Understanding soil NO fluxes and their impact on the forest atmosphere

Hyunjin An

BSc, MSc.

Earth and Environmental Sciences

This thesis is submitted for the degree of

Doctor of Philosophy

April 2024

Lancaster Environment Centre

Lancaster University

Abstract

Nitrogen oxides (NO_x = NO + NO_2) are important atmospheric pollutants and major precursors of ozone (O_3) and secondary aerosol. To address air pollution issues in industrial and urban cities, anthropogenic emissions have been the main focus of attention to improve air quality. NO_x emissions from natural sources such as the soil are less intense and are frequently neglected. However, NO_x is highly reactive and even small emissions to the atmosphere can make a substantial impact in locations where anthropogenic emissions are low, such as in remote or forested regions.

In this work, soil NO_x fluxes have been measured in the field in a number of different environments, and in lab experiments with collected soil samples, and the impacts of these fluxes have been investigated using model simulations. In-situ measurements in two forests with different vegetation and soil characteristics enabled investigation of the driving factors that govern the magnitude of soil NO_x fluxes and their diel and periodic cycles. Field observations in a Eucalyptus forest and suburban greenspace found that soils are an ongoing and non-negligible emission source, and that the diel cycles are influenced by meteorology. Surprisingly, negative soil NO_x fluxes (reflecting net NO_x uptake) were found in nitrogen limited forest soils. To account for the effects of future climate changes, soils were collected under conditions of elevated atmospheric carbon dioxide (CO_2) and temperature treatments were applied. The measurements from the field campaigns and lab experiments demonstrated that climate and pedoclimate parameters affect the magnitude of soil NO_x fluxes, and that atmospheric CO_2 levels alter the optimal soil NO_x flux response to temperature. The soil NO fluxes measured in these studies were then applied in a canopy exchange model to investigate their impact on the forest atmosphere. Soil NO fluxes influenced O_3 concentrations, but also affected peroxy radical concentrations and isoprene oxidation. The model results showed that impacts were bigger under heatwave and prolonged drought conditions. Furthermore, the structure of the forest canopy affects the vertical profile of O_3 and its relationship with soil NO fluxes. As Earth's climate changes, and as anthropogenic sources reduce under the effect of emission controls, the role of soil NO_x fluxes will become increasingly important. The findings in this work motivate further interest in the role of soil fluxes on the atmosphere, and in the wider importance of biosphere and atmosphere interactions.

Contents

List of tables

List of figures

Acknowledgements

First, I want to express my unlimited gratitude to my parents, who have trusted me and supported me during my four and half years of self-funded PhD studies. Thanks to my parents, I could successfully complete my studies without giving up.

I am incredibly grateful to Dr Kirsti Ashworth, my primary supervisor. She gave me the chance to study in Lancaster Environment Centre, and has guided the direction of my research. When field observations and collaborative lab experiments were cancelled because of the COVID-19 pandemics she provided invaluable guidance and gave me opportunities for further eligible topics and science questions for my research.

Also, I express my profound gratitude to another supervisor, Prof. Emma J. Sayer. She guided me in writing my first publication and through the whole procedure of a lab experiment from design to measurements. Also, she introduced me to new analysis methods and encouraged me to solve my challenges one by one.

I thank Prof. Oliver Wild for taking over my supervision from Kirsti. He advised not only my research, but also my future plans and personal concerns.

My appraisal committee members, Dr. Andrew Jarvis and Prof. Kevin Jones provided their precious time for me, and advised me how to move forward when facing the challenges of the pandemic and my change of supervisors. They also encouraged me to adapt my plans to complete my PhD.

Also I give warm thanks to the member of my lab. Especially, Frederick Otu-Larbi helped me with the settings and operations of the model. Hattie Robert and Isla Young helped me with writing and helped me improve my poor English. Also thank you for the opportunity to chat together and for the help to get over the COVID pandemic and difficult times with supervisors.

Furthermore, I grateful to all my internal and external collaborators. Clare Benskin trained me in soil analysis, and I really appreciate her help, as those data were essential to analysis of my results. James Allan and Michael Flynn helped me during the OSCA

campaign and encouraged my works. Frances Phillips, Clare Paton-Walsh and Kathryn Emmerson also gave me a great opportunity for studying conditions in an Australian Eucalyptus forest.

To everyone I haven’t named here, and all listed above, I want to say great thanks to you all for my short (but not that short) PhD life. I wish you happiness all the day today and tomorrow, now and forever!

Declaration

This thesis is the work of the author, has not been submitted for the award nor another degree elsewhere. The results are my own work and collaborative works are specifically indicated within. The ideas in this thesis were the product of discussions with my supervisors Dr Kirsti Ashworth, Prof Oliver Wild, and Prof Emma J Sayer.

Excerpts of this thesis have been published in academic journals:

Soils are a non-negligible source of NO in a UK suburban greenspace and SE Australian Eucalyptus forest. Hyunjin An, Emma J. Sayer, James Allan, Michael Flynn, Frances Phillips, Doreena Dominick, Travis Naylor, Clare Paton-Walsh, Kathryn M. Emmerson, Malcolm Possell, Danica Parnell, Kirsti Ashworth, 2023, published in *Agricultural and Forest Meteorology*, vol. 342, 109726, https://doi.org/10.1016/j.agrformet.2023.109726

Chapter 1: Introduction

1.1 Background

Nitrogen oxides ($NO + NO_2 = NO_x$) play a key role in the photochemistry of the troposphere and ground-level ozone (O_3) production and loss. Air pollution, especially O_3, arose as a critical issue in urban areas in the 20th century. Tropospheric O_3 was first recognised as a significant issue for human health and vegetation in the Los Angeles basin (Middleton et al., 1950); it plays an important role as an oxidant in the atmosphere and as a highly reactive and harmful pollutant, e.g. damaging for the respiratory system (Bell et al., 2004) and for stomata on leaves (Bohler et al., 2007). However, not only O_3, but also NO_x itself affects health issues e.g. lung function and the respiratory system (Boningari and Smirniotis, 2016), especially under long-time exposure.

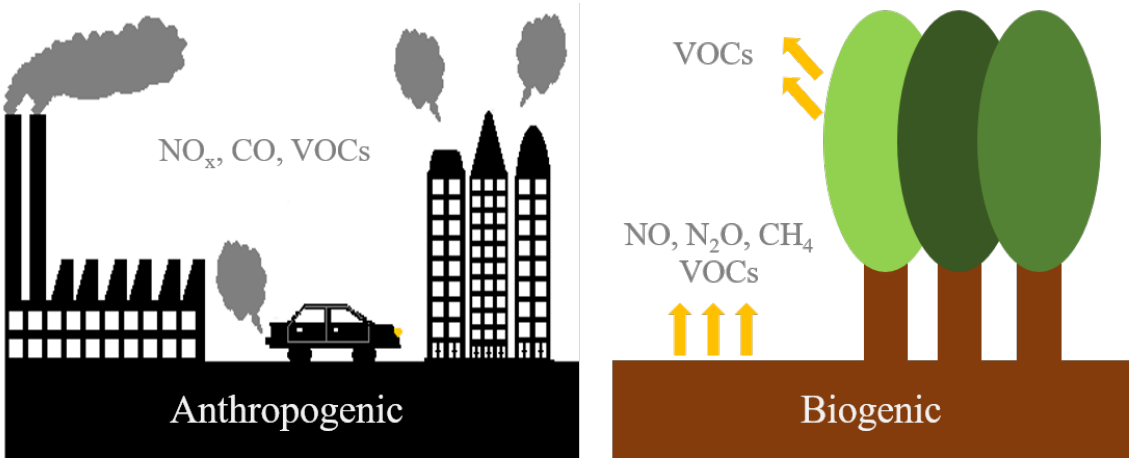

Fig. 1.1. Simplified illustration of emission sources. Urban and industrial areas are dominated by the major anthropogenic emission sources, including industrial activities, transport, and power plants. Vegetation and soils are the major biogenic emissions sources, involving plant and microbial activities.

NO_x can be emitted from both anthropogenic and biogenic sources (Fig. 1.1). As air pollution issues arose in megacities where abundant anthropogenic emission sources were distributed, NO_x has been investigated much more in urban or downwind systems

(Hidy et al., 2014; Gao et al., 2017; Crawford et al., 2021) rather than in rural regions where anthropogenic sources are relatively small.

Global NO_x emissions rapidly increased during the late 20th century, as a consequence of increased energy consumption, transport, and agricultural activities (Fowler et al., 2020). At a global scale, total annual anthropogenic NO_x emissions were estimated at 37 Tg N in 2017 (McDuffie et al., 2020). Combustion of fossil fuel (e.g. for energy generation, industry, and transportation), accounts for 50~60% of total NO_x emissions, and biomass burning, which contributes around 20%, is the other main anthropogenic source of NO_x (Delmas et al., 1997; McDuffie et al., 2020). Starting with developed countries in the late 20th and early 21st century, a range of regulations have been implemented to reduce NO_x emissions. However, global total emissions continue to rise because reductions in Europe and North America have been counterbalanced by increases in Asia and elsewhere (Fowler et al., 2020, McDuffie et al., 2020). After the smog in Beijing reached hazardous levels in 2012, NO_x emissions in China have also started to decrease, and this is contributing to a reduction in global NO_x emissions (McDuffie et al., 2020). The declines in NO_x emissions have mainly been achieved by changes in road transport; for example, of the 37% NO_x emissions reductions in the UK between 1990 and 2000, 34% were due to lower traffic emissions following improvement of engine design, catalysts, and tightened European vehicle emission standards (AQEG, 2004).

Natural NO_x sources, including lightning and microbial activity in the soils are estimated to comprise a quarter of global total NO_x budgets, and up to 80% of these biogenic NO_x emissions are believed to be from the soil (Denman et al., 2007; Skiba et al., 2021). However, estimates of biogenic NO_x emissions vary depending on the methods used (e.g. model type, top-down or bottom-up calculations, etc.), as well as the grid resolution and time period of interest (Weng et al., 2020). In addition, input information including edaphic, pedoclimate and climate or meteorological data also affects the uncertainties and the varied estimation of biogenic NO_x emissions (Kesik et al., 2005; Hudman et al., 2012). Early studies estimated that 13~21 Tg N yr^{-1} of NO are emitted from the soil to the atmosphere globally, depending on the strength of absorption onto plant canopy surfaces (Davidson & Kingerlee 1997). Later, NO_x emissions from soils from natural ecosystems and agriculture were estimated at 7.3 and

3.7 Tg N yr^{-1}, respectively, accounting for 23% of total global NO_x emissions (Ciais et al., 2013). More recent models reported 7.1~8.8 Tg N yr^{-1} during 2014-2017, depending on the resolution of the grid (Weng et al., 2020). However, according to Fortems-Cheiney et al., 2021, NO_x emissions from soils in Europe were estimated to have increased by up to 2% per year between 2008-2017, whereas anthropogenic emissions were predicted to have decreased by as much as 10% yr^{-1} during the same period. Many sources of anthropogenic NO_x are declining, but soil NO_x emissions are increasing. Hence, the importance of soil emission as a biogenic source becomes relatively more important as a potential driver of air pollution. Furthermore, in ecosystems where anthropogenic NO_x sources are limited, such as forests, the role and contribution of biogenic NO_x emissions to atmospheric chemistry and O_3 production is likely to increase with more N-deposition, which leads to fertilisation and microbial fixation, and climate change (Fowler et al., 2015; Fortems-Cheiney et al., 2021). To investigate the contributions of natural ecosystems to forest O_3, a greater focus soil NO_x fluxes and their impacts in forests and remote areas will be required.

1.2 Role of nitrogen oxides in atmospheric chemistry

Direct emissions of NO rapidly oxidise to NO_2 by reacting with O_3 (Eq. 1.1), while NO_2 is converted back to NO (Eq. 1.2) by photolysis in sunlight ($h\nu$). The photolysis of NO_2 also forms atomic oxygen, $O(^3P)$, which combines with an oxygen molecule to re-form ozone in the presence of an inert molecule, M (Eq. 1.3). Equation 1-1 ~ 1-3 represent a null cycle in which there is no net production or loss of NO or O_3 (e.g. in the stratosphere).

$$NO + O_3 \rightarrow NO_2 + O_2 \quad \text{Eq. 1.1}$$

$$NO_2 + h\nu \rightarrow NO + O(^3P) \quad \text{Eq. 1.2}$$

$$O(^3P) + O_2 + M \rightarrow O_3 + M \quad \text{Eq. 1.3}$$

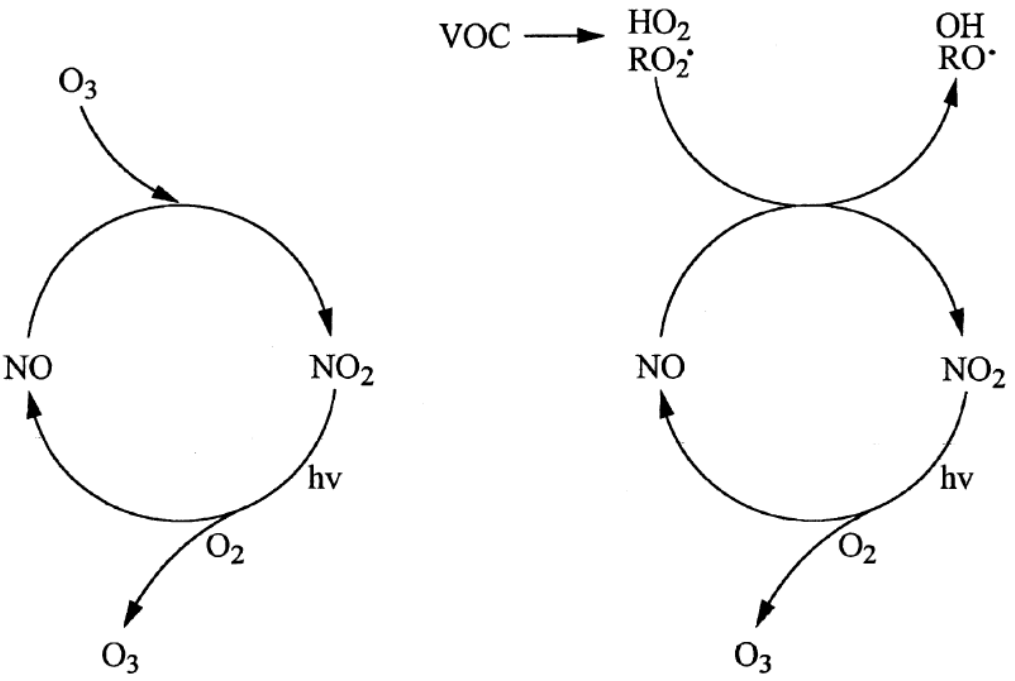

Fig. 1.2. Schematic diagram of the nitrogen oxide conversion (NO-NO_2) and O_3 formation reactions under the absence and presence reactive organic radicals (HO_x and RO_x) produced through oxidation process of the volatile organic compounds (VOCs).

This rapid cycling between NO_x-O_x occurs throughout the atmosphere (Jacob, 1999). However, in the presence of Volatile Organic Compounds (VOCs) in the troposphere, this cycle can be disturbed if NO_x conversion along other reaction pathways is energetically more efficient and competes with these reactions (Fig. 1.2; Atkinson, 2000). In particular, the NO-NO_2-O_3 cycle is disturbed by the preferential oxidation of NO by peroxy radicals (Eq. 1.5), which replaces the O_3-NO oxidation reaction (Eq. 1.1). These, often highly reactive organic peroxy radicals (RO_2), are produced by the oxidation of emitted VOCs by OH or NO_3 radicals or by direct reaction with O_3, depending on the chemical structure of the VOC and the availability of each oxidant. Further oxidation of the products of these radicals produces the highly reactive hydroperoxyl radical (HO_2; Eq. 1.6). The RO_2 and HO_2 radicals produced by atmospheric oxidation (Eq. 1.4 & 1.6) very efficiently convert NO to NO_2 (Eq. 1.5 & 1.7) and compete with the NO-O_3 reaction shown in Eq. 1.1. The net result is the reactions shown in Eq. 1.4 ~ 1.7, where the presence of VOCs enables conversion of

NO to NO_2 without consuming O_3. As the NO_2 produced via Eq. 1.5 & 1.7 can still produce O_3 via Eq 1.2 & 1.3, even a small amount of VOC in the presence of NO_x produces more O_3 than NO_x alone. Therefore, the null cycle of NO_x-O_3 chemistry is disrupted by VOCs and their oxidation processes result in additional production of O_3 in the troposphere.

$$RH + OH\ (+O_2) \rightarrow RO_2 + H_2O \qquad \text{Eq. 1.4}$$

$$RO_2 + NO \rightarrow RO + NO_2 \qquad \text{Eq. 1.5}$$

$$RO + O_2 \rightarrow R'CHO + HO_2 \qquad \text{Eq. 1.6}$$

$$HO_2 + NO \rightarrow OH + NO_2 \qquad \text{Eq. 1.7}$$

In urban areas, human activity generates abundant anthropogenic VOCs (AVOCs) such as toluene and benzene, providing a source of peroxy radicals to fuel net O_3 production (Eq. 1.4 ~ 1.7) in the presence of NO_x. In more rural, remote and forested areas, biogenic VOCs (BVOCs) such as isoprene and monoterpenes, which are emitted from vegetation, replace the role of AVOCs, although here sources of NO are more limited. When NO_x is available, however, these BVOCs have significantly higher reactivity with the OH radical than AVOCs (Atkinson, 2000), which results in O_3 concentrations being unexpectedly high in forested and rural areas (Sari et al., 2016). Considered globally, total BVOCs emissions are estimated to be an order of magnitude higher than AVOC emissions (Goldstein and Galbally, 2007; Guenther et al., 1995), and are present even in urban areas. Isoprene (C_5H_8) is one of the most prevalent VOCs, accounting for as much as 70% of global BVOCs emissions (Sindelarova et al., 2014). Several long-term observational studies have reported that urban O_3 levels increase with increasing isoprene concentrations, even when NO_x emissions are reduced (Zhang et al., 2008; Bao et al., 2010; Geng et al., 2011; Ran et al., 2011, Sartelet et al., 2012). These studies indicate that biogenic emissions of VOCs have a critical impact on atmospheric chemistry in all areas where NO_x and AVOCs emissions are limited. However, isoprene emissions are difficult to predict because they are strongly dependent on temperature, plant species, growth stage, CO_2, and land use changes (Lantz et al., 2019). Furthermore, total OH reactivity, which is the inverse of the OH lifetime, is significantly greater than expected in natural environments (Di Carlo et al., 2004; Goldstein and

Galbally, 2007; Sanchez et al., 2021). The difference between models and measurements is referred to as missing OH reactivity, ranging from 30~80% in forest environments. The major contributions to this missing reactivity are unknown BVOCs yet to be measured and oxygenated VOCs from oxidation of known BVOCs. Thus, missing OH reactivity also increases with temperature in the forest environments (Di Carlo et al., 2004).

Estimates and predictions of both VOCs and O_3 are highly uncertain because there are limited emission inventory data and there are substantial uncertainties in precursors and in the complexity of their oxidation (Fowler et al., 2008; Mcduffie et al., 2020). As the majority of air pollution issues arise in urban and industrialised areas, more time and effort has been spent on establishing anthropogenic emission inventories, but there are still high uncertainties in human activity data (e.g. transport, power plants, solvent use, and etc.), emission factors, and time-spatial quantification. NO_x emissions from natural sources such as soils are also poorly quantified (Fowler et al., 2008), which hampers efforts to improve predictions of O_3 production through reactions between NO_x and VOCs. As NO_x emissions from soils are the result of both abiotic and microbial processes that involve a variety of micro-organisms, there is high uncertainty in the response of NO_x emissions to potential controlling parameters (Pilegaard, 2013). The uncertainty in soil NO_x emissions urgently needs to be resolved, firstly because in natural ecosystems their impact on O_3 production is greater than in more polluted environments, due to high emissions and reactivity of BVOCs, and secondly because urban greenspaces are expanding with expanding urban area (Haaland and Van Den Bosch, 2015), and therefore natural emissions from urban green spaces including BVOCs from plants and NO_x from soils cannot be neglected even in urban environments.

1.3 NO formation in soils

Soil NO_x is predominantly emitted in the form of NO, and this is oxidised to NO_2 which is then deposited onto the soils (Schindlbacher et al., 2004; Schaufler et al., 2010). Hence, soil NO_x flux measurements have concentrated on NO, which is produced in the soil through microbial activity and abiotically under aerobic and anaerobic conditions.

The main pathway for soil NO production is considered to be microbial activities involving nitrification and denitrification (Fig. 1.3) which also produce nitrous oxide (N_2O), one of the major greenhouse gases in the atmosphere (Butterbach-Bahl et al., 2013; Pilegaard, 2013; Medinets et al., 2015), whereas the abiotic process is called chemodenitrification, which produces NO through chemical reactions in the soil. In general, both NO and N_2O are produced by the same processes. However, the partitioning condition and fraction between these NO and N_2O is not yet clearly determined. As global climate change has arisen as an environment challenge, there has been a much stronger focus on N_2O because it is an important greenhouse gas. NO contributes to climate change only indirectly through O_3 production and aerosol formation. Therefore, it is important to investigate soil NO fluxes and their impact on O_3 production and interactions between the biosphere and atmosphere.

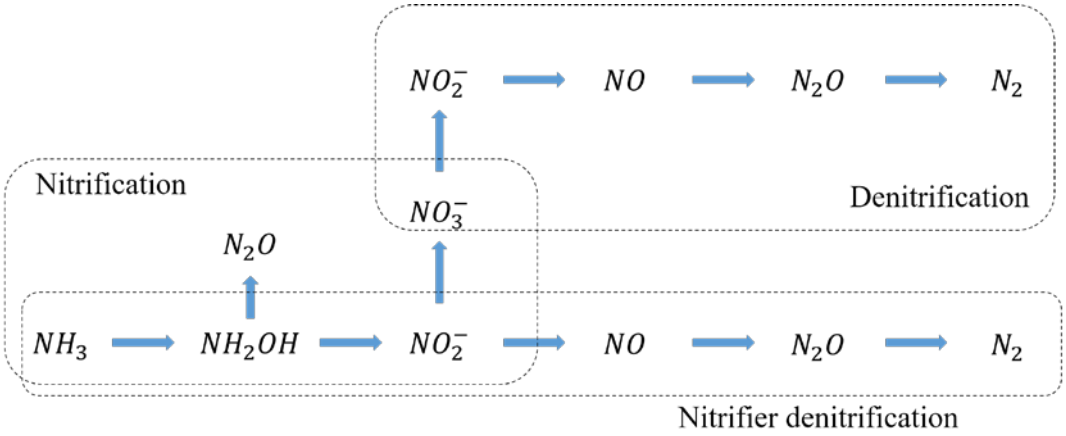

Fig. 1.3. Schematic diagram of the nitrification and denitrification process in the soils. Nitrogen species transform in gaseous and ion phase interact through atmosphere and soils via microbial activities.

1.3.1 Nitrification

Nitrification is a sequence of steps converting ammonium (NH_4^+) via hydroxylamine (NH_2OH) to nitrite (NO_2^-) and further to nitrate (NO_3^-) by biological oxidation processes (Eq. 1.8 ~ 1.9). Nitrification is carried out by *nitrosobacteria* through Eq. 1.8 following this sequential pathway (Firestone & Davidson, 1989). Nitrite is oxidised into nitrate by

nitrobacteria (Eq. 1.9). NO can be released as a by-product of nitrate (NO_3^-) formation during nitrification as well as intermediates of NO_3^- reduction during denitrification.

$$NH_4^+ \rightarrow NH_2OH \rightarrow HNO \rightarrow NO \uparrow \rightarrow NO_2^- \quad \text{Eq. 1.8}$$

$$NO_2^- \rightarrow NO_3^- \quad \text{Eq. 1.9}$$

In soil solution with sufficient oxygen supply (aerobic conditions), the availability of the ammonium (NH_4^+) ion predominantly controls the nitrification process (Robertson, 1989; Ludwig et al., 2001). Previous research has investigated this process and found that nitrification (plus nitrifier denitrification) in a wide range of soils is a significant process for soil NO production from NH_4^+ oxidation through NH_2OH to NO_2^- and further gas phase emissions (Garrido et al., 2002; Wan et al., 2009; Mei et al., 2011). The rates of NO formation during nitrification are not clearly determined yet, but are estimated as 0.1~10% (Ludwig et al., 2001) or 0.6~2.5% (Garrido et al., 2002) of gross NH_4^+ oxidation.

1.3.2 Denitrification

Denitrification is the reduction process of nitrate (NO_3^-) to nitrite (NO_2^-), which further produces gaseous NO, N_2O and nitrogen gas (N_2) (Eq. 1.10). This is called heterotrophic or classical denitrification. The process can take place both under aerobic and anaerobic conditions. Most denitrifiers are active in aerobic conditions (e.g. bacteria, fungi, and archaea), but they can switch to anaerobic respiration using NO_3^- as electron acceptor under low O_2 (Hayatsu et al., 2008; Shoun et al., 2012).

$$NO_3^- \rightarrow NO_2^- \rightarrow NO \uparrow \rightarrow N_2O \uparrow \rightarrow N_2 \uparrow \quad \text{Eq. 1.10}$$

The other process producing gaseous NO is nitrifier denitrification, which is followed by nitrification (Eq. 1.8), whereby NO_2^- is reduced to gaseous NO by ammonium

oxidation bacteria with NH_4^+ as an electron donor under the O_2 limitation (Poth and Forcht, 1985; Wrage et al., 2001).

1.3.3 Chemodenitrification

Chemical decomposition of nitrite (chemodenitrification) describes non-enzymatic (abiotic) chemical conversion of NO_2^- or NO_3^- to gaseous nitrogen species. Chemodenitrification occurs at low pH (below 5) and normally requires NH_4^+, amines or reduced metals such as ferrous iron (Fe_2^+), as well as high soil organic matter (Chalk and Smith, 1983; Zumft, 1997) and soil water contents (Venterea et al., 2005). The essential reaction of chemodenitrification (Eq. 1.11) is the formation of NO through nitrous acid (HNO_2 in aqueous phase, HONO in gaseous phase; Van Cleemput and Baert, 1976, 1984; Chalk and Smith, 1983; Venterea et al., 2005). If reduced metals are available, Eq. 1.12 can also contribute to gaseous NO formation in the soil. In addition, gaseous nitrous acid, HONO, is produced by reversible acid-base reaction of nitrite with H^+ ions shown in Eq. 1.13 (Su et al., 2011; Oswald et al., 2013). Aqueous HNO_2 can be released to the atmosphere as gaseous HONO followed by the equilibrium of gaseous and aqueous nitrous acid, which is determined by soil pH and nitrite concentrations (Eq. 1.13). Finally, HONO in the atmosphere is rapidly photolyzed to release NO and OH radicals (Eq. 1.14).

$$3NO_2^- + 3H^+ \leftrightarrow 3HNO_2 \rightarrow 2NO \uparrow \rightarrow + HNO_3 + H_2O \quad \text{Eq. 1.11}$$

$$NO_2^- + Fe^{2+} + 2H^+ \rightarrow NO \uparrow \rightarrow + Fe^{3+} + H_2O \quad \text{Eq. 1.12}$$

$$NO_2^- + H^+ \leftrightarrow HNO_2 \leftrightarrow HONO \uparrow \quad \text{Eq. 1.13}$$

$$HONO + h\nu \rightarrow OH + NO \quad (\lambda < 400nm) \quad \text{Eq. 1.14}$$

For chemical NO formation in the soil, H^+ ions are the critical component as shown through Eq. 1.11 ~ 1.14, and therefore pH is the major controlling factor. Additional factors that control the process are: NO_2^- concentrations, which represent nitrogen (N) availability (Ludwig et al., 2001), temperature (Kesik et al., 2006) and soil water

content (Schindlbacher et al., 2004; Venterea et al., 2005; Schaufler et al., 2010; Pilegaard et al., 2013).

1.4 Soil NO consumption

Soils can also be an important potential sink for NO (Slemr and Seiler, 1984; Skiba et al., 1992; Ludwig et al., 2001; IPCC, 2007). However, there are so few studies demonstrating NO uptake by soils that the underlying processes and controls are poorly described, and we do not know whether soil NO uptake is widespread.

Both NO_2^- and NO are involved in nitrosation in the soil and considered as nitroso and nitrosyl donors (Spott et al., 2011). Particularly, the nitrosation with humic substances have been investigated and reported as an abiotic, chemical consumption and a pathway of nitrogen incorporation into soil organic matter (Thorn and Mikita, 2000).

There is strong evidence for NO consumption by soils, as NO production through denitrification and nitrifier denitrification in the soils is greater than the NO emitted out of the soil surface (Firestone and Davidson, 1989; Skiba et al., 1997), with only 13% of production released to the atmosphere (Skiba et al., 1997). A significant fraction of produced NO is consumed by the energy production of denitrifiers (Zumft and Cárdenas, 1979). Furthermore, NO can be consumed by soil denitrifiers as an electron acceptor to produce N_2O (Eq. 1.10), which generally occurs in anoxic conditions. However, soil micro-organisms can also oxidise NO to N_2O under oxic conditions (Pilegaard, 2013), especially when there is insufficient or limited soil nitrogen availability (Skiba et al., 1992; Schindlbacher et al., 2004). Thus, there is evidence that soils in N-limited ecosystems could represent a sink for NO, but this has not been widely investigated, and the potential for soils to act as a sink for NO has been largely ignored.

1.5 Drivers of soil NO emission

Soil NO formation pathways are either biological or chemical, and are significantly influenced by the surrounding environment through variables such as soil moisture, soil

temperature, pH, nitrogen availability, soil type and vegetation. However, the varied effects of these pedoclimate parameters on the biological and chemical processes involved in NO formation can produce high temporal and spatial variability. For instance, increasing temperature would boost NO emissions from the soil to the atmosphere in unplanted soils (Chapter 2, section 2.3.4), but greater nitrogen uptake of plant roots under higher temperatures could limit soil NO production (Denef et al., 2007). In addition, the biotic and abiotic processes involved in NO formation are sensitive to the pH and nitrogen availability of the soils and thus, NO emissions are strongly influenced by interactions between plants, microbial processes, and environmental conditions. Nonetheless, quantifying soil NO emissions is important because soil NO emissions can be expected to become increasingly important in the future due to climate changes (especially increasing temperatures and changes in patterns of precipitation) and on-going efforts to reduce NO emissions through e.g. fossil fuel combustion (Fig. 1.4.).

1.5.1 Nitrogen availability

While nitrification and denitrification processes are the transformation of the nitrogen species, soil N availability is the most important factor governing the magnitude of soil NO production or consumption. As nitrogen transformations in soil are largely driven by biological processes, the balance of elemental nitrogen and carbon contents in the soil, the C:N ratio, is likely to be a reasonable proxy for N availability (Davidson et al., 2000; Klemedtsson et al., 2005) because it indicates the balance of the food (represented by carbon) and nutrients (nitrogen; essential component in protein) required for microbial growth.

There are several major N inputs to soils: nitrogen fixation by microorganisms, deposition from the atmosphere, and fertiliser/manure input. Although fertiliser or manure input is highly relevant in agricultural systems, atmospheric nitrogen fixation and deposition represent the main inputs of inorganic nitrogen to natural ecosystems.

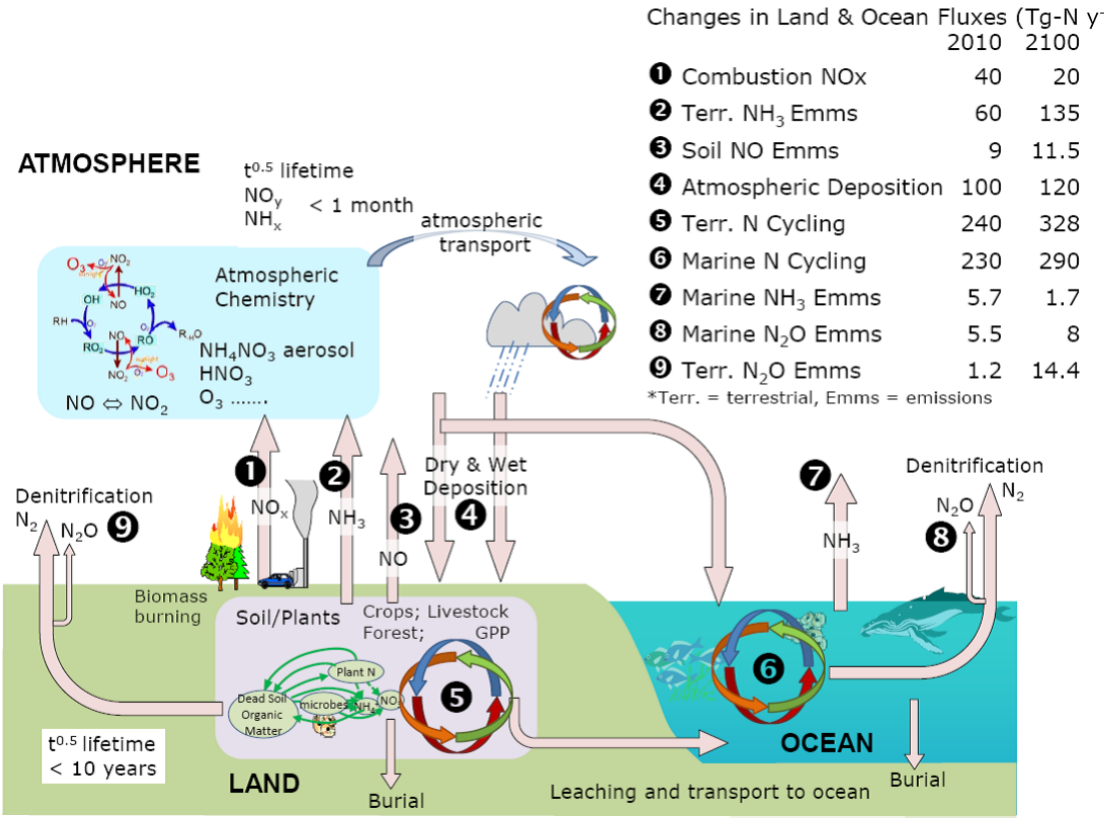

Fig. 1.4. Global reactive nitrogen (Nr) fluxes through terrestrial, marine and atmosphere between 2010 and 2100 projection, adapted from Fowler et al., 2015.

As N_2 gas is a very stable molecule with a triple bond, it has little interaction with the soil. Thus, atmospheric N_2 requires transformation to reactive nitrogen (any form of nitrogen species except N_2) to enable uptake and use of the N in soil. The transformation of N_2 to reactive N species is referred to as nitrogen fixation. Atmospheric N_2 can be fixed through both anthropogenic and biological processes: Anthropogenic fixation occurs during industrial ammonia (NH_3) production by the Haber-Bosch process. Biological nitrogen fixation is carried out in soil by microorganisms termed "diazotrophs" or "N_2-fixers", which reduce N_2 to NH_3 (Burris and Wilson, 1945; Zhang et al., 2020).

Nitrogen fixation represents a major nitrogen input to soils. Global total reactive nitrogen fixation is estimated to be 473 Tg N yr^{-1}, and terrestrial fixation by biological processes is estimated to be 128 Tg N yr^{-1} in 2010, which is predicted to increase to 170 Tg N yr^{-1} by 2100, reflecting increasing temperature and atmospheric CO_2 levels (Fig.

1.5, Fowler et al., 2015). Furthermore, atmospheric reactive nitrogen species can also be deposited through both wet and dry deposition, which are estimated to account for 100 Tg N yr^{-1} (Fowler et al., 2013; Fowler et al., 2015). As soil and marine organisms consume the nitrogen as an essential nutrient for growing, the amount of the atmospheric deposition is exceeding emission from the soil. The changes in N deposition affect the soil NO emissions (Kesik et al., 2005), as N addition significantly stimulates nitrification and denitrification (Barnard et al., 2005) and provides more available nitrogen in the soil, resulting in a greater magnitude of soil NO emissions from e.g. forest soils (Pilegaard et al., 2006). On the other hand, insufficient N input could limit available nitrogen in the soil, which could uptake the NO from the atmosphere (e.g. boreal forest in Finland, Schindlbacher et al., 2004; Pilegaard et al., 2006; Schaufler et al., 2010). However, N availability in soils differs so strongly in space and time, depending on vegetation, climate and pedoclimate conditions that we do not know when soils might switch from a sink to a source of NO or how much additional N might be required to initiate this switch.

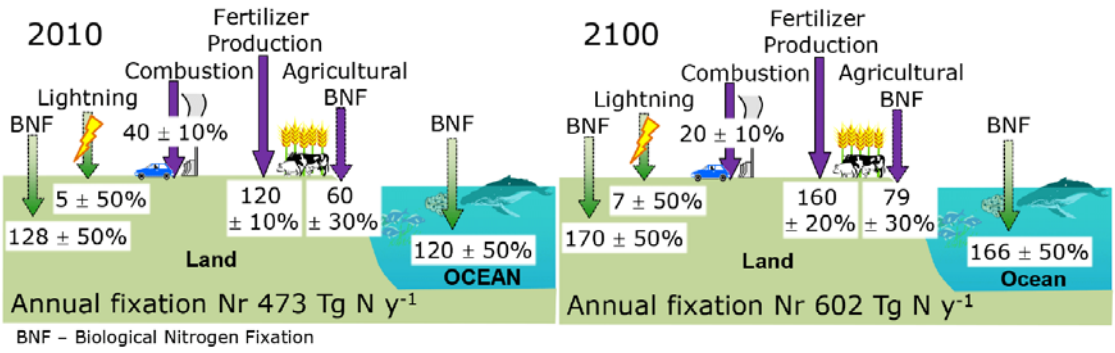

Fig. 1.5. Global nitrogen fixation over terrestrial and marine systems, adapted from Fowler et al., 2015, where BNF is biological nitrogen fixation, green arrows represent natural processes (biological nitrogen fixation and lightning) and purple arrows indicate nitrogen fixation as a consequence of anthropogenic influences. Percentages indicate uncertainties of each estimation.

1.5.2 Soil moisture

Soil water is a transport medium for NO_3^- and NH_4^+, and a supply of O_2 that controls aerobic process (nitrification) or anaerobic process (denitrification). Various studies have investigated the relationship between soil water content and NO emission rates (Schindlbacher et al., 2004; Venterea et al., 2005; Schaufler et al., 2010; Pilegaard, 2013). In general, NO production and emission rate decrease with increasing soil moisture content (Venterea et al., 2005; Schaufler et al., 2010). The nitrification tends to be inhibited at higher water contents, whereas denitrification and reductive microbial NO consumption increase. Gaseous diffusion, and thus NO emission, is often limited at high soil water contents, because the pore space is filled with water, which can even result in greater NO consumption. Several studies have found that the soils have different optimal soil water content for soil NO flux (Schindlbacher et al., 2004; Pilegaard, 2013), depending on soil characteristics (e.g. soil texture and vegetation). For example, the moisture optimum for NO emission ranged from 15 to 65% of water filled pore space (WFPS) in different locations: around 45% at German forest soils, around 15% in Italian sandy floodplain soils, and around 65% in Austrian beech forest soils. In addition, plant litter on the soil surface helps regulate soil water content (Sayer, 2006; Deutsch et al., 2010), and reduce soil NO emissions (Chapter 2, section 2.3.4). However, prolonged drought and rewetting effect can trigger microbial activities, leading to a temporary boost in NO production in the soil (Muhr et al., 2008; Leitner et al., 2017).

1.5.3 Soil temperature

As long as N availability and soil moisture are not limiting, soil NO emission increases with soil temperature (Schindlbacher et al., 2004; Schaufler et al., 2010; Medinets et al., 2016). Most biological processes initially increase exponentially with temperature, including enzyme activities and microbial processes in the soil, which affects nitrification (Machefert et al., 2002; Robertson and Groffman, 2007) and denitrification (Butterbach-Bahl et al., 2013). However, microbial processes become limited if the temperature is too high, and the optimal temperature for biological activity differs among microbial communities depending on their adaptation to the prevalent climatic

conditions (Medinets et al., 2015). For example, typical temperature optima for ammonium oxidising bacteria in temperate soils are 22~30 ℃ (Stark, 1996), whereas the nitrification optima in tropical soils is over 35 ℃ (Sierra, 2002). Therefore, although soil temperature is an important parameter that affects NO production in the soil, it is not the primary controller but rather a modulating factor that leads to short-term variations in NO emissions (Ludwig et al., 2001).

1.5.4 Soil pH

Soil acidity (pH) is another important parameter that governs biological and chemical processes. Soil pH affects not only microbial communities and their composition (Schreiber et al., 2012) but also their biological activity (Kesik et al., 2006). Furthermore, low pH indicates more H^+ ions that enhance electron transfer and the chemical process of chemodenitrification (Kesik et al., 2006). Chemodenitrification accounts for 62% of NO production below pH 4.0, but nitrification and denitrification dominate when the pH is 4.5 or higher. NO production through nitrification and denitrification can occur between a wide range of soil pH values (pH 5~9 for nitrification and 3.5~11.2 for denitrification), but both processes are optimal around pH 7 (Wang et al., 2015). Soil NO production was found to be lowest at a pH of 5.0 (Kesik et al., 2006), because neither abiotic nor biotic processes favour NO production at this soil pH. On the other hand, soil NO production is highest at pH values of 3 or 4, when chemodenitrification dominates, and at pH 7, when microbial NO production is favoured.

1.5.5 Vegetation

Although pedoclimate factors directly influence NO formation by nitrification and denitrification processes in the soil, the vegetation of an ecosystem also affects NO emission indirectly via nutrient uptake and the influence of plant inputs on microbial processes. Plant roots interact with soils, taking up nutrients and exuding organic carbon and nitrogen into the soil. Plant growth, root production, and exudation rates differ among plant species, which in turn could influence carbon and nitrogen availability and

microbial activities that produce NO in the soil (Blackmer et al., 1982; Denef et al., 2007; Pilegaard, 2013). Different tree species affect not only soil C and N pools and net N mineralization (Finzi et al., 1998), but also soil respiration and gross nitrification in the organic layer (Bruggemann et al., 2005). For example, many comparison studies (e.g. Butterbach-Bahl et al., 1997; Schindlbacher et al., 2004 ; Kesik et al., 2005; Pilegaard et al., 2006; Schaufler et al., 2010) found higher NO emission rates in coniferous forest soils than deciduous forest soils. Spruce forest in particular has significantly higher soil NO emissions than forest with other tree species (Schindlbacher et al., 2004), presumably related to higher soil respiration rates and gross N mineralisation in the organic layer (spruce > beech > larch > oak > pine, Bruggemann et al., 2005). In addition, moss cover (Pilegaard et al., 1999) and litter on the soil surface (Chapter 2, section 2.3.4) significantly reduce NO emission from soils by regulating soil water content (Sayer, 2006) and blocking light penetration.

1.6 Motivation

Focus on soil emissions of the major greenhouse gases N_2O, CO_2 and methane (CH_4) has increased due to ongoing climate change. To date, most studies of gaseous nitrogen emissions from soils have concentrated on N_2O, whereas the impact of soil NO fluxes on the atmospheric chemistry has been largely neglected because the contribution of soils were considered to be small compared to anthropogenic NO emissions. Studies of NO_x in several field observations and laboratory measurements have improved our understanding of the importance of soil NO emission rates in various ecosystems. However, the majority of studies on soil NO emissions to date have been conducted in agricultural and forest soils, have been short-term intensive studies, or have quantified NO emissions in the lab using soil samples, which hampers our ability to identify general patterns in soil NO emissions. Hence, we still lack sufficient data on the temporal variations in soil NO emissions and their driving parameters to accurately predict NO_x emissions from soils. Therefore, it is important to investigate the temporal variations of the soil NO_x fluxes and driving parameters. Furthermore, it is essential to seek for the following impacts on the atmospheric chemistry (e.g. O_3 production). This knowledge gap needs to be filled, as NO_x are highly reactive gasses in the atmosphere,

with a major impact on atmospheric chemistry, particularly through O_3 and aerosol formation.

1.7 Thesis aims and objectives

This research aims to improve our understanding of soil NO emissions in distinct ecosystems and under different environmental conditions by identifying and modelling the variation in and controls of soil NO emissions.

The main objectives are to:

- Quantify NO fluxes from novel locations (suburban green space in UK, mixed deciduous forest in UK, Eucalyptus forest in Australia) and identify temporal variations and cycles through in-situ field observations and a lab experiment.
- Investigate the pedoclimate components affecting the magnitude of soil NO fluxes, and the meteorological parameters that influence their temporal cycles.
- Quantify potential future soil NO flux in response to the climate changes such as rising temperatures and CO_2 elevation in the atmosphere.
- Determine the impacts of soil NO flux on atmospheric chemistry in forests, where the anthropogenic impacts are limited.

This research combines in-situ observations, modelling and a novel lab experiment to quantify the magnitude of soil NO fluxes and temporal variations (e.g. diel cycle) of soil emission rates and their driving factors. Furthermore, NO_x fluxes will be measured from soils following treatment with elevated CO_2 concentrations. This study will provide another insight of climate change response, not only rising temperature but also atmospheric CO_2 elevation impact. In addition, model simulations will be undertaken using the measured soil NO fluxes. This modelling will investigate the impact of soil NO fluxes on forest O_3 and oxidation capacity with vertical profile considering the canopy structure, and time series of different heights. Throughout the work, the importance of soil NO flux will be highlighted, not only for the nitrogen cycle through atmosphere and biosphere, but also the role of soil NO fluxes in atmospheric chemistry, and the implications now and under future climate change.

1.8 Structure of the thesis

This work consists of three separate but coordinated research studies. Chapter 2 describes *in-situ* observations in field campaigns to quantify soil NO emissions and their diel cycles and investigate the relationship between soil NO fluxes and meteorological parameters. Chapter 3 is a novel lab experiment with soils collected from a free-air CO_2 enrichment (FACE) experiment to identify soil NO_x fluxes in an N-limited system, and to determine the response of soil NO_x fluxes to elevated atmospheric CO_2 concentrations. Chapter 4 describes a modelling study simulating the impact of soil NO fluxes on the forest atmosphere, focussing on O_3 and oxidation potential through HO_x radicals.

Chapter 2 : Soils are a non-negligible source of NO in UK suburban greenspace and SE Australian Eucalyptus forest (This work is published in *Agricultural and Forest Meteorology,* Nov. 2023)

This chapter is composed of field measurements in two different locations, Eucalyptus forest in SE Australia and suburban greenspace in Manchester, UK. The research demonstrates that soils are non-negligible natural NO emission sources during both day and night, not only in forest soils but also in suburban greenspace. Furthermore, continuous in-situ measurements allowed investigation of the diel patterns of soil NO emissions and the relationship between meteorological parameters, such as solar radiation, air temperature, and vapour pressure deficit, which influence biological activities. The diel cycles provide evidence that soil NO fluxes are closely connected to biological activities. This research also introduced the relationship between soil NO fluxes and pedoclimatic components, such as elemental concentrations, soil moisture and soil temperature, the magnitude of soil NO emissions could vary with different environmental conditions. This chapter suggests that soils are a non-negligible source of NO in both remote and strongly human-influenced systems.

Chapter 3 : Impact of soil temperature and elevated CO_2 on the soil NO_x fluxes in deciduous forest (in preparation for submission to a journal such as *Geophysical Research Letter*)

In this chapter, a laboratory experiment was performed to determine NO_x fluxes in nitrogen limited soils collected from the Birmingham Institute of Forest Research (BIFoR) free-air CO_2 enrichment (FACE) experiment. The comparison of FACE and control soils provides important insights into the potential impacts of rising atmospheric CO_2 concentrations on soil NO fluxes. Furthermore, the soils were incubated at different temperatures to investigate the response of soil NO fluxes to the combined impact of elevated CO_2 and rising temperatures. This research demonstrated negative NO fluxes, indicating that the soils are taking up NO from the atmosphere. Several soil properties, such as elemental (carbon and nitrogen), inorganic nitrogen (nitrate and ammonium) contents and soil pH likely contribute to soil NO uptake. Importantly, the incubation of soils at different temperatures demonstrated that elevated CO_2 alters the temperature optimum of NO uptake by soils, which provides valuable information for future projections of soil NO_x fluxes under climate change.

Chapter 4 : Impact of heatwave and soil NO fluxes on the forest canopy atmosphere in UK deciduous forest (in preparation for submission to a journal such as *Atmospheric Chemistry and Physics*)

In the final study, I used model simulations to investigate the impact of soil NO fluxes on the forest atmosphere. Three different soil NO fluxes were applied to the 1-D canopy exchange model FORCAsT (model of FORest Canopy Atmosphere Transfer): positive fluxes, observed at the Eucalyptus forest site in Chapter 2; negative fluxes measured in the BIFoR soils in Chapter 3; and zero fluxes as a control scenario. The formation of O_3 and HO_x radicals were then analysed to understand the role of soil NO fluxes on forest atmospheric chemistry, including photochemistry and isoprene oxidation. Comparisons at four different heights and during a heatwave period demonstrated the impact and importance of the soil NO fluxes on forest O_3 formation and HO_x radical chemistry, especially at locations where anthropogenic emissions of NO_x are limited. This study provides the novel insight that soil NO fluxes cannot be neglected in studies of the

forest atmosphere. The scenarios demonstrate the potential consequences of different environmental conditions and highlight how soil NO fluxes affect atmospheric chemistry and oxidation capacity in the forest canopy.

The last chapter (Chapter 5) draws conclusions from the body of work presented in the thesis, highlighting how the research has elucidated the importance of the soil NO_x fluxes and their impact on the forest atmosphere, and discussing the implications of the findings from the three research chapters. Combining the field studies, lab measurements and model simulations, I will show how my work has advanced research into soil NO fluxes, highlight remaining knowledge gaps, and propose future research directions.

Chapter 2: Soils are a non-negligible source of NO in a UK suburban greenspace and SE Australian *Eucalyptus* forest

Authors contributions

Hyunjin An: Designed experiment methodology, carried out practical observations, compiled and analysed data, visualised data, participated in result interpretations, prepared and submitted manuscript.

Emma J. Sayer: Participate in result interpretations and manuscript preparation

James Allan: Advised observation planning, supplied observed datasets, participate in manuscript preparation

Michael Flynn: Advised observation planning, supplied observation datasets

Frances Phillips: Carried out practical observations, supplied observed datasets, participate in manuscript preparation

Doreena Dominick: supplied observation datasets

Travis Naylor: Carried out practical observations, supplied observed datasets, participate in manuscript preparation

Clare Paton-Walsh: Carried out practical observations, supplied observed datasets, participate in manuscript preparation

Kathryn M. Emmerson: Carried out practical observations, supplied observed datasets, participate in manuscript preparation

Malcolm Possell: Supplied observation datasets, participate in manuscript preparation.

Danica Parnell: Supplied observation datasets

Kirsti Ashworth: Designed experiment methodology, participated in result interpretations and manuscript preparation.

Highlights

- Soil emissions were a continuous source of NO to the atmosphere at both sites
- Meteorological conditions affect soil NO emission
- Diel variations of solar radiation and VPD partly explain soil NO diel patterns
- Diel patterns indicate both anthropogenic and biogenic sources of NO
- Soils contributed a small but significant fraction of atmospheric NO_x at both sites

Graphical Abstract

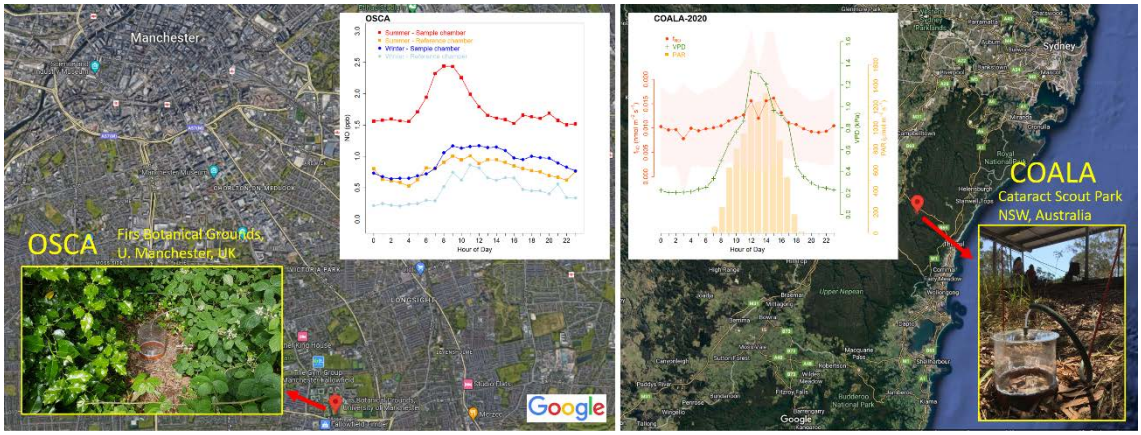

Submission to journal

Soils are a non-negligible source of NO in a UK suburban greenspace and SE Australian Eucalyptus forest. Hyunjin An, Emma J. Sayer, James Allan, Michael Flynn, Frances Phillips, Doreena Dominick, Travis Naylor, Clare Paton-Walsh, Kathryn M. Emmerson, Malcolm Possell, Danica Parnell, Kirsti Ashworth, 2023, published in *Agricultural and Forest Meteorology*, vol. 342, 109726, https://doi.org/10.1016/j.agrformet.2023.109726

Abstract

Nitrogen oxides, particularly NO and NO_2 (NO_x), are primary air pollutants that also play an essential role in the atmospheric oxidation of volatile organic compounds, resulting in ozone and secondary organic aerosol formation. It is therefore critical to fully characterise NO_x sources and sinks to understand tropospheric photochemistry and hence local- to regional-scale air quality. Human activities such as transport and power plants are well-known NO_x emission sources in urban areas, whereas natural sources such as soils have been considered to contribute more substantially in rural and remote areas. However, soil NO emissions are poorly characterised and therefore underrepresented in models. To improve our understanding of soil as a source of NO, we measured diurnal patterns in soil NO concentrations at a suburban site in the UK and a remote field site in Australia to determine whether soils contribute to local atmospheric NO, and to identify the potential drivers of soil NO emissions.

Mean soil NO concentrations in both UK campaigns (1.76±0.92 ppb in summer and 0.91±0.37 ppb in winter) were higher than those measured in Australia (0.73±0.73 ppb). The diel patterns of NO concentrations (both sites) and emissions rates (Australia) showed a clear peak corresponding to local emission sources, but variation in NO was also related to either vapour pressure deficit (R^2 = 0.88 in UK summer, R^2=0.51 in Australia, both $p < 0.05$) or solar radiation (R^2 = 0.06 with $p > 0.4$ in UK summer, R^2=0.71 with $p < 0.05$ in Australia) during the daylight hours, indicating biogenic origin of soil NO.

Our work demonstrates that biogenic soil emissions of NO are non-negligible, estimated at around 1.32% of total NO emissions at the remote site, and 0.22% at the urban site, and must be accounted for in global and regional atmospheric chemistry-climate modelling and NO_x reduction strategies.

Keywords: Soil NO emission, Natural NO_x source, Soil chamber

2.1 Introduction

Nitric oxide (NO) is a major component of nitrogen oxide (NO_x = NO + NO_2) which plays a key role in tropospheric photochemistry. NO_x is one of the most significant primary air pollutants, not only directly harmful to human and ecosystem health (see e.g., COMEAP, 2018) but also a major precursor of secondary pollutants such as tropospheric ozone (O_3) and aerosols (e.g., Fowler et al., 2008). Unlike stratospheric O_3, tropospheric O_3 contributes to global warming and damages living cells, adversely affecting human health and plant growth (Fowler et al., 2008).

NO_x emissions are predominantly anthropogenic, originating wherever human activities involve fossil fuel combustion (e.g. transport, power generation, industry; WHO, 2006). Consequently, NO_x emissions tend to be highest in urban areas. Natural sources, such as lightning and soils, are estimated to account for ~25% of global NO_x emissions, with soil emissions contributing around 80% of these (Denman et al., 2007; Skiba et al., 2021). Given that anthropogenic emission sources are concentrated in more populous regions, the contribution of soil NO_x has generally been understood to be of most importance in rural and remote areas (see e.g., Bertram et al., 2005). However, the contribution of biogenic emissions from soils to the total tropospheric NO_x budget has been estimated to range as high as 40% (Denman et al., 2007; Butterbach-Bahl et al., 2009). As anthropogenic NO_x emissions are now falling in many industrialised regions, soil NO_x emissions could play an increasingly important role in the future. For example, NO_x emissions from soils in Europe were estimated to have increased by up to 2 % yr^{-1} between 2008-2017, while anthropogenic emissions decreased as much as 10 % yr^{-1} during the same period (Fortems-Cheiney et al., 2021).

NO_x is usually emitted from the soil in the form of NO which rapidly equilibrates to NO_2. NO is produced in soils as a result of both microbial activities and chemical reactions (Heil et al., 2016; Medinets et al., 2015). The major microbial pathways responsible for NO production are the processes of nitrification and denitrification (see e.g. Butterbach-Bahl et al., 2013; Pilegaard, 2013) that also produce nitrous oxide (N_2O), the potent greenhouse gas which has been extensively studied (starting with Bremner and Blackmer, 1978), particularly in agricultural contexts (e.g. Buckingham et al., 2014). As a product of nitrification-denitrification, soil NO emissions are influenced

by a range of pedoclimatic factors (e.g. pH, nitrogen availability, mineral content and structure, soil moisture, soil temperature), and surrounding vegetation (Kesik et al., 2006; Pilegaard, 2013). Soil NO emissions generally increase with decreasing soil moisture to a peak at a moisture content of between 15 to 65% water-filled pore space, depending on the soil type (Schindlbacher et al., 2004). Interestingly, soil NO emissions increase with soil temperature in well-aerated soils, in a pattern similar to soil CO_2 efflux (soil respiration), whereas N_2O emissions are driven by nitrification and denitrification, which increase under anaerobic conditions (Medinets et al., 2016).

Hence, while the soil processes responsible for N_2O production are reasonably well known, NO emissions from soils have been almost entirely overlooked. NO and NO_2 are of most interest as air pollutants and their emissions are therefore considered a more critical issue in urban areas where anthropogenic NO_x emission rates are high and natural sources are considered negligible (Goldberg et al., 2021). However, the downward trend of anthropogenic NO_x emissions is coupled with changes in land use and landcover, most notably increased forested areas. Driven by countries' commitments to Net Zero targets and the wider ecosystem services and well-being benefits of trees, suburban and peri-urban forests are being extensively created. These changes make it more important than ever to understand the magnitude and drivers of soil emissions from natural and semi-natural vegetation and elucidate where their relative contributions are high.

While soil NO emissions have been measured in the field (Chen et al., 2019; Medinets et al., 2019) and using soil cores in the laboratory (Schaufler et al., 2010; Medinets et al., 2021; Yu and Elliot, 2021), our understanding of the real-world determinants and hence magnitude and significance of NO fluxes across different environments and ecosystems is still limited. This paper addresses this gap by characterising soil NO emissions from contrasting understudied ecosystems. The first, a suburban site in a large UK city represents a typical urban greenspace with high transport-related NO_x emissions, while the second, a relatively remote semi-arid forest in south-east Australia, could be expected to be more important in terms of the relative contribution of soil NO to the local NO_x budget. This paper provides insight into soil NO fluxes under distinct seasons, vegetation cover, soil characteristics, and environmental conditions and highlights the importance of soil NO_x emissions to local air quality.

2.2 Methods

2.2.1 Study sites and measurement set-up

Soil NO_x emissions were measured at two different sites: a suburban air quality monitoring supersite in Manchester, UK (Fig. 2.1a) as part of the Observing System for Clean Air (OSCA) project, and a remote forest observatory in Australia (Fig. 2.1b) during the Characterising Organics and Aerosol Loading in Australia in 2020 (COALA-2020) project. While these sites offer different environmental conditions, e.g., soil characteristics, vegetation type and meteorology, which might be expected to influence the biological, and bio- and physico-chemical activities underpinning soil NO emissions, more importantly, they represent very different background levels of NO_x. The former represents a typical urban site where anthropogenic emissions could be expected to dominate, while the latter is a more remote location where anthropogenic influences would be expected to be small. Furthermore, we conduct field sampling during two different seasons in Manchester. Our samples therefore offer an important 3-way comparison: between two contrasting locations during their respective summer periods and one site across two seasons: one of peak biological activity and one relative dormancy. We are hence able to explore the importance of biogenic soil NO emissions from forest soils under a range of conditions.

2.2.1.1 Suburban air quality monitoring supersite in Manchester, UK

One subset of the OSCA project took place at the Manchester Air Quality Supersite, hereafter MAQS, which is located in Firs Botanical Grounds, Manchester University, UK (53°26’39” N, 2°12’52” W). The study site is a relatively large green space within a suburban residential area ~4 km south of the centre of Manchester (Fig. 2.1a), a large city with a population of ~2.75 million. The MAQS observatory at the site records air pollutant concentrations and meteorological measurements. The present study was conducted in an area of mixed deciduous vegetation (inset photograph in Fig. 2.1a). The dominant species in the tree canopy were *Laburnum*, *Acer pseudoplatanus*, and *Ilex aquifolium*, while *Rubus fruticosus* and *Hedera helix* dominated the understorey (Fig.

2.S1). Soil emission rates were measured during two intensive observational periods: the first from 15th June to 30th July 2021 (hereafter OSCA Summer) and the second from 21st January to 28th February 2022 (hereafter OSCA Winter). During OSCA summer, the average air temperature at the observatory was 17.4±3.9 ℃ and the relative humidity was 75.1±15.2 %. Conditions during OSCA Winter were much colder and more humid with an average air temperature of 7.1±2.5 ℃ and relative humidity of 83.8±9.6 %.

A pair of soil chambers were placed on bare soil ~5 m behind the MAQS observatory and a CAPS (Cavity Attenuated Phase Shift) NO_x analyser (Teledyne API Model N500) was positioned in the ground floor cabin of the observatory to sample outlet air from one chamber at a time. An external pump was used to pull the air from the chamber to the main observatory. A bypass line was connected to the NO_x analyser and a filter was fitted to remove water vapour, ozone and volatile hydrocarbons from the sampled air. The air was drawn continuously from the sample chamber during both of the campaigns, aside from brief periods when the reference chamber was sampled. Due to Covid-19 travel restrictions, reference chamber datasets were collected at the start (15th – 18th June), around the mid-point (1st – 6th July), and on the last day (29th – 30th July) of the summer campaign (see Fig. 2.S2 for a calendar of sampling periods). During the winter campaign, reference chamber concentrations were continuously measured at the start (21st – 24th January) and mid-point (16th – 18th February), with additional sampling for 20 minutes per hour during the daytime (09:00 ~ 16:00 local time) every 2-3 days. The winter sampling schedule is shown in Fig. 2.S3. The soil chamber was removed for the rest when the reference chamber was connected to the NO_x analyser.

2.2.1.2 Remote forest observatory in Australia

The COALA-2020 field campaign took place from January-March 2020 at Cataract Scout Park in the coastal forest region of SE Australia (34°14’44” S, 150°49’26” E; see Simmons et al. (2021) and references therein). The COALA-2020 observatory was located in an area of open dry sclerophyll forest dominated by *Eucalyptus* trees (Fig. 2.1b). The chambers were installed under a *Eucalyptus haemastoma,* which was being used for periodic leaf and branch enclosure measurements, in an area of thin sandy soil

approximately 100 m west and downhill from the main observatory. Soil NO measurements occurred from 24th February to 23rd March, during the latter part of the COALA-2020 campaign after an extreme rain event had ended a prolonged drought and extinguished the widespread “Black Summer fires” (Simmons et al., 2021; Mouat et al., 2022). During the sampling period, the average air temperature was 18.9±4.1 °C, higher than either OSCA campaign but, at 76.0±18.0 %, the relative humidity was similar to that observed during OSCA Summer.

Two pairs of soil collar arrays, each with and without litter on the soil surface (hereafter WL and NL, respectively), were prepared on either side of the *Eucalyptus haemastoma* and the chambers rotated between the two pairs daily, so that measurements over NL or WL were made on alternate days, with one exception (Fig. 2.S4). The reference chamber was placed on the spare collar at each sampling location (see Fig. 2.S4 for detailed measurement dates). Soil emissions at the COALA-2020 site were measured with two chemiluminescence NO_x analysers (Thermo Fisher Scientific Inc. Model 42i), which were set-up in a gazebo ~10 m from the soil collars. They were used to retrieve NO_x concentrations from the sample and reference chambers simultaneously.

At both sites, sampling lines were enclosed in opaque tubing to reduce photolysis and the short line length (< 11-m) and small inner diameter (3 mm) reduced residence time to minimise loss or production of NO_x inside the lines (Butterbach-Bahl et al., 1997). All analysers were calibrated at the start and end of each measurement campaign (OSCA winter and COALA-2020), or in the middle and at the end of the campaign (OSCA summer).

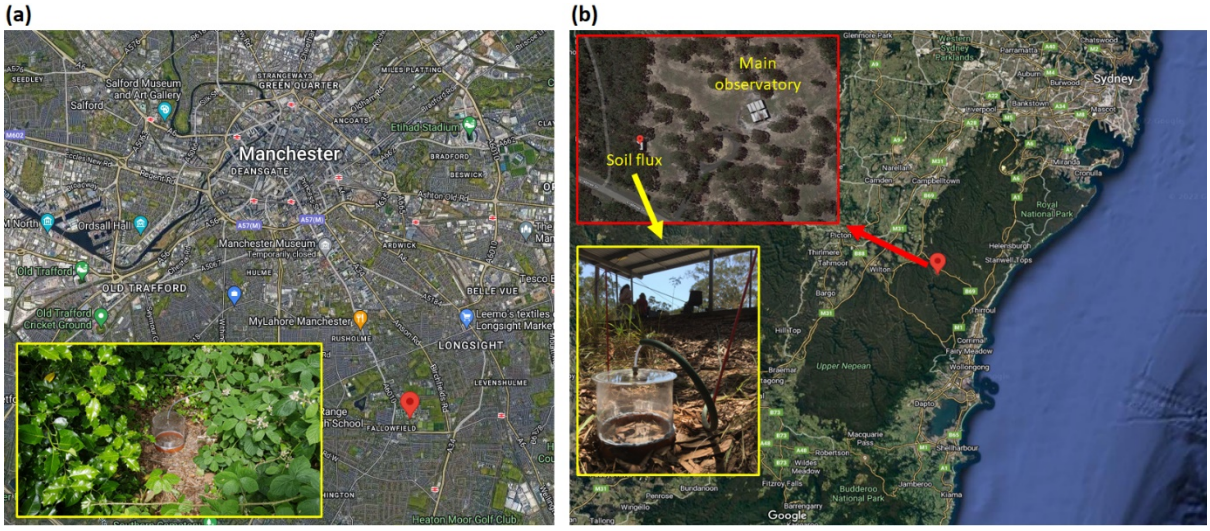

Fig. 2.1. Satellite images (©Google) of the locations of the OSCA (a) and COALA-2020 (b) measurement campaigns. The inset images in the yellow boxes show the installed sample chambers. At the OSCA site, the sample chambers were located at 5-m distance from the main observatory; the inset in the red box in (b) shows the location of the sample chambers relative to the COALA main observatory (~100 m distance).

2.2.2 Dynamic soil chambers

Soil emissions at both sites were determined by sampling concentrations of NO_x from the headspace of Lancaster University Dynamic Soil Chambers (LU-DySCs). The LU-DySCs are a pair of transparent acrylic chambers (Fig. 2.2), which are placed and sealed onto previously installed soil collars. Each chamber consists of a cylindrical tube (200 mm diameter and 150 mm height), with four inlet holes located 20 mm above the base of the chamber, and an outlet port comprising a quarter (¼) inch union fitting installed in the centre of the lid, to which gas analysers are connected. The two chambers differ only in the construction of their bases. The base of one chamber (hereafter ‘sample chamber’; Fig. 2.2a) is open to allow emissions from the soil to enter the chamber. By contrast, the base of the second chamber (hereafter reference chamber; Fig. 2.2b) is sealed with an acrylic disc isolating the chamber headspace from the soil. The sample chamber thus contains a mixture of soil emissions from the soil collar and ambient air drawn through the inlet holes, whereas the reference chamber contains only ambient air. Hence, the difference between gas concentrations in the sample and reference chambers

represents emissions from the soil. It should be noted that the LU-DySCs are suitable for sampling any target species, depending solely on the analyser connected to the outlet port. Although NO, NO_2 and NO_x were sampled during all three campaigns, we focus our analyses and discussions on NO, as this is the primary compound emitted and taken up by soil organisms, and the component of NO_x that initiates the photochemistry leading to secondary air pollutant production.

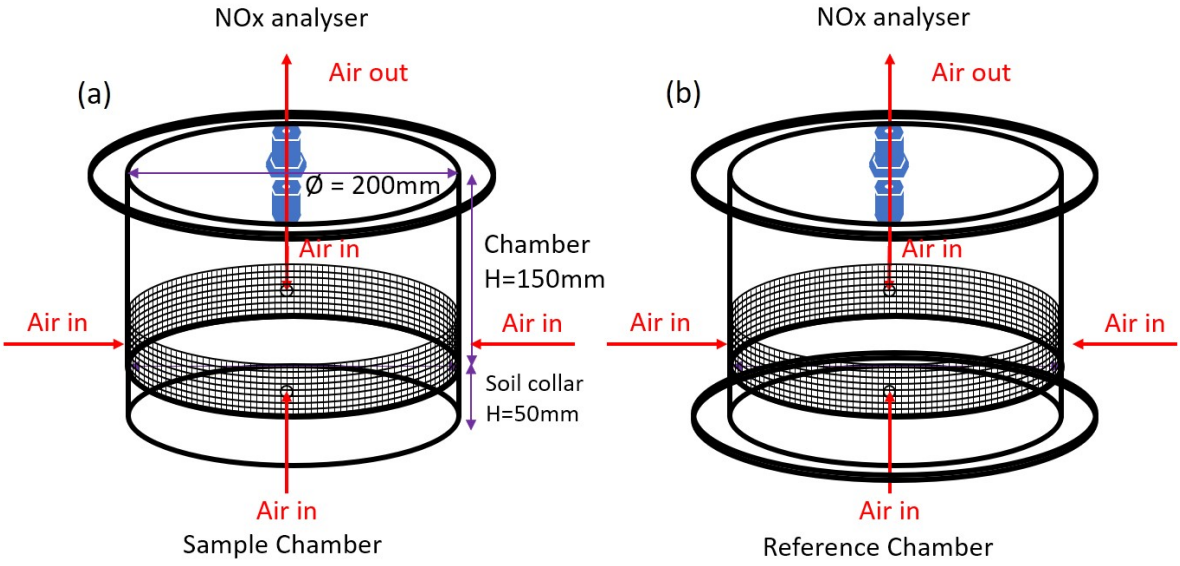

Fig. 2.2. Diagram of the Lancaster University Dynamic Soil Chambers (LU-DySCs) used here for measuring nitrogen oxide (NO_x) emissions from the soil. The sample chamber (a) has an open base for ingress of emissions from the soil collar, while the reference chamber (b) has a closed base to exclude soil emissions and therefore samples only the ambient air drawn through the inlet holes (denoted "Air in"). Air is drawn from the chambers into the NO_x analyser via the outlet port in the centre of the lid of each chamber (shown in blue; denoted "Air out"). "H" is the height of the chamber headspace.

2.2.3 Soil sampling and laboratory analysis

Soil moisture (volumetric, %) and temperature were recorded periodically during the OSCA Winter and COALA-2020 campaigns. In addition, bulk soil samples were collected from the sample chamber locations after each field campaign using a soil core sampling kit consisting of plastic tubes ~55 mm diameter and ~120 mm height. A total of 3 replicates of soil were sampled from the soil next to the sample chamber locations

in Manchester and from between the pairs of soil collars in Australia. The soil samples were immediately bagged and transferred to Lancaster Environment Centre, where they were placed in cold storage at ~5 ℃ until the elemental analyses could be run.

During the OSCA Winter campaign period, soil moisture and soil temperature were measured at the changeover times between sample and reference chamber sampling (indicated in the sampling schedule shown in Fig. 2.S2). Soil moisture and soil temperature were measured using portable devices (an ML3 ThetaKit from Delta-T devices and a Jumbo-Display Dial Thermometer from Traceable®, respectively). The probes were installed in the surface sub-layer, at depths of ~60 mm (moisture) and ~130 mm (temperature) during chamber changeover. Following a 5-min stabilisation period, soil moisture and temperature were manually recorded. The recorded values are presented in Table. 3.S1.

Soil moisture and temperature at the COALA-2020 site were measured inside the soil collar used for sampling at the end of the measurement period at each of the two pairs of collars (~12:00 local time) 4-5 times per week. Soil moisture was measured with a MPM-160-B (ICT international Armidale NSW) probe at a depth of 60 mm. Soil temperature was also recorded at a depth of 60 mm with a Digitech Probe Temperature meter model QM7217 which has a resolution of 0.1 ˚C and an accuracy of 1.5%. Measurement dates are listed in Table. 3.S2, which also shows the manually recorded soil temperature and moisture. We note that the periodic measurements of soil water content preclude the identification of NO pulses as a result of wet-dry cycles.

Three replicates of each soil sample were randomly subsampled from the bulk soil samples. The replicates were oven-dried at 65 ℃ for 24 hours and ball-milled in preparation for carbon (C) and nitrogen (N) elemental analysis. 20 mg of each of the grounded soil samples was used for the analysis of the total soil C and N content by combustion oxidation (Vario EL III, Elementar Analysensysteme GmbH, Germany; Sayer et al., 2021; Matejovic, I, 1997). Dry combustion elemental soil analysis was also conducted independently by University of Sydney on three soil cores, taken using the same procedures, from three locations around the *Eucalyptus haemastoma* before the start of COALA-2020 soil chamber sampling. The three replicates from each location were used for combustion oxidation analysis by Elementar VarioMACRO Cube

(Elementar Australia Pty Ltd, Sydney NSW) of C and N content. We use their findings from the first pair of soil collars as a validation of our estimates.

2.2.4 Calculations and statistical analysis

Soil NO emission rates at the COALA-2020 site were calculated from the difference in NO concentration between the sample and reference chambers using the following equation:

$$f_{gas} = f_{NO} = \frac{(C_{Samp} - C_{Ref}) \cdot Q \cdot P}{R \cdot T \cdot A_{soil}} \cdot \frac{1}{60} \quad \text{Eq. 2.1}$$

where f_{gas} is the soil emission rate of the target gas-phase species (here NO; f_{NO}) in nmol·m^{-2}·s^{-1}, and C_{Samp} and C_{Ref} represent its mixing ratio (ppb) in the sample and reference chamber, respectively, as measured by the NO_x analyser. Q is the flow rate of air drawn through the analyser from the chamber; set to 0.7x10^{-3} m^3·min^{-1} (0.6 – 0.8 x10^{-3} m^3·min^{-1}) during COALA-2020 and 1.0x10^{-3} m^3·min^{-1} (±10%) during both OSCA Summer and Winter campaigns. A_{soil} is the soil surface area (m^2) enclosed by the soil collar, which here is equal to the base of the LU-DySC. P and T are the air pressure (Pa) and air temperature (K) observed at the main observatory (at 4.5 m height above ground level during COALA-2020, and 6.5-7.5 m height during OSCA). R is the ideal gas constant (8.314 m^3·Pa·mol^{-1}·K^{-1}). Thus, f_{NO} was calculated at a 1-minute resolution and then averaged over each 24h period for analysis. As sample and reference NO concentrations at the OSCA site were not measured simultaneously, we only present data for NO mixing ratios.

We used vapour pressure deficit (VPD) as a proxy for biogenic activity within the wider soil-plant system because it is regarded as a measure of the “drying power” of air, and plays an important part in determining the relative rates of growth and transpiration in plants (Monteith and Unsworth, 1990). VPD is calculated as the difference between the saturation and ambient vapour pressure and is therefore dependent on the temperature and relative humidity of the air:

$$VPD = SVP \times \frac{100 - RH}{100} \quad \text{Eq. 2.2}$$

$$SVP = 610.7 \times 10^{7.5T/(2373+T)} \quad \text{Eq. 2.3}$$

where *SVP* (Pa) represents saturation vapour pressure, *RH* is the relative humidity (%) and *T* the temperature (°C) of the air. We used meteorological data recorded at the main observatories to estimate the VPD at 1-minute intervals during the measurement periods at both sites.

NO concentrations, air temperature and air pressure were all recorded as 1-minute averages during all three measurement campaigns, and used to calculate f_{NO} (at the COALA site) and VPD at the same time resolution. All variables were then transformed from the frequency of measurements to produce average hourly diurnal profiles for each of the three campaigns. To determine the relationships between soil NO concentrations and VPD or solar radiation (OSCA Summer and Winter) and f_{NO} and VPD or photosynthetically active radiation (*PAR*, COALA-2020) we used Pearson's correlations.

Differences in soil NO concentrations or fluxes and micro-meteorology were determined between OSCA Summer and Winter campaigns and COALA NL and WL measurements using non-parametric Mann-Whitney U-tests.

Statistical analyses and generation of figures were performed in R version 4.0.5 (R Core Team 2021). Differences were assumed to be significant for $p<0.05$. Although the low spatial replication of measurements at both sites precludes a full site-level quantification or comparison of NO concentrations or fluxes, we use our data to evaluate and discuss how diurnal patterns can help reveal hitherto ignored sources and processes of NO emissions.

2.3 Results and Discussion

2.3.1 OSCA Summer

During the OSCA Summer campaign in the UK, the average NO mixing ratio in the sample chamber was higher than that observed in the reference chamber, at 1.76±0.92 ppb and 0.79±0.85 ppb respectively (Fig. 2.3a). Average ambient atmospheric NO mixing ratios, measured at the main observatory at 6.5-m height and 5-m (hereafter, ambient) to the north of the sample chamber, were very similar to the reference at 0.72±1.33 ppb (sample period = 0.73±1.38 ppb, reference period = 0.67±1.13 ppb). The standard deviations in concentration were around one-third lower in either chamber than in the ambient air. This difference in variability likely reflects the highly localised nature of the different emission sources, with ambient levels most affected by traffic emissions, which fluctuate widely over short distances and timescales (AQEG, 2004), and chamber concentrations are likely to be moderated by the relatively slower variations in soil emissions.

Ambient NO concentrations in both sample and reference periods (Fig. 2.3a) showed clear and similar diel patterns (significance p-value = 0.85, correlation $R^2 = 0.87$ with $p < 0.05$), increasing rapidly from 04:00 to a maximum at 08:00 (2.10 & 1.65 ppb, respectively), corresponding to the peak of morning commuting traffic (AQEG, 2004). NO levels in the ambient air then decreased continuously until 22:00, reaching a minimum of 0.03 ppb. NO remained low, <0.1 ppb, between 21:00 and 04:00. The pronounced peak during morning rush hour and near-zero nighttime NO concentrations are characteristic of anthropogenic influences and are often observed in urban settings (e.g. Brune et al., 2016).

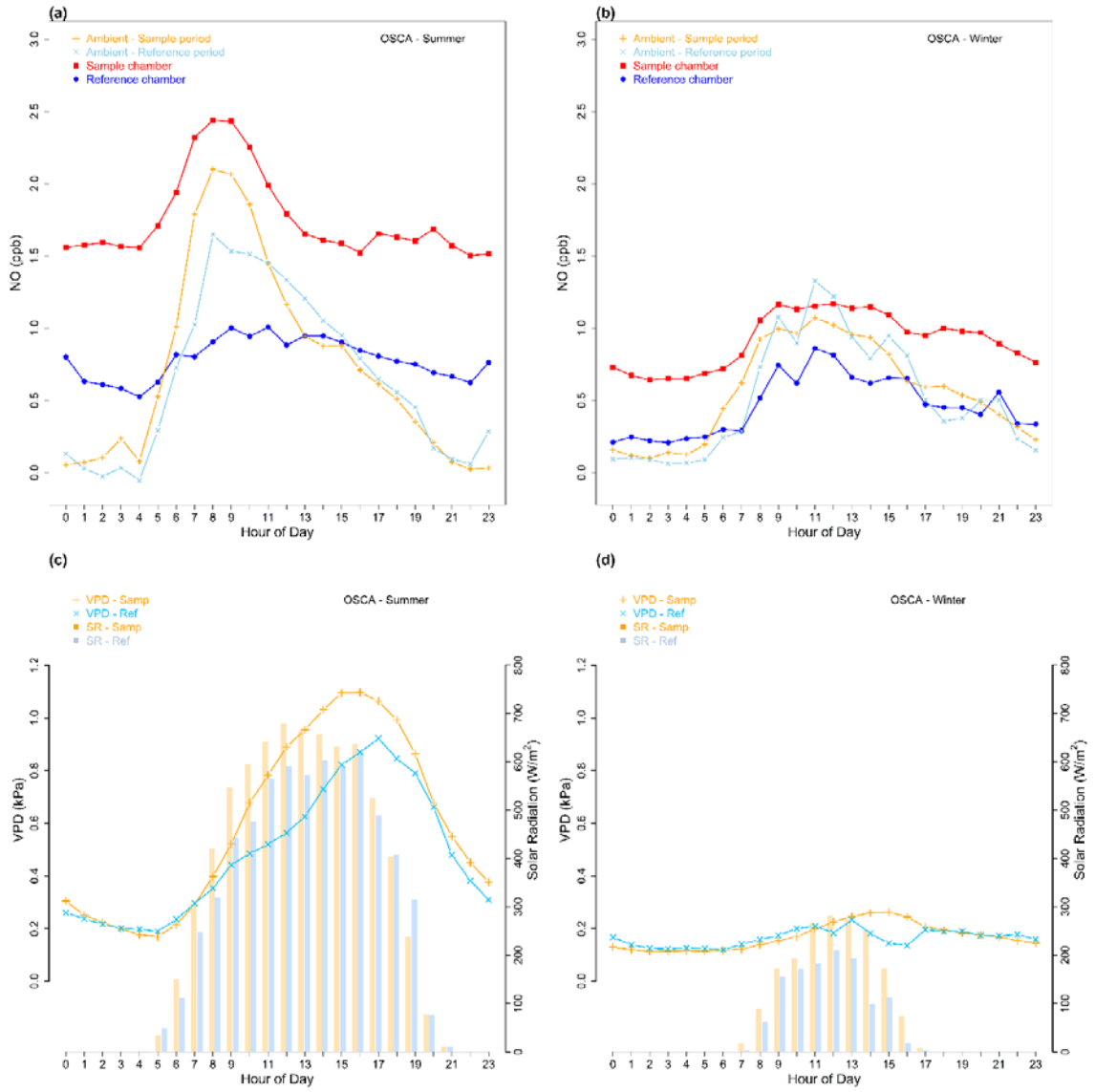

Fig. 2.3. Diel patterns of the observations in summer campaign (left, a & c) and in winter campaign (right, b & d). NO mixing ratios (ppb) in summer (a) and winter (b) campaign; red with square dotted lines (■) represent sample chamber measurements, the blue with closed circle lines (●) indicate reference chambers. Orange with cross-mark (+) and light blue with x-mark (×) lines display the ambient NO mixing ratio observed at the main observatory, each data split into the measurement period in accordance with sample (orange) & reference (light blue) measurements. Panel (c) and (d) illustrate vapour pressure deficit (VPD) using cross-mark and x-mark lines, and the bars represent solar radiation (SR) observed at the main observatory. Orange lines and bar plots remarks sample chamber measurement period, light blue lines bar plots are observed in reference measurement periods. All data has recorded in 1 minute resolution and averaged in 1 hour resolution in the figures. Hour of day refers to local time (LT).

The diel patterns of NO mixing ratios differed significantly between the sample and the reference chambers (p <0.05). However, although sample and reference chambers were measured during distinct time periods, NO concentrations showed quite consistent diel patterns. NO concentrations in both chambers also increased from 04:00 local time, immediately following sunrise, and peaked at ~08:00 (Fig. 2.3a). Sample chamber NO then decreased sharply from a maximum of 2.44 to 1.65 ppb at 13:00, thereafter remaining between 1.50 to 1.68 ppb throughout the afternoon and night until the following early morning. By contrast, the NO mixing ratio in the reference chamber continued to rise through the morning, reaching a maximum of 1.00 ppb between 09:00 and 11:00, which was a slightly later peak than seen in either the sample chamber or ambient air. It is also worth noting that NO concentrations in the reference chamber were lower than ambient from 06:00 to 13:00, possibly because local traffic emissions affected the ambient observations, but the tree canopy moderated NO concentrations close to the soil surface (e.g., Seok et al., 2013). On the other hand, reference chamber NO concentrations were higher than ambient during the rest of the day, likely due to emissions from the surrounding soil accumulating and mixing with the ambient air near the ground (Geyer & Stutz, 2004). These differences in peak timing and duration also perhaps suggests that reference chamber NO concentrations were less influenced by fluctuating emission sources, i.e. traffic or direct soil emissions, and instead reflect a well-mixed stable atmosphere near the ground.

Sample chamber NO concentrations were consistently higher than ambient and reference chamber concentrations, indicating that the soil is a key emission source at this suburban site. The diel pattern of the sample chamber NO concentration was followed VPD during the daylight hours (07:00~20:00) more closely than the ambient concentration (Fig. 2.3c). However, both sample chamber and the ambient NO mixing ratios declined with increasing VPD (R^2 = 0.88 and 0.72, respectively, both p< 0.05), but were not related to solar radiation (both R^2 <0.06, p> 0.4). The stronger relationship between NO concentrations and VPD in the sample chamber compared to the ambient air suggests that sample chamber NO concentrations are highly influenced by biological activities, including plants and soil microbes (Mcdowell et al., 2004; Jauregui et al., 2018). The slightly weaker relationship between ambient air NO concentrations and VPD reflects the influence of anthropogenic NO sources, as well as biological sources.

By contrast, the reference chamber NO mixing ratio was not related to either VPD (R^2 = 0.18, p> 0.1) or solar radiation (R^2 = 0.23, p> 0.05), even though ambient NO concentrations during the reference measurement period were clearly related to VPD (R^2 = 0.62, p< 0.05).

The diel variation range of NO concentrations also highlights the importance of soil NO emissions. Sample and reference NO concentration ranges were 0.94 and 0.53 ppb, respectively. The greater diel variation in the sample chamber compared to the reference chamber likely indicates the influence of soil NO emissions. The difference between the hourly maximum and minimum ambient NO concentrations were 2.08 and 1.70 ppb during the sample and the reference period, respectively. These large diel variations in ambient NO mixing ratios are characteristic of anthropogenic impacts (AQEG, 2004). Importantly, during the night, the ambient NO mixing ratio dropped to near zero in both measurement periods, whereas sample and the reference chamber NO mixing ratios remained above 1.5 and 0.5 ppb, respectively. These observations suggests that NO is emitted from the soil not only in the daytime, but also at night.

2.3.2 OSCA Winter

During the OSCA Winter campaign, NO mixing ratios were again highest in the sample chamber (Fig. 2.3b), although the average of 0.91±0.37 ppb was only around half that observed during the summer. Average NO levels in the reference chamber and ambient air were almost identical, at 0.48±0.37 in the reference chamber, and 0.54±0.84 or 0.55±0.70 ppb in the ambient air during the sample and the reference period, respectively, which was around two-thirds of the concentrations observed during the summer. Variability in NO concentrations was much lower than in the summer, and the highest fluctuations were again observed in ambient NO concentrations.

Ambient NO concentrations in urban environments are usually reported to be higher in winter than in summer because of increased fossil fuel use for heating and meteorological conditions that promote NO_x accumulation below 1 km height (e.g. AQEG, 2004). However, we observed the opposite during the OSCA campaigns. The lower NO concentrations at this site during winter are likely due to the meteorological conditions reducing activity and hence soil NO fluxes, in conjunction with increased

atmospheric losses. Data from MAQS monitoring reported more rainy days in the winter with near double the duration of precipitation (206 hours compared to 112 hours in the summer), which would result in greater removal of NO from the ambient atmosphere through wet deposition to plant and soil surfaces (Luria et al., 1990). Higher wind speeds in winter (2.03±1.27 m s^{-1}) than in summer (0.98±0.75 m s^{-1}) would lead to faster dispersion of local emissions, again reducing ambient NO concentrations, although this effect would probably be small near the ground surface where the chambers were sited. However, given that the study site is located in a large green space, biogenic emissions would be expected to have a stronger influence than anthropogenic sources, unlike many urban observations (e.g. Sillman et al., 1999; Im et al., 2013). Reduced biological activities during the winter due to lower temperatures would therefore result in lower soil emissions and hence NO concentrations near the soil surface (Medinets et al., 2019).

Winter ambient NO concentrations followed similar diel patterns (R^2 = 0.88 with p <0.05) to summer, but with much smaller values and ranges (Fig. 2.3b). Ambient NO concentrations in both sample and reference chamber periods increased rapidly from 04:00 to 09:00, reaching a maximum (1.07 and 1.33 ppb, respectively) at 11:00. Winter night-time minimum ambient NO mixing ratios were below 0.15 ppb between 01:00 to 04:00. However, the variability in ambient winter NO concentrations was much reduced compared to the summer with a range of only 0.97 and 1.26 ppb in sample and reference period. The lower daytime NO concentrations in winter might be related to meteorological conditions, i.e. colder air temperatures and shorter daylight hours resulted in less consumption of NO through photochemical reaction during the daytime or titration at night (Sillman, 1999). By contrast, higher nighttime concentrations could reflect the suitability of conditions for accumulation near the ground at night due to the stability of the nighttime boundary layer (Doran et al., 2003) and longer nighttime duration.

There was a clear and significant difference (p<0.05) in diel patterns in sample chamber NO mixing ratios between the OSCA Summer and Winter campaigns most likely due to the significant (p<0.05) seasonal differences in meteorological conditions (air temperature, relative humidity, solar radiation, and VPD). The early morning rise in concentrations in both the sample and reference chambers, from 07:00 to 09:00 in

winter, was later than during the summer due to the reduced day length at this latitude. In the reference chamber, the pattern of daytime NO concentrations was otherwise similar to that observed in the summer, with peak concentrations at 09:00 and 11:00. However, winter nighttime NO concentrations in the reference chamber differed from summer, with mixing ratios well above zero and which increased slightly from 0.21 to 0.29 ppb between 00:00 to 07:00 (Fig. 2.3b). In the sample chamber, the early morning peak in NO concentrations observed during the summer was absent in the winter, but high levels of NO (~1.15 ppb) were instead observed in the sample chamber through the morning and midday period 09:00-14:00. The differences in the patterns of NO concentrations between sample chambers and ambient air again suggests the difference in NO sources, whereby ambient concentrations that are largely anthropogenically influenced remain the same through the seasons (Carslaw, 2005), contrasting with the clear seasonality of sample chamber NO concentrations which suggests a biogenic origin (Fumagalli et al., 2016).

Winter VPD and solar radiation are far lower than in summer and therefore smaller diel variations in NO were observed in the winter period (Fig. 2.3d). Sample chamber NO diurnal patterns under the daylight hours (08:00~17:00) were not related to VPD (R^2 = 0.01, p <0.05) but increased with solar radiation (R^2 = 0.72 with p <0.05). By contrast, reference chamber concentrations increased weakly with both VPD (R^2 = 0.10 with p >0.05) and solar radiation (R^2 = 0.38 with p >0.05). In addition, the ambient NO concentrations throughout the day increased with solar radiation (R^2 = 0.51 with p <0.05 and R^2 = 0.53 with p <0.05 during sample and reference periods, respectively) but were not related to VPD (both R^2 = 0.16 with p >0.05). The lack of a strong relationship between NO concentrations and VPD in winter suggests that the influence of the biological activities is very small. However, the stronger relationship with solar radiation implies that plant activity stimulated by sunlight can still influence NO concentrations at ground level even under low temperatures and wet conditions.

Total soil nitrogen and carbon contents were almost identical in summer and winter (nitrogen: 0.47±0.13% and 0.50±0.12%; carbon: 8.41±1.92% and 9.12±1.93% in summer and winter, respectively). The resulting low C/N ratio at the site (18.09±1.30 in summer and 18.27±0.70 in winter) is likely to be conducive to nitrification and

denitrification processes (Huang et al., 2004; Klemedtsson et al., 2005; Toma and Hatano, 2007), and therefore favour NO production in soils.

2.3.3 Differences in potential soil NO drivers between summer and winter

Lower VPD and solar radiation in winter likely play a role in limiting biological activities in both non-dormant plant species and soil organisms, which would explain why winter NO mixing ratios in the sample chamber were lower than those in summer and less variable through the day. Wintertime VPD was generally lower and less variable than in summer (0.16 kPa *vs.* 0.57 kPa; Fig. 2.3b & 2.3d) and solar radiation was substantially reduced in both magnitude and duration. Hence, VPD and solar radiation intensity were likely too low for the vegetation or soil micro-organisms to activate soil NO production. However, the increase in sample chamber NO concentrations in winter with solar radiation could indicate that biological activity was stimulated by sunlight (plants) or the increase in temperature (plants and soil organisms). Nonetheless, the consistently higher NO concentrations in the sample chamber, compared to the reference chamber, during both summer and winter campaigns, indicates that NO is emitted from the soil throughout the day, and depends on the soil moisture and temperature.

The summer period was not only warmer and drier than the winter with an average air temperature of 17 *vs.* 7 °C and relative humidity of 75 *vs.* ≲85 %. Daylength, recorded at the main observatory, was considerably longer in the summer than the winter at this latitude with 16.5 hours of daylight in July *vs.* 9.5 in February. Solar radiation was also more intense in summer, stimulating photosynthesis and plant growth. Hourly average incoming radiation peaked at ~658.2 Wm^{-2} in summer and ~270.8 Wm^{-2} in winter. More species are active during the summer and conditions are far more suitable for biological activity in vegetation, roots and soil organisms (Campbell et al., 2019; Jakoby et al., 2020), resulting in increased production of NO via nitrification and denitrification, and hence higher emission rates and stronger diurnal patterns in summer. The winter period, with near-dormant organisms, could therefore be considered as a baseline of biological activities and soil emissions for a site at this latitude.

Furthermore, although the total accumulated precipitation at the OSCA site was slightly more during the summer campaign (155.9 mm against 148.7 mm in winter), the duration was roughly twice as long in the winter and cloud cover was greater (6.42 *vs* 5.67 oktas in summer). A prolonged wet period ahead of the winter campaign, coupled with cool damp conditions during the observation period, kept soil moisture high throughout OSCA Winter. In-situ soil moisture monitoring during the winter showed soils were saturated for most of the observation period, with a soil water content of 52.5±7.6 % and range of 39.4-66.1 % (see Table. S1), which could have supressed biological activity (Venterea et al., 2005). Despite the high precipitation during the summer campaign, higher air temperatures and lower relative humidity would have resulted in rapid evaporation from and drying of the soil surface layers. These key seasonal differences in meteorological and surface conditions would have affected many soil processes to produce the diel patterns of soil NO emissions that are also characteristic of soil respiration rates observed during late summer and winter at other locations (Makita et al., 2018).

2.3.4 COALA-2020

In contrast to either OSCA campaign, the average ambient NO mixing ratio measured at the main observatory (4.7 m height and 100-m away from the soil collars) during the COALA-2020 campaign were much higher than the sample chamber, at 1.65±0.59 ppb (NL period = 1.63±0.62 ppb, WL period = 1.67±0.56 ppb, respectively) compared to 0.73±0.73 ppb in the NL collar (Fig. 2.4a) and 0.19±0.35 ppb in the WL collar (Fig. 2.4b). This is likely due to the distance of the sampling location from the main observatory (Fig. 2.1b) combined with changes in wind direction (Fig. 2.S5). In the reference chambers in both collars, the observed NO concentrations were below the lower detectable limit (<0.4 ppb) for a long period, and the mean concentrations during the campaign were 0.01±0.37 ppb in the NL collar and 0.08±0.19 ppb in the WL collar.

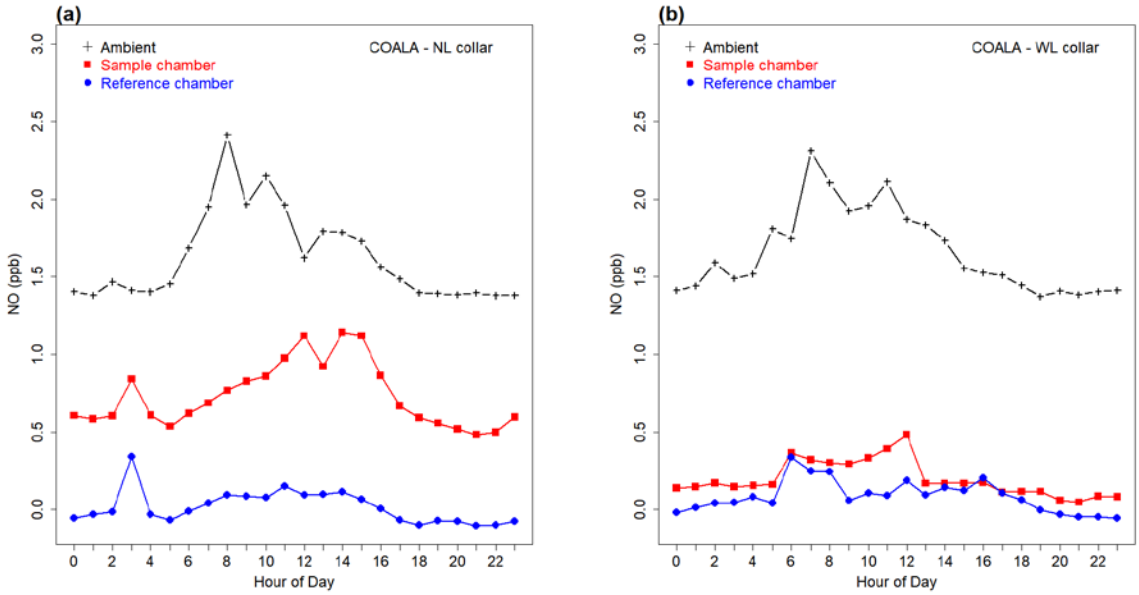

Fig. 2.4. Diel patterns of NO concentrations (ppb) at the main observatory, showing ambient air (black crosses), sample chamber (red squares), and reference chamber (blue circles) in soil collars without litter (NL) and with litter (WL) during the COALA-2020 campaign. Hour of day refers to local time.

Daytime ambient NO levels during the COALA-2020 campaign were higher and more variable than those measured in the soil chambers, increasing from ~1.5 ppb at 04:00 to a peak of 2.26 ppb around 08:00 (2.31 ppb at 07:00 during NL measurements, and 2.41 ppb at 08:00 during WL measurements). Ambient NO concentrations then followed a fluctuating but generally declining trend until 13:00 before decreasing steadily until

19:00. By contrast, night-time ambient NO mixing ratios were relatively low and stable from 18:00 to 01:00, at ~1.40 ppb, which was nearly an order of magnitude higher than at the OSCA site. Interestingly, the diel pattern of ambient NO levels was similar to those observed during the OSCA campaigns when the wind was blowing from the north-east (Fig. 2.S5b), which suggests a strong anthropogenic source in this direction. Potential anthropogenic sources of NO are most likely a combination of vehicle emissions from site staff and park visitors (north to north-east, ~1 km), a colliery ~2 km to the north (Simmons et al., 2021), a municipal waste management facility which is located ~25 km to the northwest (Ramirez-Gamboa et al., 2020), and the more moderate influence of urban pollution transported from the broader Sydney metropolitan area ~50 km northeast of the study site.

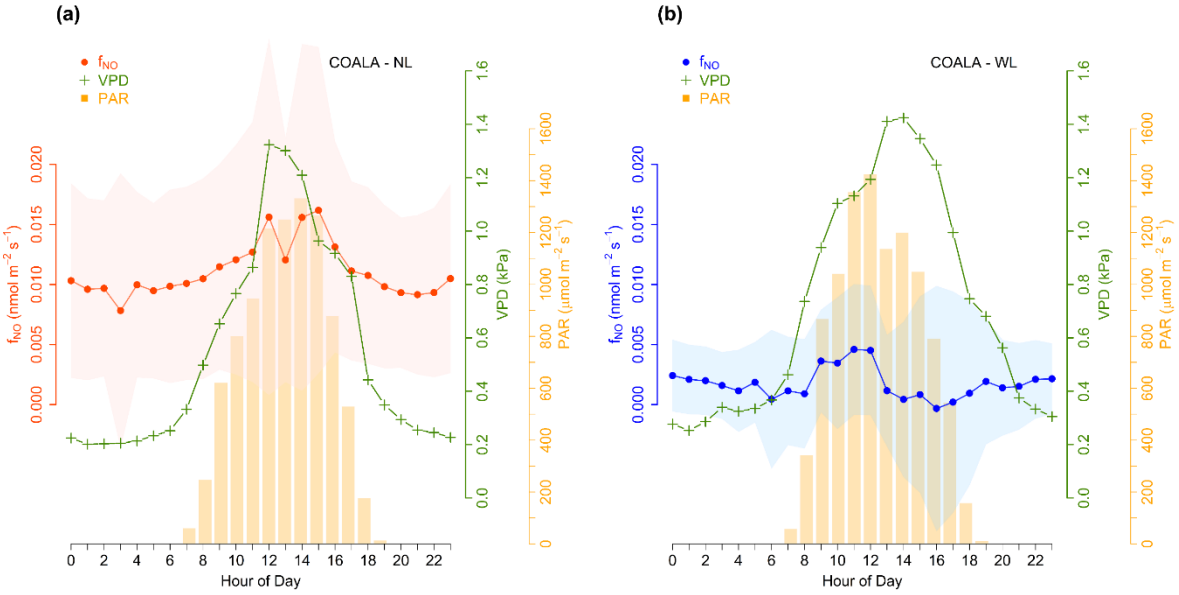

Fig. 2.5. Diurnal pattern of soil NO emissions (f_{NO}) during the COALA-2020 campaign in SE Australia, at (a) no litter collar (NL) and (b) with litter collar (WL). The red and blue lines illustrate the diel patterns of the soil NO flux of each collar and the shaded area indicates ±1σ above and below average f_{NO}. Green with (+) marked lines show the diel variations of the vapour pressure deficit (VPD), and the orange bars indicate the photosynthetically active radiation (PAR). Hour of day refers to local time.

The diel patterns of NO concentrations in both soil chambers during COALA-2020 (Fig. 2.4) differed markedly from the profiles observed during the OSCA campaigns

(Fig. 2.3). In the NL collar (Fig. 2.4a), the sample chamber NO mixing ratios were always higher than the reference. The soil chambers were measured simultaneously, so the difference between the sample and reference chambers strongly indicates that NO was continuously emitted from the soil. NO concentrations in both chambers increased slightly at 03:00, perhaps in response to the increase in ambient concentrations at 02:00. This spike in ambient NO is likely due to the reduced wind speed at 01:00 leading to local atmospheric stagnation and an accumulation of gas species at the surface (Geyer & Stutz, 2004; AQEG, 2004; Fig 2.S5b). The increment in the reference chamber around this time (0.35 ppb) was greater than in sample chamber (0.24 ppb), which indicates that the increase was due to external sources, rather than soil NO emissions. Sample chamber NO concentrations increased throughout the morning until 12:00, declined around 13:00, recovered between 14:00 and 15:00, to then decline constantly until 21:00 (Fig. 2.4a). Although the diel patterns of NO in the ambient air during NL measurements were very similar to ambient concentrations measured during the OSCA summer sampling period (R^2=0.88, p<0.05), the diel patterns of NO measured in the sample chambers differed significantly (p<0.05) between OSCA and COALA. Furthermore, sample chamber NO concentrations in the NL collar (Fig. 2.5a) increased strongly with VPD (R^2=0.59, p<0.05) and PAR (R^2=0.83, p<0.05) during daylight hours (i.e. when PAR>90, between 08:00~19:00), which is in contrast to the lack of a relationship between NO concentrations and solar radiation at the OSCA site in summer.

In the WL collar sample chamber and both NL and WL reference chambers, NO concentrations were close to zero (below the lower detectable limit, <0.4 ppb) throughout the day and showed weak diel patterns (Fig. 2.5). It is likely that near-surface NO in WL collars and reference chambers was rapidly removed by chemical reaction with biogenic volatile organic compounds (VOCs), which have much higher reactivity toward NO than anthropogenic VOCs (Atkinson, 2000; Atkinson and Arey, 2003). These VOCs most likely originated from the thick layers of litter on the soil surface at our sampling location (Ramirez-Gamboa et al., 2020) under *Eucalyptus haemastoma,* as *Eucalyptus* species generally contain high concentrations of VOCs (Vuong et al., 2015). Given that only the NL sample chambers showed strong diel patterns, we present estimated soil NO fluxes for the NL but not the WL sample chambers.

The average soil NO flux ($f_{NO;}$ Eq. 2.1) in the NL collar was 0.011±0.009 nmol·m^{-2}·s^{-1} and exhibited a clear diel pattern (Fig. 2.5a). As fluctuations in NO concentrations in the reference chamber were negligible, the diurnal pattern of f_{NO} tracked that of sample chamber NO concentrations, with higher fluxes during the daytime and a return to lower night-time values from around 17:00. There was a particularly marked increase from 08:00, with f_{NO} peaking at 0.016 nmol·m^{-2}·s^{-1} at 12:00. The sharp decline in f_{NO} at 13:00 (0.012 nmol·m^{-2}·s^{-1}) mirrored that observed in sample chamber concentrations. Overnight, from 17:00 to 08:00, emissions of NO were below average.

The soil NO flux at the COALA-2020 site was much lower than previously reported for sites in Europe (Schaufler et al., 2010), which could be partly due to differences in soil characteristics and vegetation. Importantly, soil nitrogen content at the COALA site was only 0.12±0.03 % and the C/N ratio was 30.4±3.1. Previous studies have reported that nitrous oxide (N_2O) emissions and emission efficiency decline with increasing soil C/N ratio (Huang et al., 2004; Toma and Hatano, 2007), as high soil carbon content apparently inhibits the nitrification and denitrification processes. Indeed, Klemedtsson et al. (2005) reported that N_2O fluxes were negligible at C/N levels >25. As NO is also a product of the nitrification and denitrification processes, NO emissions are also likely to be inhibited above this same threshold of C/N ratio. Hence, although soil and meteorological conditions appeared more conducive to soil NO emissions at the COALA site, the higher soil C/N ratio and lower nitrogen availability substantially reduced soil nitrification and denitrification and hence NO production, resulting in low fluxes from the Australian soils.

Soil NO flux in the NL collar generally tracked both VPD and PAR (Fig. 2.5a). The first peak in NO emission rates was at 12:00, coinciding with the highest maximum VPD (1.32 kPa) and a dramatic increase in PAR (Fig. 2.5a). There was a substantial drop in NO flux around 13:00, but NO fluxes recovered thereafter to reach the maximum of 0.016 nmol·m^{-2}·s^{-1} at 15:00. From 16:00 onwards, soil NO emissions declined until ~21:00, which corresponded to a period of rapidly decreasing PAR and decline in VPD. Accordingly, f_{NO} increased significantly with both VPD and PAR but the relationship with PAR was stronger (R^2=0.71, p<0.05) than with VPD (R^2=0.51, p<0.05) during daylight hours (i.e. when PAR>90, between 08:00~19:00). The strong influence of VPD

and solar radiation on f_{NO} at COALA suggest that soil NO is of biological origin, such as plant and microbial activity.

While factors such as VPD directly affect soil activities, others such as sunlight stimulate or inhibit soil processes via their effect on air temperature, relative humidity, and the surrounding vegetation (McDowell et al., 2004). Although soil NO emissions were related to PAR and VPD, very high VPD and solar radiation can limit biological activity as organisms attempt to preserve water, thus reducing biochemical sources of NO (Ocheltree et al., 2014). The rapid decrease in soil NO flux at 13:00 is therefore likely due to a reduction in biological activity in response to environmental conditions (Velasco et al., 2013; Rubio & Detto, 2017). Furthermore, plant roots exude organic carbon and nitrogen to the soil, which provides fuel and activate soil micro-organisms, stimulating the denitrification process in the soil (Blackmer et al., 1982). This effect dominates in the morning, leading to the observed increase in emissions (Makita et al., 2018). However, photosynthesis increases with solar radiation during the middle of the day, which increases the amount of nitrogen required by the plant for carbon assimilation, resulting in greater root uptake of nitrogen from the soil (Denef et al., 2007). This would limit nitrogen availability for soil organisms, leading to an instant decrease in NO emission rates at 13:00. As photosynthesis declines later in the day, less nitrogen is taken up from the soil by the plant and more is thus available to soil organisms, resulting in the increase in soil NO emissions after ~16:00 (Fig. 2.4a). The soil NO emission rates with a maximum around midday are similar to diurnal patterns of soil respiration observed in wet seasons elsewhere (Adachi et al., 2009), providing further evidence that soil NO emissions are driven by biological activity.

Soil moisture and soil temperature are important driving factors of soil NO emissions (Kesik et al., 2006; Venterea et al., 2005; Pilegaard, 2013; Medinets et al., 2015). The measurements at the COALA site were made after heavy rain events in mid-January to early February 2020, which ended an extreme drought in 2019-2020 (Commonwealth of Australia, 2022). The extreme contrast of late summer meteorological conditions in SE Australia during the COALA measurements were therefore characteristic of a “wet season” climate. Nonetheless, soil moisture was only 21.99±7.98 % (range: 12.4~33.9%; Fig. 2.6a) and soil NO flux decreased with increasing soil moisture (R^2=0.48, p<0.05). Above ~20% soil moisture, soil NO flux remained low (≤0.01

nmol·m^{-2}·s^{-1}) and our regression analysis suggests that the optimal volumetric soil water content for soil NO emissions at COALA site is ~10%. Although the optimal water content for NO fluxes depends on the soil type and different soil characteristics, our results are in line with previous research demonstrating higher soil NO fluxes at lower water-filled pore space (Schindlbacher et al., 2004; Schaufler et al., 2010; Pilegaard et al., 2013).

The average soil temperature at the COALA site was 19.55±1.02 ℃ and despite the relatively narrow range of 17.6-21.1 ℃ (Fig. 2.6b), soil NO flux increased linearly with increasing soil temperature (R^2=0.13, p>0.05). Although the number of the observation points are small, the correlation coefficient was similar to that reported in (R^2=0.18, p<0.0001). This temperature-dependency of soil NO fluxes is well-established, as temperature governs the activities of micro-organisms involved in nitrification and denitrification process (Skiba et al., 1992; Schindlbacher et al., 2004; Schaufler et al., 2010; Fumagalli et al., 2016; Medinets et al., 2016).

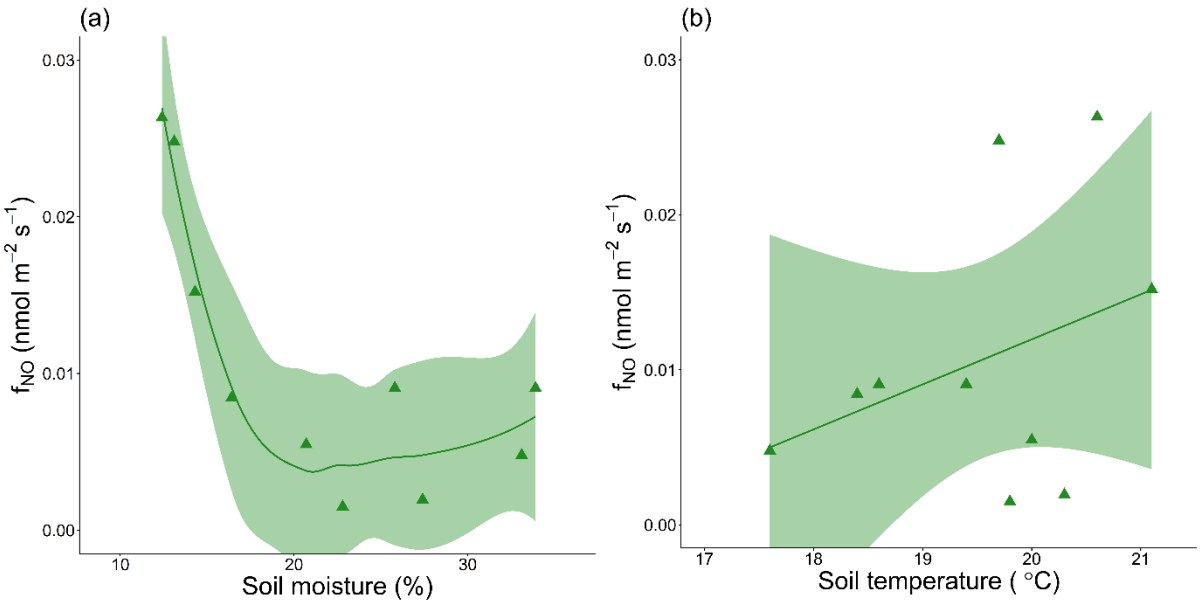

Fig. 2.6. The relationship between soil NO flux with soil moisture (a) and soil temperature (b) in collars without litter at the COALA site in Australia. Green triangles represent individual measurement values, solid lines show regressions of each relationship, using LOESS smoothing for the non-linear relationship in a). The green shaded areas denote 95% confidence intervals.

2.3.5 Contribution of the soil NO emission to the atmosphere

In 2020, total NO_x emissions in UK were estimated at 1851.65 tonnes/day with summertime soil NO emissions from urban green spaces accounting for just 2.28 tonnes/day (0.12%) of that (Ricardo Energy & Environment, 2022). At the location of the OSCA site, the UK National Atmospheric Emission Inventory (NAEI) estimated total NO_x emissions to be 25.75 kg/day with only 4.17 g/day from the natural sources. Although we cannot directly calculate soil NO fluxes at the OSCA site, due to the difference in measurement time periods for sample and reference chambers, we used the reference averages to estimate potential NO fluxes from the soil (Fig. 2.S6). Our estimates for the OSCA summer and winter campaigns suggest that soil NO emissions could be as high as 57.04 and 28.52 g/day, respectively, at this urban greenspace site. Although this is still only 0.22 and 0.11% of total NO_x emission rates, these estimates are 13.69 and 6.85 times higher than current estimates of natural NO_x sources, and soil NO emissions thus warrant further investigation. In New South Wales, Australia, total NO_x emissions in 2019-2020 were reported to be 439.39 tonnes/day (Australian Government Department of Climate Change, Energy, the Environment and Water, 2022). Our measurements of soil NO emissions at the COALA-2020 site suggest that forest soils could contribute as much as 5.81 tonnes/day, accounting for 1.32% of the total NO_x emissions for the region. While these contributions appear modest at both sites, natural NO emissions are expected to increase under climate change even as anthropogenic sources continue to fall. Our observations therefore indicate that future work should aim to understand the contribution of biogenic NO sources to the local atmosphere, and in particular its role in the formation of longer-lived secondary air pollutants.

2.4 Conclusions

Our study of diurnal patterns in soil NO concentrations and emissions at two contrasting locations reveals hitherto ignored sources and processes of NO emissions. At both sites, and during all three measurement campaigns, soil fluxes were always positive, even at night, indicating that soils act as a continuous source of NO. Concentrations and fluxes of NO from the soils exhibited a diurnal pattern very different from urban

anthropogenic NO emission sources but similar to patterns previously observed for soil respiration. This suggests that soil NO is biogenic in origin, resulting from active NO production due to soil microorganism activities. The low winter NO concentrations at the UK site are likely to represent a baseline of soil NO concentrations when microorganism activities are at a minimum. While biogenic NO emissions, including those from soils, are generally considered to have a small impact on atmospheric NO_x concentrations compared to anthropogenic NO emissions, we demonstrate here that they can become significant under the right conditions, and soil emissions are proportionally more important in more remote locations where anthropogenic influences are small. Nonetheless, from an air quality perspective, we found that hotter, drier summer weather led to substantially higher soil NO concentrations at the urban site in the UK, at a time of year when anthropogenic sources of NO tend to be at a minimum. We propose that biogenic sources of NO will gain in significance as anthropogenic emissions of NO decline. Although the low spatial replication of measurements at both sites precludes a full site-level quantification or comparison of NO concentrations or fluxes, our findings show that soil NO emissions are not negligible. Future work should focus on identifying the major drivers and characterising how soil NO emissions differ among environments and vegetation types.

Supplementary Material for Chapter 2

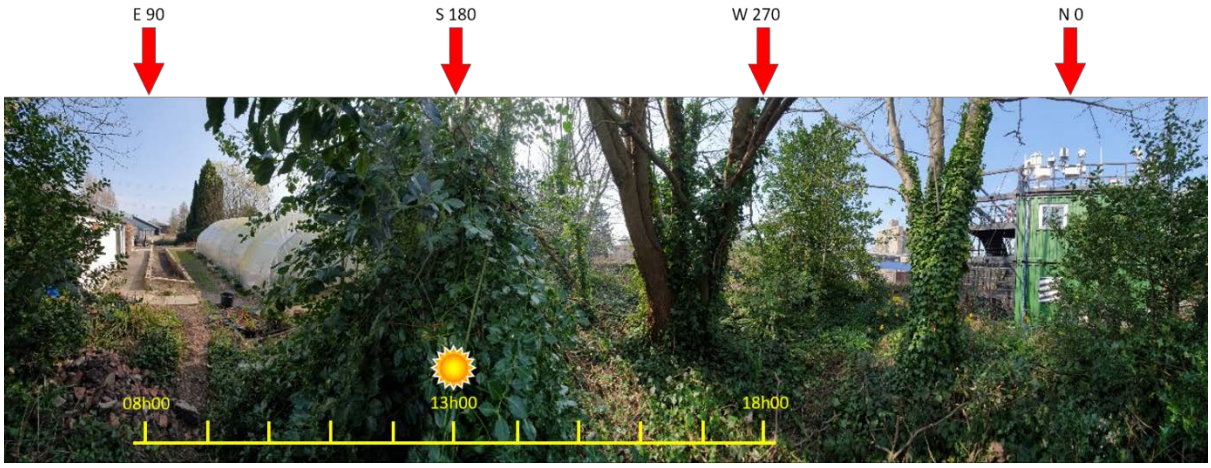

Fig. 2.S1. Panoramic photo of the surroundings of the soil chamber location at Manchester Air Quality Supersite in the UK during the OSCA Summer and Winter campaigns, showing compass directions (red arrows). The yellow scale bar at the bottom of the photo refers to the rough hour of day. The sun was located to the east during 08h00~09h00 (azimuth = 90°, altitude = 22~30°). The *Ilex aquifolium* blocked the direct sunlight (S 180) to the soil collar around the culmination time (13h00; azimuth = 180°, altitude = 55~60°).

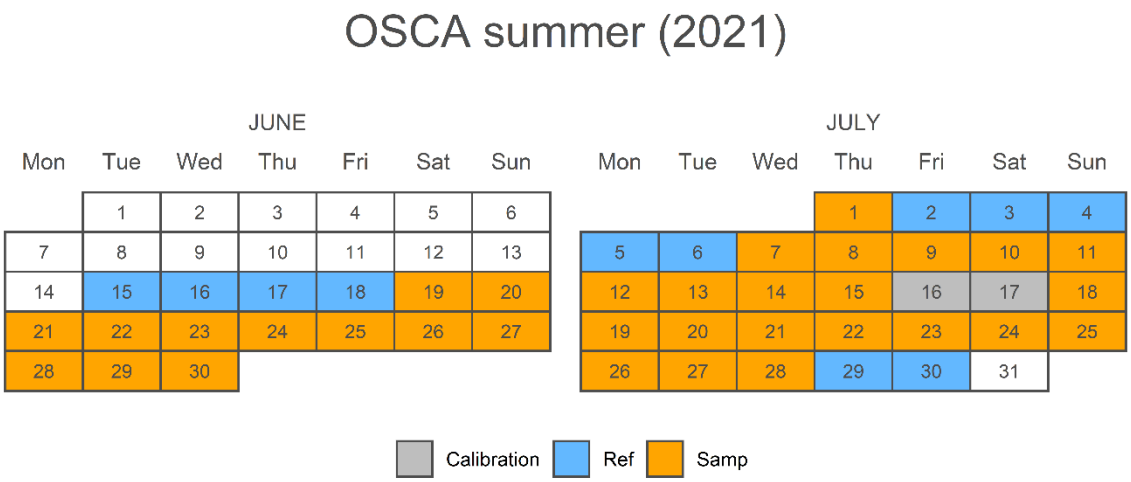

Fig. 2.S2. Calendar of observations during the OSCA Summer campaign in the UK. Orange denotes the periods when measurements were made from the sample chamber while light blue indicates the days sampling was carried out from the reference chamber (Jun-15 11:10 to Jun-18 16:05, Jul-01 17:16 to Jul-06 13:39, and Jul-29 12:35 to Jul-30 12:36). The grey shading shows

the days the NO_x analyser was off-line for calibration. No measurements were possible between Jun-29 14:32 to Jun-30 10:41, because of an unexpected loss of power at the site.

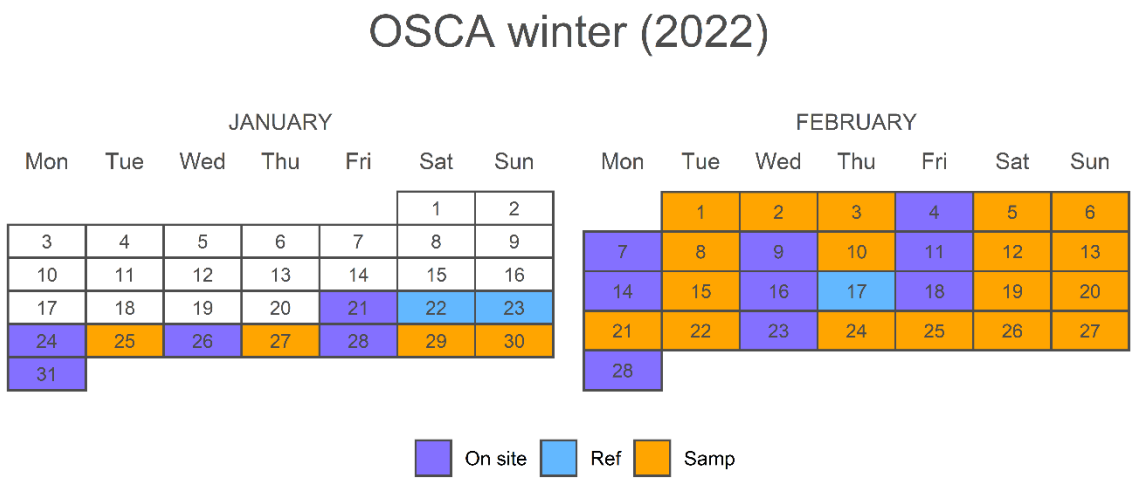

Fig. 2.S3. Calendar of observations during the OSCA Winter campaign in the UK. The reference chamber was continuously measured from Jan-21 15:20 to Jan-24 10:15, and Feb-16 15:15 to Feb-18 09:25. Purple shading indicates on-site days, when sampling alternated between measuring concentrations from the sample chamber for 40 minutes, and the reference chamber for 20 minutes each hour. In addition to NO concentration measurements, soil moisture and temperature were also collected on these days.

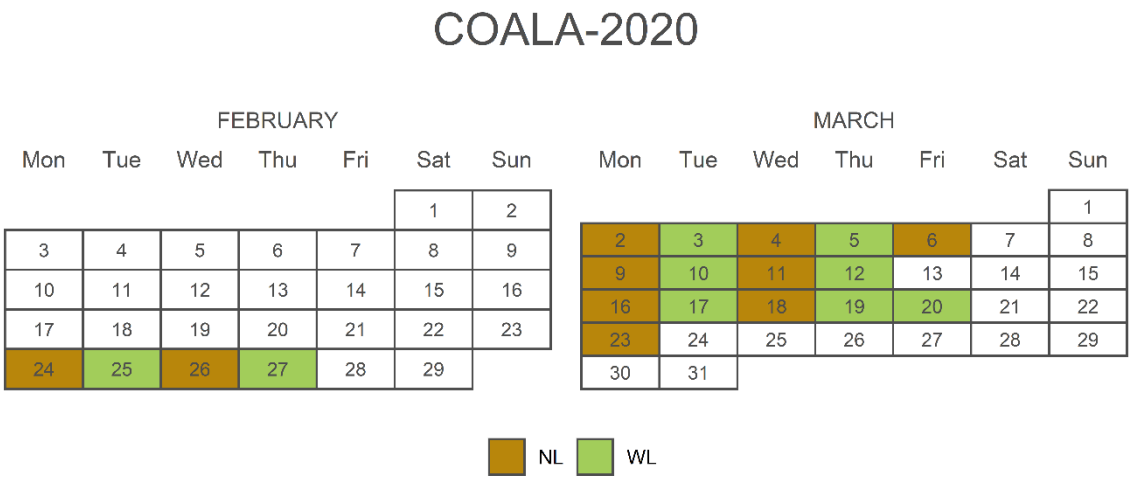

Fig. 2.S4. Soil NO emission sampling schedule during the COALA-2020 campaign in Australia. Two NO_x analysers were deployed allowing simultaneous continuous sampling from the sample and reference chambers. Brown shading indicates sampling from the soil collars with no litter (NL) and green shading indicates sampling from the soil collars with litter (WL).

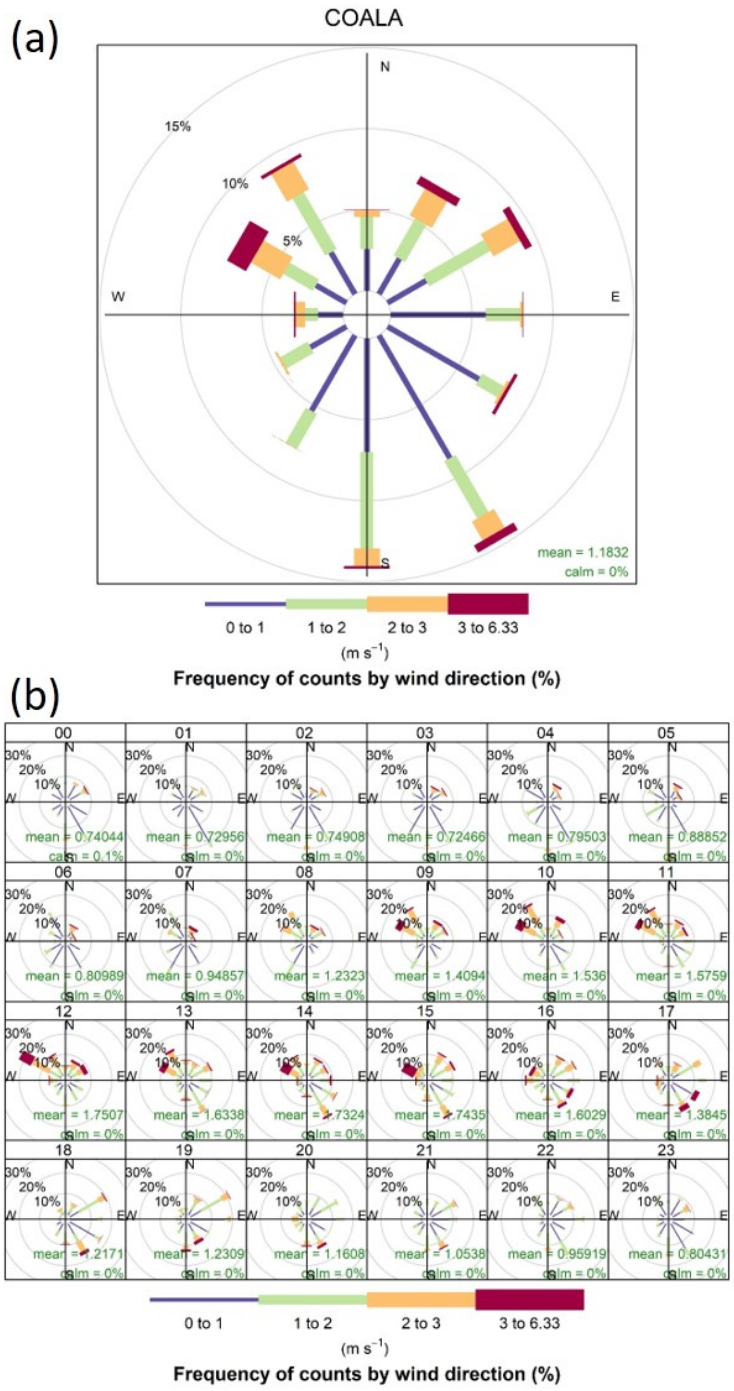

Fig. 2.S5. Windrose for the COALA site in Australia in 2020, showing (a) the campaign average and (b) hourly average windroses for the campaign period. It was relatively calm during the nighttime, with the wind speed starting to increase from dawn to early morning from the north. The shift in wind direction from the morning north-westerlies to the late afternoon south-easterlies are characteristic of the land-sea breezes previously reported in this region (Ramirez-Gamboa et al., 2020). The windrose plots were generated using R version 4.0.5 (R Core Team 2021) with the “openair” package (Carslaw and Ropkins, 2012).

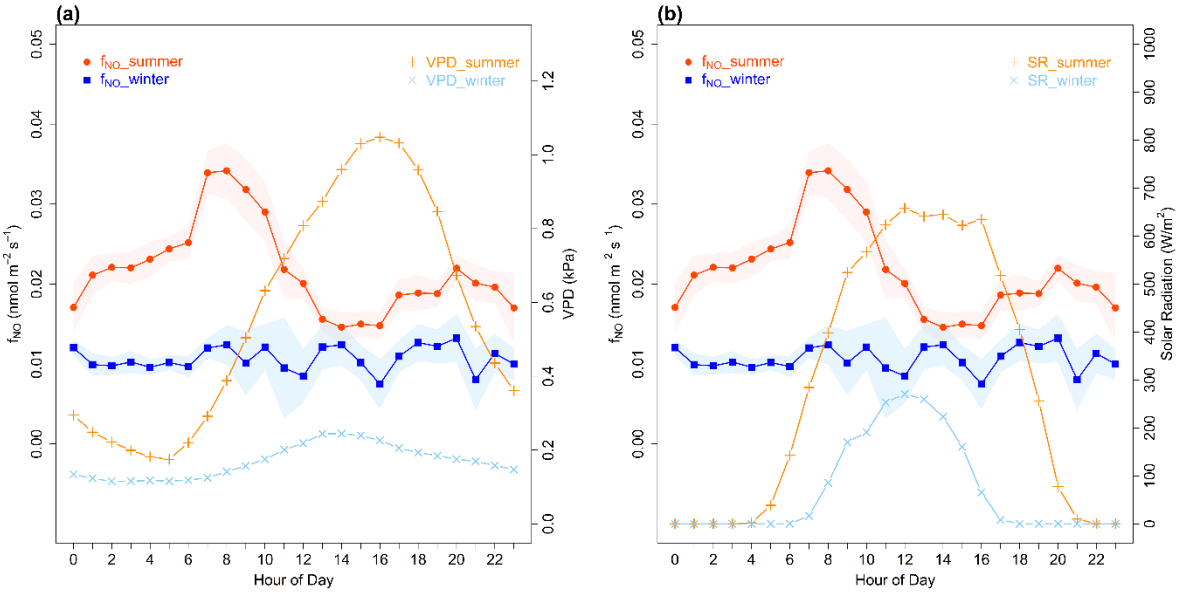

Fig. 2.S6. Estimated diel patterns of soil NO emission (f_{NO}) during the OSCA summer (red line with circles) and winter (blue line with squares) campaigns in the UK, showing (a) vapour pressure deficit (VPD) and (b) solar radiation (SR). The orange lines with (+) marks represent the observations in summer, light blue with (x) marks illustrate the winter observations. The shadings of NO flux denote ±1σ range of each estimation.

The emission rates (f_{NO}) were estimated from the NO concentration difference between sample and reference chamber (Eq. 2.1 in the main text). However, as only one NO_x analyser was used in OSCA campaigns, sample chamber and reference NO concentrations were not observed simultaneously. Thus, NO concentrations were averaged in 1 minute resolution of diel profile (24 hours in 1 minute resolution) for each campaign and observation period (e.g. 24 hours of OSCA summer sample chamber NO, and reference chamber in 1 minute resolution). The difference at each diurnal timepoint was then calculated to estimate f_{NO} in 1 minute resolution and averaged hourly. The average of the soil NO fluxes were estimated at 0.022±0.006 nmol·m^{-2}·s^{-1} and 0.011±0.003 nmol·m^{-2}·s^{-1} in summer and winter, respectively.

Table 2.S1. Manually recorded volumetric soil moisture (SM) and soil temperature (ST) during the OSCA Winter campaign in the UK.

Date	Hour	SM (%)	ST (°C)		Date	Hour	SM (%)	ST (°C)
2022-01-21	15	49.5			2022-02-09	9	54.5	8.3
					2022-02-09	10	55.15	8.2
2022-01-24	10	47.5			2022-02-09	11	55.2	8.2
2022-01-24	11	46.2			2022-02-09	12	55.25	8.2
2022-01-24	12	45.5			2022-02-09	13	55.3	8.2
2022-01-24	13	46.8			2022-02-09	14	55.4	8.2
2022-01-24	14	47.4			2022-02-09	15	55.5	8.15
2022-01-24	15	46.9						
2022-01-24	16	46.5			2022-02-11	11	50.85	6.15
2022-01-24	17	45.2			2022-02-11	12	50.8	6.2
					2022-02-11	13	50.75	6.3
2022-01-26	13	39.4	5.9		2022-02-11	14	50.7	6.4
2022-01-26	14	39.4	6		2022-02-11	15	50.7	6.5
2022-01-26	15	39.35	6.1					
2022-01-26	16	39.4	6.1		2022-02-14	10	61	7.4
					2022-02-14	13	67	7.1
2022-01-28	12	41.55	6.5		2022-02-14	14	68.2	7.1
2022-01-28	13	41.9	6.6		2022-02-14	15	68.3	7.1
2022-01-28	14	41.85	6.7					
2022-01-28	15	41.9	6.7					
2022-01-28	16	42.2	6.8					
					2022-02-16	14	58.8	8.6

2022-01-31	10	45.5	6.35					
2022-01-31	11	45.95	6.4		2022-02-18	10	63.33	7
2022-01-31	12	46	6.35		2022-02-18	11	63.45	7
2022-01-31	13	45.9	6.3					
2022-01-31	14	45.9	6.35		2022-02-23	9	57.35	6.8
2022-01-31	15	45.9	6.4		2022-02-23	10	57.05	6.7
					2022-02-23	11	56.95	6.8
2022-02-04	10	47.2	7.45		2022-02-23	12	56.9	6.9
2022-02-04	11	47.6	7.4		2022-02-23	13	56.9	6.95
2022-02-04	12	47.6	7.35		2022-02-23	14	56.85	7.05
2022-02-04	13	47.6	7.3		2022-02-23	15	56.75	7.1
2022-02-04	14	47.6	7.3					
2022-02-04	15	47.8	7.3		2022-02-28	12	58.15	6.7
					2022-02-28	13	59.1	6.8
2022-02-07	11	53.75	6.1					
2022-02-07	12	53.6	6.15					
2022-02-07	13	53.8	6.3					
2022-02-07	14	53.75	6.4					

Table 2.S2. Manually recorded volumetric soil moisture (SM) and soil temperature (ST) recorded in the sample chamber soil collars with litter (WL) and without litter (NL) at the COALA site in Australia in 2020. Measurements were conducted ~12:00 local time.

Date	SM (%)	ST (°C)	Collar
2020-02-24	12.4	20.6	NL
2020-02-25	18	20.9	WL
2020-02-26	14.3	21.1	NL
2020-02-27	25	20	WL
2020-03-02	13.1	19.7	NL
2020-03-03	15.2	19.2	WL
2020-03-04	25.8	19.4	NL
2020-03-05	31.3	20.3	WL
2020-03-06	27.4	20.3	NL
2020-03-09	33.9	18.6	NL
2020-03-10	24.1	19	WL
2020-03-11	22.8	19.8	NL
2020-03-12	18.1	18.6	WL
2020-03-16	33.1	17.6	NL
2020-03-17	23.2	17.9	WL
2020-03-18	20.7	20	NL
2020-03-19	21.6	20.2	WL
2020-03-20	15.4	19.7	WL
2020-03-23	16.4	18.4	NL

Chapter 3: Impact of soil temperature and elevated CO_2 on the NO_x fluxes in UK deciduous forest

Authors contributions

Hyunjin An: Designed experiment methodology, visit and collect soil samples, carried out practical measurements, compiled and analysed data, visualised data, participated in result interpretations and prepared manuscript.

Kirsti Ashworth: Advice on experiment design and methodology.

Emma J. Sayer: Advice on experiment design and methodology, participate in result interpretations and manuscript preparation

Clare Benskin: Participated in soil analysis

Highlights

- Nitrogen limited forest soils take up nitrogen oxides from the atmosphere
- Soil NO_x fluxes were influenced by temperature and showed clear temporal variations
- Elevation of atmospheric carbon dioxide concentrations alters the temperature response of soil NO fluxes

Abstract

Nitrogen oxides (NO_x), including nitrogen dioxide (NO_2) and nitric oxide (NO) are major precursors of air pollution. NO_x is principally considered to be of anthropogenic origin but is also emitted from natural sources such as soil microbial activity. At the same time, soils are one of the major sinks for NO_x from the atmosphere. However, we know very little about the influence of climate changes such as rising temperatures and elevated CO_2 on soil fluxes of NO_x. To address this knowledge gap, we incubated soil samples collected from a Free Air CO_2 Enrichment (FACE) experiment in oak

woodland in the UK at 4 different temperatures and tracked NO and NO_2 fluxes for 10 days.

Soil NO_2 fluxes were negative (-26.58 ± 3.56 and -14.54 ± 1.80 ng N g^{-1} $hour^{-1}$) in both the control and FACE soils, respectively, indicating that the soils are a sink for atmospheric NO_2. Although soils were expected to act as source of NO we measured negative NO fluxes in both control and FACE soils (-2.26 ± 0.72 and -1.55 ± 0.29 80 ng N g^{-1} $hour^{-1}$, respectively). Greater soil uptake of NO and NO_2 were observed for control soils than FACE soils, with peak uptake on day 3 and day 7-8 of incubation. NO fluxes increased with soil temperature, but NO_2 fluxes did not differ among temperature treatments. Importantly, the observed optimal temperature for NO uptake was 10 ºC in the controls but 15 ºC in the FACE soils, indicating that soil NO uptake could be affected by rising temperatures and atmospheric CO_2 concentrations.

Our study demonstrates unexpected patterns in soil NO_x fluxes in response to combined warming and elevated CO_2. Field studies including multiple climate change drivers are thus urgently needed to improve projections of NO_x under future climate change scenarios.

Key words: Soil fluxes, Nitrogen oxides, CO_2 enrichment, BIFoR

3.1 Introduction

Soils are an important component of the nitrogen (N) cycle. Nitrogen not only cycles in various forms within the soil, but also interacts with the atmosphere via gas exchange. Soils can act both as sources and sinks for N from the atmosphere, mainly through microbial processes. For example, soils are the most important biogenic source of nitrous oxide (N_2O), which is an important greenhouse gas (IPCC, 2007). We know much less about the role of soils in the emission and uptake of N oxides (NO_x), the other gaseous N compounds that interact with soils. NO_x comprise nitric oxide (NO) and nitrogen dioxide (NO_2), which are important primary pollutants as well as precursors of ozone (O_3) and aerosol formation (AQEG, 2004; WHO, 2006; Fowler et al., 2008). NO_x are predominantly emitted from anthropogenic sources and are

concentrated in urban and industrial areas (WHO, 2006). Given that NO_x emissions are considered to be primarily anthropogenic, emissions from natural sources have been largely neglected (Goldberg et al., 2021). However, NO_x emissions from natural sources are estimated to comprise approximately 25% of global NO_x emissions and up to 80% of biogenic NO_x emissions originate from soils (Denman et al., 2007; Skiba et al., 2021). Global NO_x emissions from soils are estimated at 3.3-20.4 Tg N $year^{-1}$ depending on the time, grid resolution and estimation methods (Davidson and Kingerlee, 1997; Pilegaard, 2013; Weng et al., 2020). Moreover, while anthropogenic NO_x emissions have declined in response to policies on air pollution, soil NO_x emissions are estimated to increase by up to 2% per year (Fortems-Cheiney et al., 2021; Goldberg et al., 2021). However, both NO and NO_2 can also be taken up by soils (Schindlbacher et al., 2004) although there are very few studies of soil NO_x fluxes and their impact on the atmosphere, especially where the NO_x emissions are limited (e.g. remote or forested areas).

Exchange of N between the soil and the atmosphere occurs predominantly through microbial activities (e.g. nitrification and denitrification) and chemical reactions called chemo-denitrification (Medinets et al., 2015; Heil et al., 2016). These processes are highly influenced by pedoclimatic parameters (e.g. soil moisture, soil temperature, soil pH, available nitrogen contents, soil texture) and vegetation (Pilegaard, 2013). A few studies have investigated soil NO_x fluxes and their driving factors, such as soil moisture and temperature (Schindlbacher et al., 2004; Schaufler et al., 2010; Wang et al., 2015). For example, soil NO emissions increase with decreasing soil moisture (Schindlbacher et al., 2004; Venterea et al., 2005; Chapter 2, section 2.3.4), and a water-filled pore space of 15-65% is considered optimal for NO emissions, depending on the soil type (Schindlbacher et al., 2004; Feig et al., 2008; Pilegaard, 2013). Soil temperature is another important factor for microbial activities and chemical reactions that produce NO in the soil: typically soil NO emissions increase with temperature, as long as sufficient moisture is available (Medinets et al., 2016; Chapter 2). In addition, soil pH and N availability could allow a suitable condition or limit the microbial activities that produce NO in the soils (Skiba et al., 1992; Schindlbacher et al., 2004; Kesik et al., 2006; Schaufler et al., 2010). Although few studies have reported soil NO_2 fluxes, work in agricultural soils (Slemr and Seiler, 1984; Skiba et al., 1992; Skiba et al., 2021),

European forest soils (e.g. Schindlbacher et al., 2004) and a semi-arid steppe in northern China (Wang et al., 2015) demonstrate that soils can absorb NO_2 from the atmosphere. In contrast to NO, uptake of NO_2 can increase with temperature (Schindlbacher et al., 2004; Wang et al., 2015) and decline with increasing soil moisture (Wang et al., 2015) but the relationships between NO_2 uptake and soil temperature differ markedly among soils (Schindlbacher et al., 2004).

Besides current pedoclimatic conditions, future levels of carbon dioxide (CO_2) in the atmosphere could affect soil NO_x emissions by altering N cycling. Elevated CO_2 in the atmosphere increases N demand and uptake by plants, which reduces the available N for soil microbes (Hungate et al., 1997). However, elevated CO_2 also increases the plant water use efficiency (Sgouridis et al., 2023) and thus influences soil moisture, which in turn governs soil gas emissions. Previous work demonstrated that CO_2 enrichment resulted in lower NO emissions from the soils (Hungate et al., 1997; Mosier et al., 2002), which was assumed to be due to increasing plant production and N uptake from the soil and consequently reduced soil N availability (Mosier et al., 2003). However, to our knowledge, the influence of elevated CO_2 on soil NO_x emissions has only been investigated at a single experimental site. Given that NO_x directly affects tropospheric photochemistry, including O_3 formation and the oxidation of the volatile organic compounds (Atkinson, 2000), we urgently need a better understanding of how climate changes, such as elevated CO_2 and warming, could affect soil NO_x fluxes in natural ecosystems. Our overarching goal was therefore to quantify soil NO_x fluxes in a nitrogen-limited deciduous woodland in the UK, and to investigate how soil NO_x fluxes might respond to projected future climate changes. We sampled soils from treatment and control arrays in a Free-Air CO_2 Enrichment (FACE) experiment and incubated them at different temperatures to measure the response of soil NO_x fluxes to combined elevated CO_2 and temperature treatments. Specifically, we tested the following hypotheses:

H1) Soil NO_x fluxes will increase with temperature in both control and FACE soils;

H2) Soil NO_x fluxes will be lower in FACE soils due to greater N-limitation of microbial activity;

H3) The increase in soil NO_x emissions with temperature will be attenuated in FACE soils compared to controls.

3.2 Methods

3.2.1 Study site and soil sampling

The Birmingham Institute of Forest Research (BIFoR) is located in central England (52.801°N, 2.301°W), United Kingdom (Fig. 3.1). A Free-Air CO_2 Enrichment (FACE) facility was established at BIFoR in 2017 in a mature temperate deciduous dominated forest (Hart et al., 2020; Sgouridis et al., 2023; Ziegler et al., 2023). The major species are *Quercus robur* (pedunculate oak) that dominates the canopy and *Corylus avellana* (common hazel) coppice that forms the understorey. The FACE facility was set up in six circular arrays following a paired design: three arrays are maintained at +150 ppm above ambient concentration, and three arrays are control plots which do not receive CO_2 fumigation. The FACE arrays operate during daylight hours (up to 18 hours; 05:00~22:00) from budburst to leaf fall (April 1st to November 1st). Thus, the facility attempts to capture the effects of CO_2 fertilisation on the forest ecosystem under "real world" conditions to project future climate change. Details about the facility and its operation are provided in Hart et al., (2020).

Soil samples were collected on 10 July 2023, in the middle of the CO_2 enrichment period. At each array, five cores (total 30 cores) were sampled from the organic layer to up to 80 mm depth using a 20-mm diameter steel corer. Each core was immediately sealed in a zip-loc bag and transported to the lab on the same day. To determine soil properties, one sample from each array (total six samples) was kept in cold storage (~5℃) for two days prior to N extraction and for four days before analysis of total C and N and determination of soil water content and pH. The other four samples from each array were placed in 0.5L Kilner^{TM} jars (soil thickness = 21.00 ±2.97 mm, weight = 60.87±15.64 g, mean ± standard deviation) and used for NO_x flux measurements (Fig. 3.2).

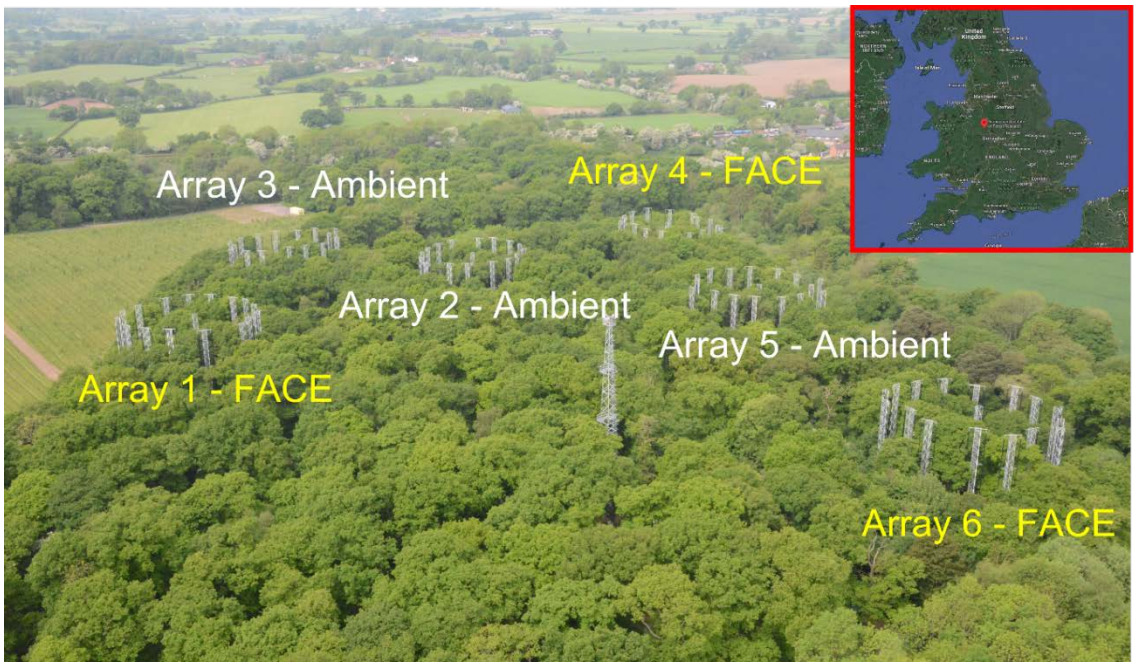

Fig. 3.1. Aerial view of the Birmingham Institute Forest of Research (BIFoR) Free-Air CO_2 Enrichment (FACE) facility (provided by BIFoR website), showing the locations of the ambient and FACE arrays. The map insert shows the location of the facility in the United Kingdom (©Google).

3.2.2 Laboratory analysis for soil characteristics

One soil core from each array (three FACE and three control arrays) was used to determine soil characteristics. The cores were divided into four subsamples to measure soil pH, total carbon (C) and nitrogen (N) content, nitrate-N (NO_3^-) and ammonium-N (NH_4^+) concentrations, and gravimetric soil water content (SWC). Soil pH was measured using a 10-g subsample from each core. The soils were placed in a 50-ml beaker with 25 ml distilled water, mixed using an orbital shaker for 30 minutes at 200 rpm and left to settle for 30 minutes, before measuring pH (Mettler Toledo, S220 SevenCompact, UK). The probe was calibrated using pH at 4.0, 7.0, and 10.0 before and after the measurements.

Total soil C and N content was determined on a 5-g subsample. The soil was oven-dried at 60 ℃ for 48 hours and ground in a ball-mill before analysing 20 mg of ground soil by combustion oxidation (Vario EL III, Elementar Analysensysteme GmbH, Germany).

Another 5-g subsample of soil was used for analysis of nitrate (NO_3^-) and ammonium (NH_4^+) concentrations after 2M KCl extraction. In brief, 20 ml of KCl was added to the soil sample, the solution was shaken on an orbital shaker for 1 hour at 200 rpm and then filtered (Whatmann 42). The extracts were stored in the freezer until analysis by colorimetry (AutoAnalyser 3 HR, Seal Analytical, Southampton, UK).

Soil water content (SWC) was measured using a 1-g subsample of fresh soil. The subsamples were oven-dried at 105 ℃ for 48 hours to determine the dry weight of the soils and SWC was calculated by the equation below;

$$SWC = \frac{soil\ fresh\ weight - soil\ dry\ weight}{soil\ dry\ weight} \times 100 \qquad \text{Eq. 3.1}$$

3.2.3 Experimental set-up

A total of 25 Kilner™ glass jars (0.5 L) were used for this study: 24 jars containing soil samples were used as 'sample chambers' (four per array), and one empty jar was used as a reference. Soil NO_x fluxes were measured immediately after returning from the field to establish pre-incubation fluxes with technical replicates. The soils were then pre-incubated at 5℃ for four days before assigning one soil sample per array to one of four temperature treatments: 5, 10, 15 or 20 ℃. The incubation temperatures were selected based on data recorded at the study site in 2019 (Mackenzie et al., 2020) to represent soil surface temperatures of annual mean (9.66 ±3.66 ℃), maximum monthly average (August, 14.97 ±1.03 ℃), minimum monthly average (January, 5.52 ±1.85 ℃), and a warming scenario which reflects the highest recorded soil surface temperature (20.08 ºC).

NO_x fluxes were measured every day for 10 days except on day 8 after the start of temperature treatments. Preliminary tests showed that it took 4-6 minutes for fluxes to

stabilise after connecting the jars to the analyser. Therefore, each sample chamber was measured for a total of 10-12 minutes but only the last 5-6 minutes of steady-state data were averaged to determine mixing ratios and calculate NO_x fluxes. Between measurements, the jars were kept closed to limit water loss but a 10 mm hole was drilled into the lid for aeration and to prevent build-up of gases in the headspace. Soil water content was maintained at field sampled values (Table 3.1) throughout the experiment, with a mean water loss of only 1% between measurements (ambient: 26.14 to 25.07 % and FACE: 22.72 to 21.71 %).

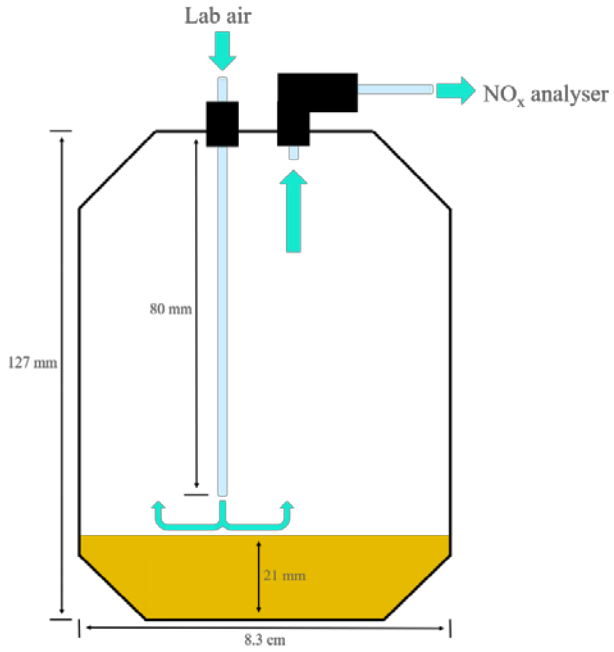

Fig. 3.2. Schematic diagram of the sample chamber (Kilner jar). Lab air is drawn into the jar and carries the soil flux to the outlet to NO_x analyser. The reference chamber is identical to sample chamber, but without soil inside.

Baseline flux measurements were conducted with a single NO_x analyser (Teledyne API, Model N500), alternating measurements of NO_x concentrations from reference and sample chambers. For temperature-treated fluxes, sample and reference chambers were measured simultaneously using two NO_x analysers (Teledyne API, Model N500 and T200UP, respectively; lower detectable limits are < 0.1 & 0.05 ppb, respectively).

3.2.4 Flux calculation and data analysis

The gas fluxes were calculated from the difference in NO_x concentrations between the sample and the reference jars using the following equation:

$$F = (C_{samp} - C_{ref}) \times \frac{M_w \cdot Q \cdot 10^9}{V_m \cdot W_{drysoil} \cdot 10^9} \times 60min \times 60g \qquad \text{Eq. 3.2}$$

where F is the net flux in ng N g^{-1} h^{-1}, M_w is the atomic weight of nitrogen (14.008 g mol^{-1}), V_m is the standard gaseous molar volume (24.055 10^{-3} m^3 mol^{-1}), C_{samp} and C_{ref} are the mixing ratios of the gas at the steady state gas concentrations (ppb) in the sample chamber and reference, Q is the mass flow rate of air through the chambers (0.00088 m^3 min^{-1} for baseline flux measurements and the sample chamber, and 0.00098 m^3 min^{-1} for the reference chamber), and $W_{drysoil}$ is the dry weight of each soil sample. The soil NO_x fluxes were standardised by soil dry weight and normalised to 60 g, which is the average soil sample weight used for the measurement.

Statistical analyses were carried out with R version 4.3.1 (R Core Team, 2023). We used linear mixed effect models in the lme4 package (Bates et al., 2015) to test whether elevated CO_2 and incubation temperature interacted to influence soil NO_x fluxes. Soil NO and NO_2 fluxes were modelled as a function of CO_2 treatment, incubation temperature, and their interactions (fixed effects). To account for the design of the field study and the repeated measurements during incubation, we included replicate array and time as random effects. Models were simplified by sequential removal of fixed effect terms, using the Akaike Information Criterion (AIC) and p-values to check for model improvement, and diagnostic plots to assess model residuals (Pinheiro & Bates, 2000). The final models were compared to appropriate null models (intercept only) using likelihood ratio tests. We used the Satterthwaite method to generate p-values and F- or t-statistics for fixed effect terms (treatment or incubation days) using the *anova* and *summary* functions in the lmerTest package (Kuznetsova et al., 2017). We report results as significant at $p < 0.05$.

3.3 Results and discussions

3.3.1 Overview of soil properties and pre-incubation NO_x fluxes

Surprisingly, pre-incubation soil NO_x fluxes at BIFoR were generally negative, indicating NO_x uptake from the atmosphere (Fig. 3.3). Contrary to our first hypothesis, soils from control arrays exhibited more negative fluxes, with 46.33 % greater uptake of NO (-2.26 ± 0.72 ng N g^{-1} h^{-1}) and 82.83 % greater uptake of NO_2 (-26.58 ± 3.56 ng N g^{-1} h^{-1}) compared to FACE soils (-1.55 ± 0.29 and -14.54 ± 1.80 ng N g^{-1} h^{-1} for NO and NO_2, respectively). According to Schindlbacher et al. (2004), NO_2 fluxes in Europe are often negative but NO fluxes are mostly positive; with only one exception in boreal forest in Finland (Schindlbacher et al., 2004; Schaufler et al., 2010) and one in lowland agricultural soils in the UK, where NO uptake was observed (Skiba et al., 1992).

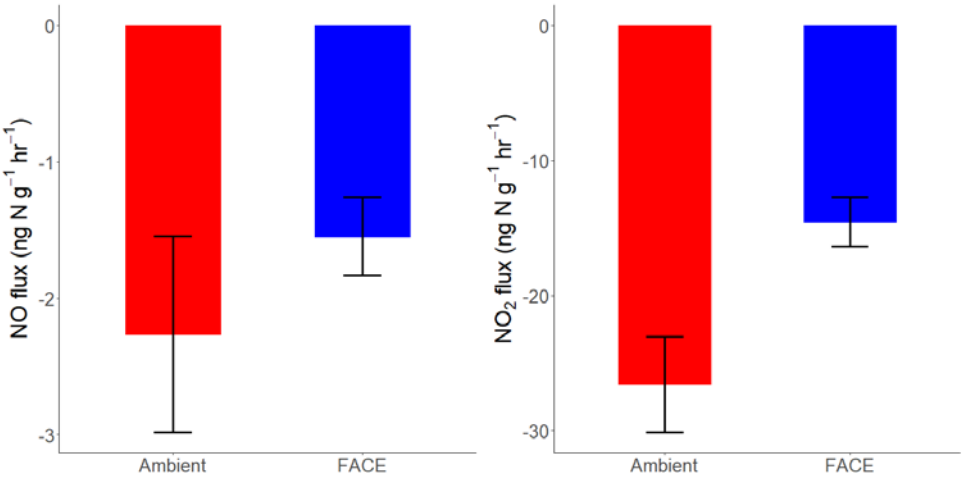

Fig. 3.3. Summary of the pre-incubation fluxes of NO and NO_2 from the ambient (red boxes) and CO_2 elevated (FACE, blue boxes) soils. The error bars represent the standard errors for n=12.

Given that Boreal forests are often strongly N-limited (Schindlbacher et al., 2004) and NO uptake by agricultural soils was greater in non-fertilised soils (Skiba et al., 1992), N-limitation at the BIFoR FACE site offers a plausible explanation for the observed uptake of NO_x in our study. Indeed, in areas with low rates of N deposition and lack of available nitrogen, soils can absorb NO from the air (Skiba et al., 1992; Schindlbacher

et al., 2004). If available nitrogen is insufficient, NO can be consumed by denitrifiers because they use it as an electron acceptor (Pilegaard, 2013). Consumption of NO_x can also occur during the denitrification process through chemical transformation of nitrite and nitrate (Blackmer and Cerrato, 1986; Galbally, 1989; Yamulki et al., 1997). Further evidence that NO_x uptake is driven by low N availability is provided by our soil analyses: although we had predicted greater N-limitation in the FACE soils, the concentrations of both nitrate-N and ammonium-N were lower in the control arrays (Table 3.1). Greater uptake of NO and NO_2 fluxes in the control than FACE soils is therefore in line with our measurements of available nitrogen in the soils. Thus, low N-availability likely contributes to uptake of NO_x by soils. Soil C/N ratios did not differ between FACE and control soils (16.00 and 15.73, respectively; Table 3.1). However, lower total carbon and nitrogen contents in the control soils could also limit microbial activity (Her and Huang, 1995; Klemedtsson et al., 2005) and promote uptake of NO_x.

Table 3.1. Pre-incubation soil properties for samples collected at 0-8 cm depth in free-air CO_2 enrichment (FACE) and control (ambient) arrays in a mature oak woodland in the UK. All values are given as means ± standard errors for n=3 per treatment.

Array	FACE	Ambient
SWC (%)	22.72 ± 2.96	26.14 ± 2.71
pH	4.21 ± 0.18	4.30 ± 0.03
Nitrate (NO_3^-; ppm)	1.06 ± 0.51	0.36 ± 0.02
Ammonium (NH_4^+; ppm)	0.55 ± 0.12	0.22 ± 0.04
Carbon content (%)	13.73 ± 2.55	5.75 ± 1.38
Nitrogen content (%)	0.86 ± 0.16	0.36 ± 0.07
C/N ratio	16.00 ± 0.05	15.73 0.70

Although soil pH was similar in the FACE (4.21) and control arrays (4.30), soil pH is an important parameter affecting microbial community composition (Schreiber et al., 2012) and biological activity (Kesik et al., 2006), including nitrification and denitrification processes. Soil NO production is favoured by specific soil pH values (Kesik et al., 2006). Production of NO in soils is generally lowest at pH value of 5, and

highest at pH values of 3, 4 and 7, but the mechanisms underpinning the high NO fluxes differ according to pH: chemo-denitrification accounts for 62% of NO production below pH 4.0, but nitrification or denitrification dominates above pH 4.5. Hence, BIFoR soils were in-between the production phase of biological and chemical processes that limits NO production. In consequence, NO_x were consumed by soils, but production processes were likely to be limited due to insufficient N availability and the pH of the soils.

3.3.2 General patterns of NO and NO_2 fluxes during incubation

During the ten days of incubation, soil NO fluxes were mostly negative, indicating uptake of NO from the atmosphere regardless of incubation temperature. Similar to the pre-incubation measurements, the mean NO uptake in the control soils was slightly higher (-24.10 ±2.27 ng N g^{-1} $hour^{-1}$) than in the FACE soils (-22.76 ± 2.23 ng N g^{-1} $hour^{-1}$). Although mean NO fluxes on the first day of the temperature treatments were positive (1.09±2.24, 1.19±2.49 ng N g^{-1} $hour^{-1}$, respectively), there was a switch to NO uptake from the second day of the incubation onwards, and the observed maximum NO uptake occurred on day 3 for both FACE soils (-49.84 ±7.55 ng N g^{-1} $hour^{-1}$) and control soils (-58.81 ±9.07 ng N g^{-1} $hour^{-1}$). NO uptake then declined until day 6, but a second uptake peak occurred on day 7 in both soils. The decline in NO uptake was steeper during the period from day 3 to day 6 than during the period from day 7 to day 10 (Fig. 3.4).

Soil NO_2 fluxes showed a similar temporal pattern to NO fluxes, whereby fluxes were generally negative, and the lowest fluxes were observed on day 3 and day 7 of the incubation (Fig. 3.4). However, the magnitude of NO_2 uptake was much greater than NO uptake. The switch from peak uptake of NO_x on day 3 to values closer to zero by day 6 suggest a shift in biological processes in the soil that influence N availability and cycles of the nitrification and denitrification (Hungate et al., 1997; Mosier et al., 2003).

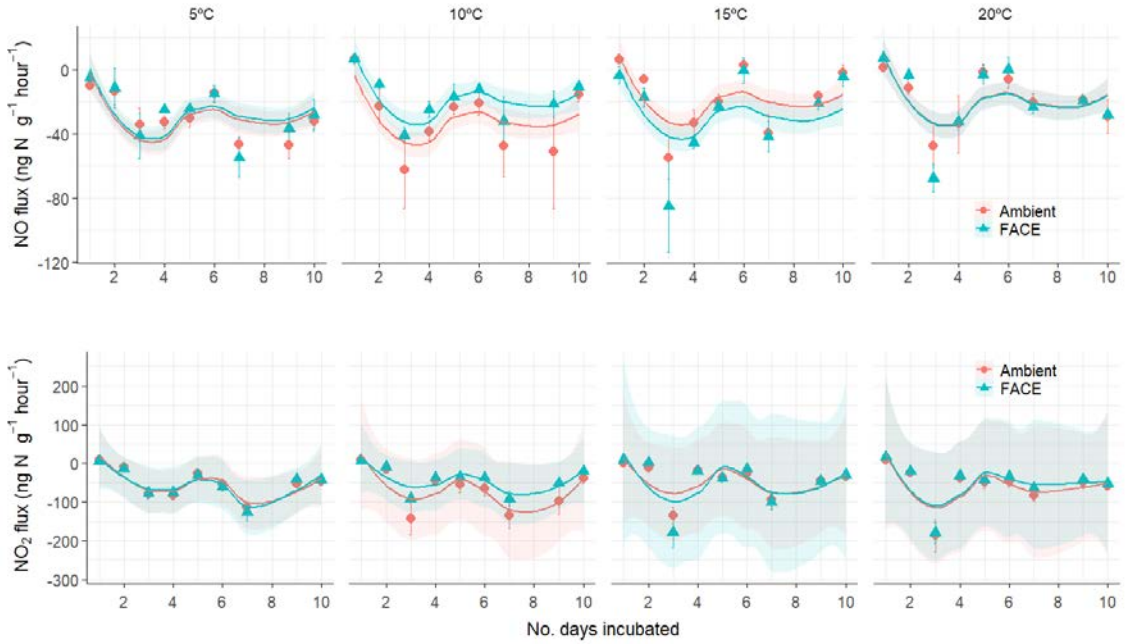

Fig. 3.4. Nitric oxide (NO) and nitrogen dioxide (NO_2) fluxes from soil collected in free air CO_2 enrichment arrays (blue triangles) and control plots (red dots) in a mature oak woodland in the UK, during a 10-day incubation at four different temperatures. Symbols and whiskers show means ± standard errors for n = 3 plots per treatment; dashed lines and shading show predicted fluxes based on linear mixed effects models and 90% confidence intervals, respectively.

NO fluxes were positive at the start of the incubations at all temperatures except the 5 °C treatment (Fig. 3.4). Temperatures below 10 °C limit biological activity (Borowik and Wyszkowska, 2016) so NO fluxes on the first day of incubation were close to zero. However, at all other temperatures we observed NO production in the soil on the first day of the incubation. Fluxes of NO_2 from the soil showed a strikingly similar pattern to NO fluxes, although positive fluxes were observed on day 1 in all temperature treatments. The peaks in NO_2 uptake also mirrored those for NO, with the greatest NO_2 uptake on day 3 at higher temperatures, but on day 7 in soils incubated at 5 °C. Maximum uptake of both NO and NO_2 occurred at day 7 in the 5 °C soils, compared to day 3 in all the other temperature treatments, and this also suggests that biological activity was greatly reduced at low temperatures. Overall, the switch from NO_x emissions to uptake after the first day of incubation indicates that the available N in the soils was insufficient to sustain microbial activity.

3.3.3 Interactive effects of temperature and elevated CO_2 on soil NO_x fluxes

Soil NO fluxes were strongly influenced by temperature, but the response of NO fluxes to increasing temperature differed between elevated CO_2 and controls (treatment × temperature interaction: $\chi^2 = 20.72$, $p = 0.005$; Fig. 3.4). Across both treatments, soil NO fluxes generally increased with temperature (temperature effect: $F = 3.01$, $p = 0.031$), with higher fluxes at 15ºC ($t = 2.47$, $p = 0.015$) and 20ºC ($t = 2.38$, $p = 0.018$) compared to 5ºC or 10ºC, which did not differ. Although there was no overall effect of elevated CO_2, NO fluxes in the FACE soils were slightly higher than in the controls at 10ºC (marginally significant trend $t = 1.69$, $p = 0.093$), indicating reduced uptake under elevated CO_2, but slightly lower than in the controls at 15ºC ($t = -3.44$, $p < 0.001$). There was no difference between treatments at 20ºC (Fig. 3.4). Thus, elevated CO_2 appears to alter the temperature optimum for NO uptake in these soils.

By contrast, neither the magnitude nor the temporal pattern of NO_2 fluxes from the soil were affected by temperature or elevated CO_2 ($\chi^2 = 11.75$, $p > 0.1$).

It is well documented that soil NO emissions (positive fluxes) increase with temperature (Pilegaard, 2013; Medinets et al., 2016; Chapter 2). However, we demonstrate here that NO uptake is also temperature-dependent, and that elevated CO_2 alters the relationship between NO uptake and temperature. Mean soil NO uptake was greater at the lower incubation temperatures (5 and 10 ℃) in both control soils (-29.03 and -30.66 ng N g^{-1} $hour^{-1}$, respectively) and FACE soils (-18.17 and -18.53 ng N g^{-1} $hour^{-1}$, respectively). Reduced uptake of NO in the FACE soils compared to the controls at 10ºC but greater uptake at 15ºC suggests that elevated atmospheric CO_2 alters soil N cycling and shifts the temperature optimum for biological processes involved in NO consumption. Increased photosynthesis and plant growth under elevated atmospheric CO_2 requires greater uptake of nitrogen from the soil (Drake et al., 2011), which could reduce soil NO fluxes. At the same time, greater water uptake from soils could also reduce soil water content and increase soil NO fluxes. Although, the small measured difference in pre-incubation soil water content (22.72% in the FACE and 26.14 % in the ambient soils) is unlikely to have a major impact on soil NO fluxes, the combined effects of nitrogen availability and soil water content could have altered the temperature optimum

for NO_x uptake in our study. Future work should assess shifts in nitrification and denitrification processes in soils exposed to elevated CO_2, as well as potential changes in the microbial communities involved.

3.4 Conclusions

This research demonstrates soil uptake of NO_x in mature deciduous forest. Although soil NO_2 uptake has been reported in previous studies, we also found NO uptake by soils, which is in line with limited soil nitrogen availability at our study site. Furthermore, we demonstrate that the uptake of NO is influenced by temperature and atmospheric CO_2. As we observed negative fluxes indicating that soil absorbs NO from the atmosphere, which is opposite to our expectation, our original hypotheses were not fully satisfied. This suggests that soil absorption may be more common than we had anticipated, and deserves further study. Throughout this series of experiments, the relationship between soil NO_x fluxes to temperature and atmospheric CO_2 concentrations were not clearly determined. Although soil flux measurements in laboratory experiments are highly controlled and exclude interactions with plants, the results of our experiment indicate interactive effects of two major climate change drivers that urgently need to be investigated under natural conditions in the field. By combining soil temperature treatments with elevated CO_2, our study suggests that future projections of soil NO_x fluxes should consider NO_x uptake by N-limited soils, as well as changes in biological processes in response to temperature and elevated CO_2 that will influence biogenic NO_x emissions under future climate change. Thus, our results lay the foundations for novel laboratory experiments and in-situ measurements of NO_x uptake and emissions from woodland soils to improve our understanding of the nitrogen cycle and biosphere – atmosphere interactions.

Chapter 4: Impact of soil NO flux on the forest canopy atmosphere

Authors contributions

Hyunjin An: Designed experiment methodology, carried out practical observations, compiled and analysed data, visualised data, participated in result interpretations, prepared and submitted manuscript.

Frederick Otu-Larbi: Supplied observed datasets, advice on model setup, operation, and evaluation.

Kirsti Ashworth: Participate in planning, advice on model setup and operation, participate in result interpretations.

Oliver Wild: Participate in result interpretations and manuscript preparation

Highlights

- Soil NO fluxes affect O_3 formation and loss and the photochemistry of isoprene and HO_x radicals in forest
- Vertical distributions of gas species reflect the different forest emission sources
- Soil NO emissions increase HO_x radicals more near the ground surface than at heights above
- Higher soil NO flux non-linearly decreases O_3 concentration at the ground surface, but linearly increases O_3 at heights above
- O_3 concentrations during the heatwave period are more sensitive to soil NO fluxes

Abstract

Nitric oxide (NO) is a major precursor of O_3 and aerosol formation. It is predominantly emitted from anthropogenic sources, hence air pollution issues are more common in industrial areas and urban regions. Unlike in urban areas, forest regions have limited NO emission sources but are relatively rich in biogenic volatile organic compounds (BVOCs; e.g. isoprene). Thus, even a small input of NO can influence atmospheric composition and produce more O_3 than expected. This study aims to provide a comprehensive understanding of the impact of soil NO on atmospheric chemistry in forests using a 1-D canopy exchange model with different soil NO flux inputs.

A constant soil NO emission flux of 0.011 nmol m^2 s^{-1}, matching that observed in Eucalyptus forest in Australia (Chapter 2), increased O_3 in the forest canopy below 30m height during the growing season by 0.6±1.0 ppb. O_3 concentrations near the ground surface were decreased by direct chemical removal through titration by NO, and O_3 decreased by 1.1±1.5 ppb at 0.8m. On the other hand, O_3 increased at all heights above 4m (e.g. 0.8±0.6 ppb at 15.6m) and there was an overall increase in O_3 through column below 30m height. O_3 increased by 0.4±0.2 ppb at the canopy top (15.6m), but this increase was 3.2 times greater (1.4±0.5 ppb) during the heatwave period. On the other hand, the O_3 decrease near the surface was very similar over this period. Moreover, soil NO emissions affect isoprene oxidation. With soil NO emissions the lifetime of isoprene to OH was estimated to be 1.3 hours in the early afternoon, 58% shorter than without soil NO flux. In contrast, soil NO uptake (-0.005 nmol m^2 s^{-1}) removes NO from the atmosphere, and contributed to an O_3 decrease of 0.5±0.5 ppb below 30m. Near the ground surface O_3 decreases in the heatwave period (-0.9±0.6 ppb) and this decrease is more than four times greater than that before the heatwave period (-0.2±0.4 ppb). These results indicate that forest O_3 can be influenced by soil NO emission and uptake, especially where anthropogenic sources are limited.

Key words: soil NO fluxes, atmospheric chemistry, 1-D canopy exchange model, biosphere – atmosphere interactions.

4.1 Introduction

Nitrogen oxides (NO_x = NO + NO_2) are key drivers of atmospheric chemistry and major precursors of air pollution through contributions to ozone (O_3) production and aerosol formation (AQEG, 2004). O_3 in the troposphere contributes to global warming and at the surface it is damaging to living cells, affecting human health and plant growth (Fowler et al., 2008). NO_x is dominantly emitted from anthropogenic sources, especially fossil fuel combustion associated with traffic, industry and power plants (WHO, 2006). These major emission sources are typically located in urban and industrialised areas.

NO_x produces O_3 in the daytime through photolysis of NO_2 (Eq. 4.1 ~ 4.3) and then reaction of the O_3 with NO removes it again, leading to a null-cycle in NO-NO_2 photochemistry. However, the lower troposphere contains abundant volatile organic compounds (VOCs) which are highly reactive and enhance O_3 production through oxidation processes (Atkinson, 2000). The oxidation of VOCs produces peroxy radicals such as hydroperoxyl (HO_2) and organic peroxy radicals (RO_2). These radicals have a high potential for converting NO to NO_2 (Eq. 4.4 ~ 4.5), which competes with the null-cycle and leads to O_3 production.

$$NO + O_3 \rightarrow NO_2 + O_2 \qquad \text{Eq. 4.1}$$

$$NO_2 + h\nu \rightarrow NO + O \qquad \text{Eq. 4.2}$$

$$O + O_2 + M \rightarrow O_3 + M \quad (M = air) \qquad \text{Eq. 4.3}$$

$$RO_2 + NO \rightarrow RO + NO_2 \qquad \text{Eq. 4.4}$$

$$HO_2 + NO \rightarrow OH + NO_2 \qquad \text{Eq. 4.5}$$

VOCs are emitted not only by anthropogenic sources (AVOCs; e.g. from solvent, transport and fossil fuel combustion) but also biogenic sources (BVOCs; e.g. from plants and algae). In fact, biogenic emissions (~1150 Tg C $year^{-1}$, Guenther et al., 1995; Goldstein and Galbally, 2007) are estimated to be approximately 10 times larger than anthropogenic sources (~100 Tg C $year^{-1}$, Stewart et al., 2003; Kansal, 2009), and constitute about 90% of the global VOC emission inventory. Moreover, BVOCs typically have higher photochemical reactivity than AVOCs (Chameides et al., 1988;

Atkinson, 2000). For example, isoprene (C_5H_8), which is the dominant VOC emitted from broadleaf vegetation, comprises about half of the total global biogenic VOC emissions (Guenther et al., 2012). The lifetime of isoprene is only about 1.4 hour for reaction with hydroxyl radical (OH), 1.6 hour with nitrate (NO_3) radical and 1.3 day with O_3 (Atkinson, 2000; Atkinson and Arey, 2003), and these are shorter than those of most AVOCs (e.g. the lifetime of toluene is 1.9 day, 1.9 year, and 4.5 years to OH, NO_3, and O_3, respectively).

Global isoprene emissions of 600 Tg $year^{-1}$ originate from the biosphere (Guenther et al., 2006), and this is more than five times higher than total anthropogenic VOCs emissions. Emissions of isoprene from anthropogenic sources (e.g. from vehicular exhaust; Borbon et al., 2001) are also observed, but the concentrations are only about 2% of those of benzene (Wagner et al., 2014). As forested regions have limited NO_x emission sources but abundant VOCs supplied by natural vegetation, even a small amount of NO_x input may have a substantial impact on atmospheric chemistry. Although NO_x is predominantly emitted from anthropogenic sources, there are also biogenic sources from lightning and soils. The contribution of these biogenic sources to the global NO_x emission inventory is estimated to be ~25%, with around 80% from soil emissions (Denman et al., 2007; Skiba et al., 2021). Soil NO_x emissions are mainly in the form of NO and have been estimated to be up to 21 Tg N $year^{-1}$ (Davidson and Kingerlee, 1997; Pilegaard, 2013; Weng et al., 2020), in the same range as NO emissions associated with fossil fuel combustion (Davidson and Kingerlee, 1997). However, soil NO emissions are very uncertain and vary strongly depending on the surrounding environment (Pilegaard, 2013), with a reported range over land of 0.2~32 kg N ha^{-1} $year^{-1}$ (Davidson and Kingerlee, 1997; Stehfest and Bouwman, 2006). Soil NO emissions are less well studied than those of nitrous oxide (N_2O), one of the most important greenhouse gases emitted from biogenic sources via nitrification and denitrification.

NO is produced by both biological and chemical processes in the soil (Medinets et al., 2015; Heil et al., 2016). The major processes are nitrification and denitrification, which involve microbial activity (Butterbach-Bahl et al., 2013). Therefore, these mechanisms are closely influenced by pedoclimatic factors (e.g. soil moisture, soil temperature, soil pH, nitrogen availability, mineral content and structure, soil texture) and vegetation

(Pilegaard, 2013). Soil NO emissions typically increase with decreasing soil moisture (Schindlbacher et al., 2004; Chapter 2, section 2.3.4), and are thought to peak at a specific water filled pore space between 15~65% depending on the soil type (Schindlbacher et al., 2003; Pilegaard, 2013). Soil temperature is an important parameter that activates micro-organism activities and chemical reactions, and is believed to increase soil NO emissions (Medinets et al., 2016; Chapter 2). Furthermore, not only soil temperature, but also soil pH provides a suitable condition for NO production (Kesik et al., 2006) and nitrogen availability (e.g. ammonium and nitrate) could govern the magnitude of soil NO fluxes and even lead to NO uptake (Skiba et al., 1992; Schindlbacher et al., 2004; Kesik et al., 2006; Schaufler et al., 2010). The soil NO flux to the atmosphere is the net effect of both emission and uptake processes, and thus soils can take up NO when the soil available nitrogen is insufficient (as found in chapter 3; Skiba et al., 1992; Schindlbacher et al., 2004; Schaufler et al., 2010).

Although NO_x in the atmosphere directly affects photochemistry and the concentrations of O_3 and VOCs, soil NO emissions are not often considered in many environments because they are assumed to be small compared to anthropogenic sources and atmospheric transport from these sources. In consequence, the contribution and impact of soil NO on atmospheric chemistry has only been investigated in a few model studies (e.g. Visser et al., 2022; Shen et al., 2023), and therefore substantial uncertainty remains. In addition, anthropogenic NO_x emissions are decreasing in many industrialised and urbanised regions, and yet soil emissions are estimated to be increasing (Fortems-Cheiney et al., 2021). Therefore, the contribution of soil NO flux to atmospheric composition and O_3 production may become more important in the future following global warming and climate change.

Therefore, this study aims to provide new insight into the importance and impact of soil NO fluxes on forest photochemistry and their contributions to O_3 production. Atmospheric chemistry in the forest canopy will be investigated using a 1-D canopy exchange model. For this purpose, Wytham Woods was selected for this study, as observations are available from 2018 at a range of heights in the canopy, and the summer included a prolonged heatwave period. Different soil NO fluxes considering both emission and absorption scenarios were used and compared to a reference scenario with no soil flux. These scenarios allow exploration of the role and significance of soil

NO fluxes in the forest atmosphere, considering both time scales (e.g. diel cycles), and the vertical structure of the impacts.

4.2 Methods

4.2.1 Site description

Wytham Woods (51°46’23.3” N, 1°20’19.0” W) is a temperate mixed deciduous forest located ~5 km north-west of the centre of Oxford, United Kingdom. The forest canopy consists of a mixture of trees including Sycamore (*Acer pseudoplatanus*), pedunculate oak (*Quercus robur*), European Ash (*Fraxinus excelsior*), and European beech (*Fagus sylvatica*) and these account for over 60% of the canopy cover. The soil textures are mostly clayey (60% clay, 22% silty clay, 15% clay roam, <5% silty clay loam). Detailed descriptions of the site are available in Thomas et al., 2011; Bolas et al., 2020; Ferracci et al., 2020; and Otu-Larbi et al., 2020.

Field measurements were conducted using a custom-built portable gas chromatograph with photo-ionization detection (GC-PID) called “iDirac” to determine isoprene mixing ratios in the atmosphere (Bolas et al., 2020) between June and October in 2018 during the “Wytham Isoprene iDirac Oak Tree Measurements (WIsDOM)” campaign (Bolas et al., 2020; Ferracci et al., 2020; Otu-Larbi et al., 2020). Isoprene was monitored at four different heights; 0.53m, 7.25m, 13.17m and 15.55m during the campaign period (Ferracci et al., 2020). The soil moisture at a 20cm depth and meteorological parameters (e.g. wind speed, wind direction, solar radiation, air pressure, air temperature and relative humidity) were observed by automatic weather station (AWS) at the Upper Seed area, located ~480m from the isoprene observation system (Otu-Larbi et al., 2020). The observation dataset and meteorological data were averaged to 30-minute resolution and isoprene mixing ratio measurements were used to evaluate the model performance. The growing season of 2018 can be split into three periods based on air temperature: before heatwave, heatwave, and post heatwave. The heatwave lasted from 22 June to 8 August (UK Met Office, 2019) and the average air temperature was 19.6℃, which is as much as 7℃ higher than the climatological average during 1992 – 2015 over the same period (Ferracci et al., 2020).

4.2.2 Model description

The FORest Canopy Atmosphere Transfer (FORCAsT) is a 1-D canopy exchange model that combines atmosphere and land surface components (Ashworth et al., 2015), and is based on the CACHE canopy exchange model (Forkel et al., 2006). Gas-phase atmospheric chemistry reactions are represented using the Caltech Atmospheric Chemistry Mechanisms (CACM, Griffin et al., 2002, 2005). Algorithms of CUPID (Norman, 1979; Norman and Campbell 1983), a plant-environment model incorporating soil-plant-atmosphere interactions, are used to calculate the energy balance and radiative transfer within the canopy. The model represents the processes occurring within and above the canopy, including emissions, advection, deposition, vertical exchange, and chemical production and loss. The vertical resolution of the column can be configured to have between 20 and 60 vertical layers in the atmosphere. The thickness of the layers increases with height, but there is greater resolution in the canopy levels. In addition to the atmosphere, 15 soil layers are included in the model for computing heat and moisture storage and transfer to the atmosphere (Forkel et al., 2006). In the canopy, biogenic emissions of BVOCs are calculated using the mechanisms introduced by Guenther et al. (1995) and modified by Steinbrecher et al. (1999), and the dry deposition of gases and particles on vegetation (leaf surfaces) are calculated by a resistance scheme (Gao et al., 1993).

The model has been upgraded from version 1.0 (Ashworth et al., 2015) in several perspectives. Otu-Larbi et al. (2020) introduced three updated isoprene emission factors associated with leaf temperature and soil moisture. Wei et al. (2021) changed the process splitting to reduce the runtime, updated the eddy diffusivity, implemented the Reduced Caltech Isoprene Mechanism (RCIM) rather than the CACM, and extended the aerosol module to include isoprene derived secondary organic aerosols. Further, Otu-Larbi et al. (2021) incorporated a coupled stomatal conductance – photosynthesis model. Most of the major updates are related to isoprene, modelling schemes and chemical mechanisms.

This study aims to investigate the impact of soil NO emissions, and soil moisture is one of the major components governing soil fluxes. Therefore, the soil moisture

parameterisation from the upgraded version of Otu-Larbi et al. (2020) is selected for this study.

4.2.3 Model setup

Most of the model settings including vertical layers (40 layers) and vegetation parameters were adopted unchanged from Otu-Larbi et al. (2020), and the observed meteorological data and soil moisture record were used. However, the soil NO emission scheme was adapted for this study. Soil NO fluxes were directly applied to the lowest model level (0.8m) of the atmosphere. Three different soil NO fluxes were used; a positive soil NO flux (f_{NO} = 0.011 nmol m^2 s^{-1}) matching that measured at a Eucalyptus forest in Australia (Chapter 2, section 2.3.4), a negative soil NO flux (f_{NO} = -0.005 nmol m^2 s^{-1}) derived from measurements at Birmingham Institute Forest of Research (BIFoR) in 2023 (pre-incubation data from Chapter 4), and no soil NO flux (f_{NO} = 0) for reference. The soil fluxes are applied uniformly at every time point (30 minute resolution) day and night. In addition, advection of background pollutants (O_3, NO and NO_2) were considered above the tree canopy (~18m) at layers 22-26 (21.2~34.9m). Unfortunately, no direct measurements of O_3 and its precursors were made at Wytham woods, and therefore advection of background O_3 and NO_x were parameterised using data measured at a Holm oak (*Quercus ilex*) forest at Castelporziano (Fares et al., 2019). As the canopy height is 18m, this study used heights up to 30m (25 levels from the ground surface out of 40 layers) to investigate biosphere–atmosphere interactions considering not only the impact of soil NO emissions but also canopy gas exchanges.

4.2.4 Model evaluation and data analysis

For evaluation of the model performance, the observed isoprene at four different heights at 30-minute resolution was compared with the model reference scenario (Fig. 4.1). All four heights were reasonably well correlated with observations, with R^2 >0.66, and the canopy top at 15m height correlated best with R^2 = 0.82. In particular, the best correlation was found for the heatwave period at all heights. In contrast, lower heights (0.8m and 7.1m) during the post heatwave period show the worst correlations with the observations (R^2 = 0.04 and R^2 = 0.03, respectively). One possibility for the poor

agreement might be the relatively low isoprene mixing ratios modelled (period average = 0.14 ppb at 7.1m and 0.09 ppb at 0.8m) and observed (0.08 and 0.06 ppb, respectively) during the post heatwave, which were much less than those observed (0.52 and 0.40 ppb, respectively) and modelled (0.53 and 0.33 ppb, respectively) during the heatwave period.

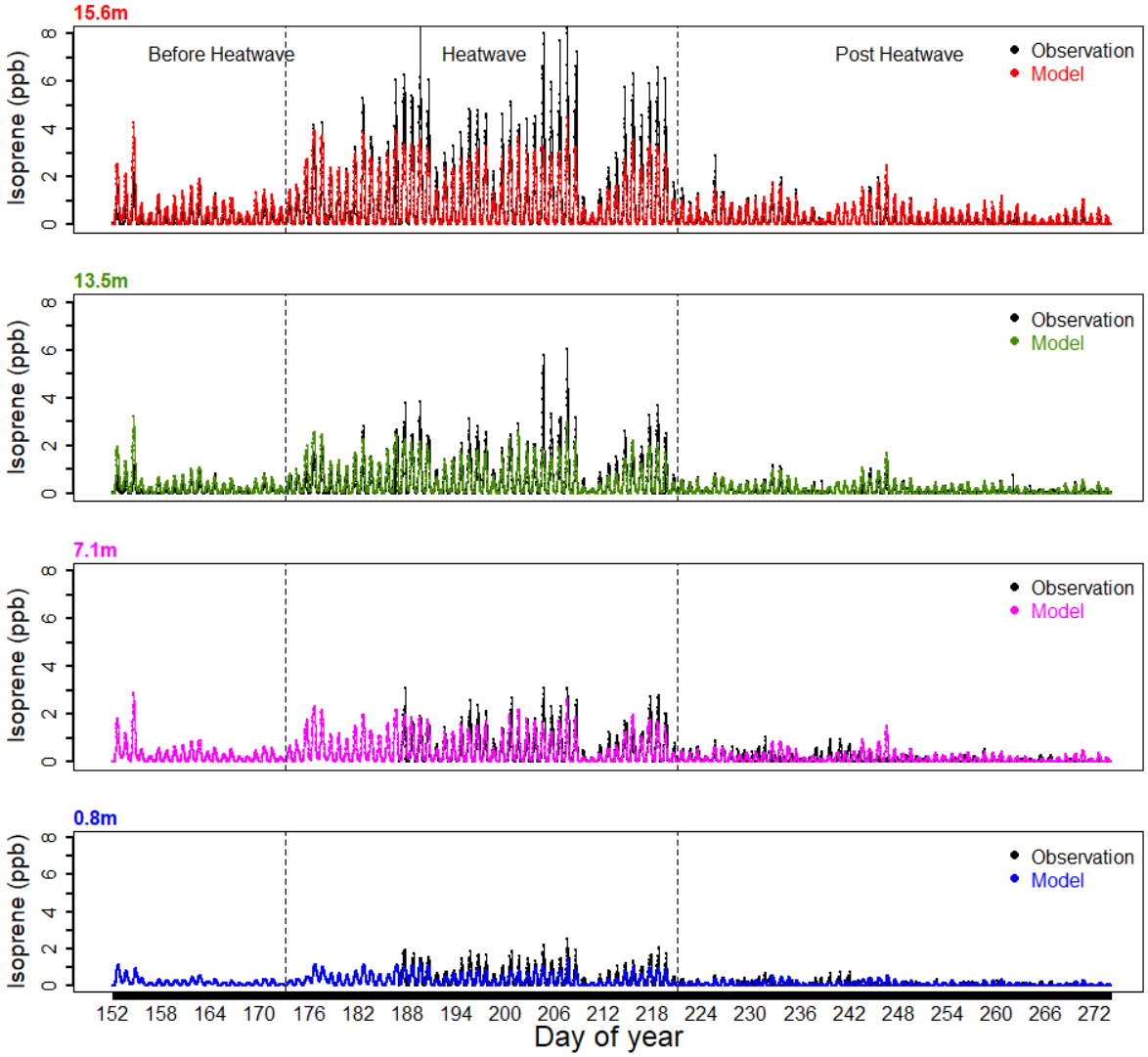

Fig. 4.1. Observed (black) and the reference model scenario isoprene concentrations (unit in ppb) at 4 heights, canopy top (15.6m) in red, mid-canopy (13.5m) in green, trunk-level (7.1m) and the ground level (0.8m) are coloured in magenta and blue, respectively. The x-axis represents the Julian date in 2018, and the vertical dashed lines highlight the heatwave period.

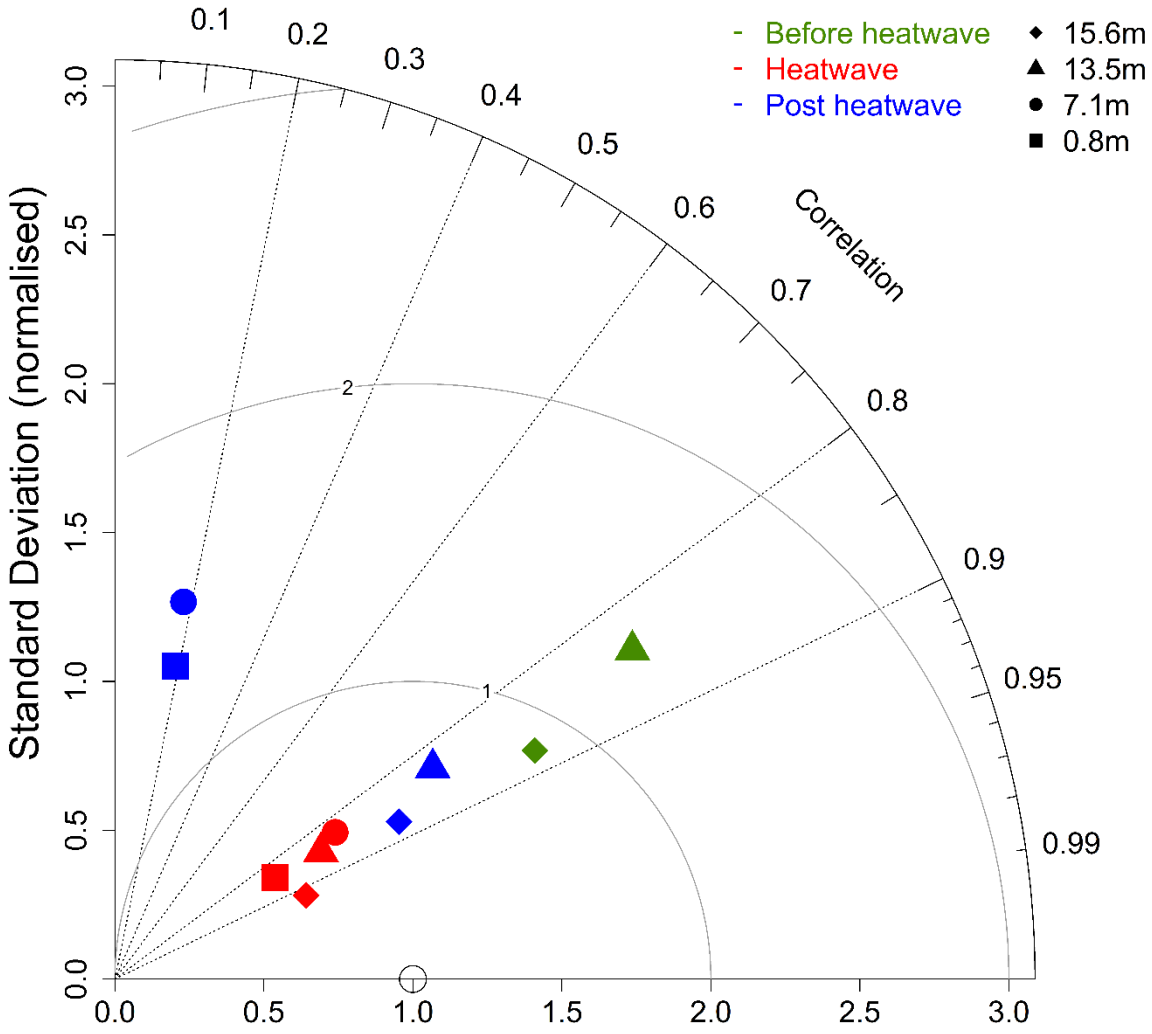

Fig. 4.2. Taylor diagram of the observed and reference scenario (soil NO flux = 0) modelled isoprene with heights. The colours represent before heatwave (green), heatwave (red), and post heatwave (blue). The shapes indicate the selected heights, ground surface (0.8m, ■), mid-trunk level (7.1m, ●), mid-canopy (13.5m, ▲) and canopy top (15.6m, ♦). Isoprene observations were not available for lower heights (0.8m and 7.1m) before the heatwave period.

For evaluation of model performance, we use a Taylor diagram that incorporates both the correlation and root mean squared error (RMSE) (Taylor, 2001). The isoprene mixing ratios from the reference simulation were evaluated with observation data at similar heights (0.8m, 7.1m, 13.5m, and 15.6m), see Fig. 4.2. The points during the heatwave period are well grouped together and show the best model performance at all

heights with a high correlation ($R^2 > 0.8$) and low RMSE. Post heatwave the higher levels (13.5 and 15.6m) also showed good correlations, but there were poorer correlations and high RMSE at lower heights. Unfortunately, observation data were not available at lower heights (ground surface and trunk level) before the heatwave, and therefore it is not possible to evaluate these conditions. In addition, the air temperature and the photosynthetically active radiation (PAR) were higher in the heatwave period (Otu-Larbi et al., 2020). These meteorological conditions enhance chemical reactions in the atmosphere, including photochemistry and oxidation processes. Therefore, we choose to analyse model results from this heatwave period to provide a clear indication of the effects of soil NO fluxes on the forest atmosphere.

Statistical analysis and graphical illustrations were carried out with R version 4.3.1 (R Core Team, 2023). We report the significance of the correlations and the differences based on a p-value <0.05.

4.3 Results & Discussions

4.3.1 O_3 in the 2018 growing season

The O_3 concentrations typically decreased with height and increased with time through the season (Table 4.1 & Fig. 4.3). One of the reasons for the decrease in O_3 from the ground surface to higher levels may be physical deposition on the leaves in the canopy. The O_3 deposition fluxes tend to be high in the canopy where the leaf density is high (Finco et al., 2018). In addition, isoprene concentrations were higher in the canopy (Ferracci et al., 2020; Otu-Larbi et al., 2020) which indicated that the tree canopy is an emission source of isoprene. Isoprene consumes not only OH radicals but also O_3 in oxidation processes. The combined effect of physical deposition in the canopy and chemical loss by isoprene leads to lower O_3 concentrations predicted at the canopy height than at the ground surface.

Table 4.1. Model simulated O_3 concentrations (ppb, mean ± 1 standard deviation) at four selected heights and the average from 0-30m for each period.

Height	Before heatwave	Heatwave	Post heatwave	Period average
15.6m	23.2±8.4	29.4±9.9	33.1±11.3	29.9±10.9
13.5m	26.6±9.9	32.5±11.2	36.7±12.4	33.3±12.1
7.1m	27.2±10.1	33.3±11.2	37.5±12.5	34.1±12.2
0.8m	28.3±9.5	35.2±9.8	39.2±11.8	35.8±11.3
Average <30m	27.2±10.1	33.4±11.1	37.5±12.5	34.1±12.2

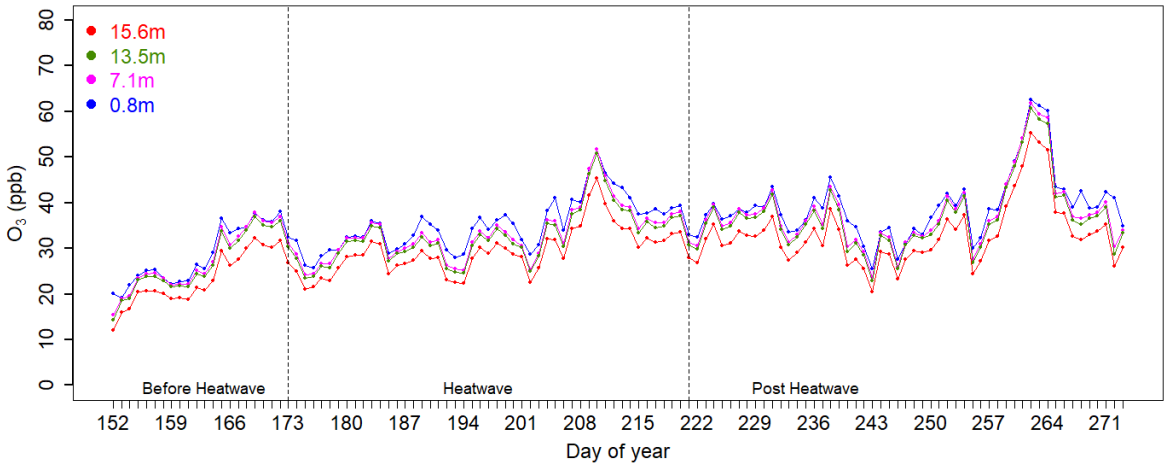

Fig. 4.3. Timeseries of the daily mean O_3 (in ppb) of the reference scenario at four different heights; 0.8m (blue), 7.1m (magenta), 13.5m (green), and 15.6m (red) during the 2018 growing season (Jun-1 ~ Sep-30) at Wytham Woods. The vertical lines highlight the three different periods.

During the heatwave period, when both solar intensity and air temperature were higher than before and after, high isoprene emissions were predicted (Bamberger et al., 2017) and high isoprene concentrations were observed (Ferracci et al., 2020). However, the atmospheric O_3 concentrations after the heatwave period were greater at all heights. Isoprene participates in enhancing both O_3 production and consumption, but increasing O_3 concentrations indicate that isoprene contributed more to production than consumption and this led to net positive O_3 production over the period.

Unfortunately, we have no observations of O_3 on-site over the period. The Oxford St. Ebbes monitoring site is the closest observation station (data archive, Department for Environment Food & Rural Affairs, UK), located approximately 6 km north-west of Wytham Woods. Model simulated mean O_3 concentrations before and during the heatwave (23.2 and 29.4 ppb, respectively) at the top of the canopy (15.6m) were very similar to those at the monitoring site (25.7 and 29.9 ppb). In contrast, there was a larger difference after the heatwave (33.1 ppb modelled vs. 18.8 ppb observed). The main wind directions during the period were south-westerly (Fig. 4.S1) especially in the post heatwave period. However, daytime O_3 was influenced by easterlies at the Oxford monitoring site (Fig. 4.S2). Furthermore, high local NO emissions during the post heatwave nighttime (Fig. 4.S3) could lead to titration of O_3, and lower observed mean O_3 concentrations. It is also possible that the boundary conditions applied here were not well suited to the post-heatwave period if it was affected by local influences. Therefore, further analysis here will focus on the heatwave period.

4.3.2 Impact of soil emission on O_3

The positive soil NO flux scenario and the reference were analysed to investigate the impact of soil NO emissions on forest O_3 concentrations. The O_3 differences between the two scenarios (dO_3 = O_3 in soil flux scenario – O_3 in the reference) are presented in Table 4.2 and the daily mean dO_3 is illustrated in Fig.4.4. Soil NO emissions directly affect both O_3 production through photochemistry and removal through titration by NO (Eq.1). Near the ground surface (0.8m), close to the soil NO emission source, O_3 reductions were predicted due to titration by NO. NO_x was transported upwards and led to enhanced O_3 production, giving significantly different dO_3 behaviour to the ground surface. The O_3 increase was about three times higher during the heatwave (Table 4.2) than during the other periods ($p < 0.001$). However, the lowest level did not show a clear difference between the periods ($p > 0.1$).

Table 4.2. Summary of the ozone differences (in ppb) due to positive soil NO emissions (mean ± 1 standard deviation). The column means were averaged up to 30 m.

Height	Before heatwave	Heatwave	Post Heatwave	Period average
H = 15.6m	0.4±0.2	1.4±0.5	0.4±0.2	0.8±0.55
H = 13.5m	0.5±0.2	1.6±0.6	0.5±0.2	0.9±0.60
H = 7.1m	0.4±0.3	1.5±0.6	0.4±0.2	0.8±0.59
H = 0.8m	-1.1±1.1	-1.1±1.9	-1.2±1.1	-1.1±1.5
Average <30m	0.3±0.6	1.2±1.2	0.2±0.7	0.6±1.0

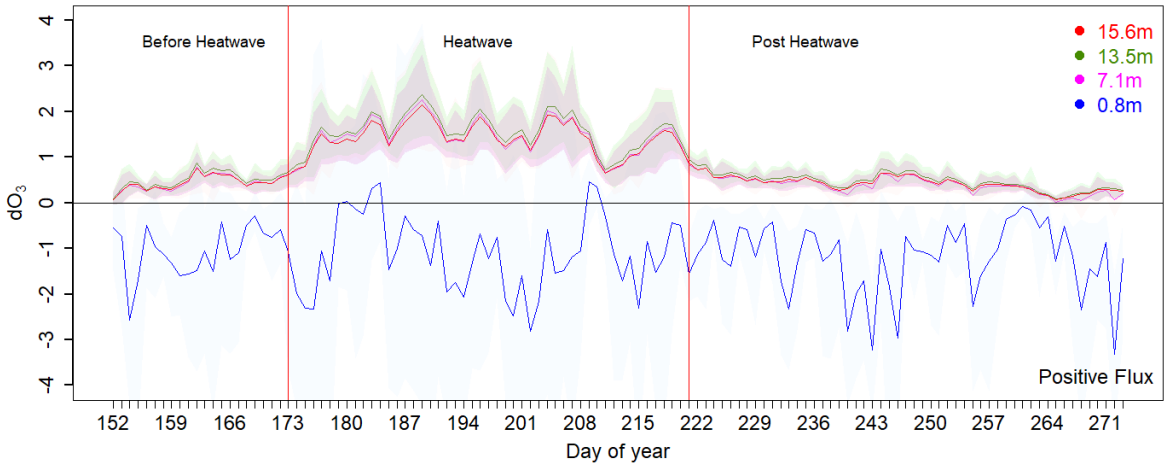

Fig. 4.4. Daily mean of the O_3 difference (dO_3, ppb) between the soil NO emission scenario and the reference. The shaded area represents the range of the daily maximum and minimum dO_3.

The range between maximum and minimum dO_3 at 30-minute resolution over the day (shaded in Fig. 4.4) also confirms that changes during the heatwave period were larger than in the other periods. Moreover, the ranges were largest at the ground surface, close to the emission source. The maximum dO_3 at 0.8m was even greater than at the three upper heights on more than 80% of the heatwave days, highlighting the large variability close to the surface. At greater heights, the more abundant isoprene (as shown in Fig 4.1) produces more peroxy radicals through oxidation. NO could then efficiently be

converted into NO_2 with peroxy radicals, without consuming O_3 (Eq. 4.4 ~ 4.5), and hence contribute to O_3 production. The maximum and minimum dO_3 are both positive, which indicates that enhancement of O_3 production always exceeds direct titration by NO.

The higher average dO_3 during the heatwave at the trunk and canopy heights suggest that O_3 production is enhanced by high air temperature and solar radiation during the heatwave period. However, the mean dO_3 at 0.8m height is negative, representing O_3 removal and there is no clear difference between the periods. Further, the positive maximum to negative minimum dO_3 during the heatwave indicates the role of NO in the atmosphere, producing O_3 in the daytime but titrating O_3 during the nighttime (Fig. 4.5).

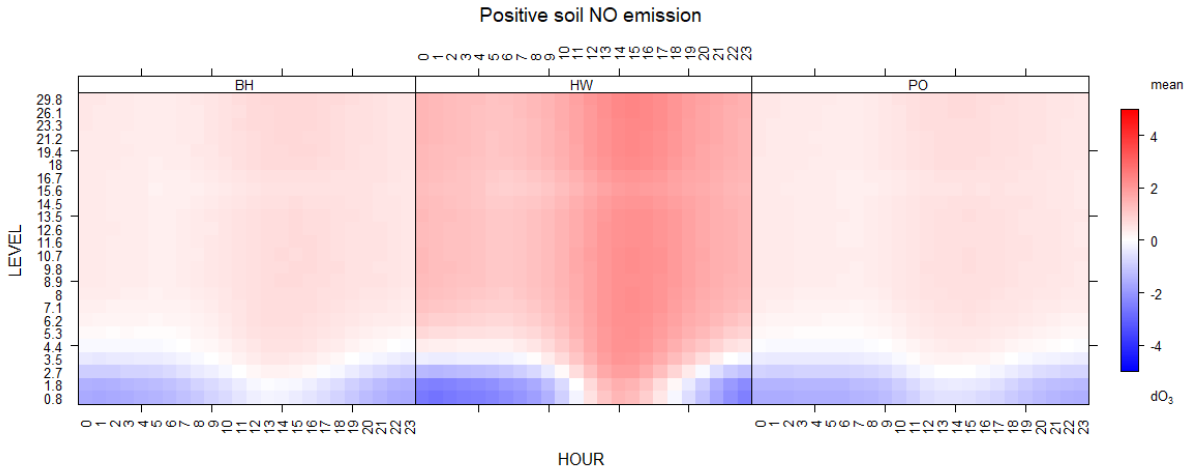

Fig. 4.5. Contour plot of O_3 difference (dO_3, unit in ppb) due to soil NO emissions. Diurnal differences are shown for three different periods: before heatwave (BH), heatwave (HW), and post heatwave (PO).

The diurnal patterns of dO_3 in the forest in the different periods look similar, but the magnitude was higher in heatwave conditions (Fig. 4.5). The diurnal dO_3 variations were different with height, and in particular the ground surface was different to the heights above. A distinctive diel pattern was found during the heatwave period near the ground surface; negative dO_3 was found in late afternoon to morning due to NO_x titration, but positive differences were found in daytime due to O_3 production through

photochemistry. In contrast, heights above 3m show enhanced O_3 (positive dO_3) day and night. Furthermore, afternoon high dO_3 indicates that the soil NO emission provided an enhancement of O_3 via photochemical reactions. Isoprene, an important BVOCs from broad leaf trees, was observed at higher concentrations during the heatwave than in other periods (Otu-Larbi et al., 2020). With high solar radiation and temperature, abundant isoprene could be oxidised and form more RO_2 radicals during the heatwave than in other periods, which contributes to higher O_3 production. As a result, the afternoon O_3 increase in the heatwave period at the ground surface could suggest vigorous O_3 production that exceeds removal. Although soil NO emissions increase O_3 at the ground surface (0.8m) in the daytime (12~18h) by up to 1.4 ppb, the titration impacts were much bigger (up to 2.7 ppb at 1:00h) and longer than the increase during the daytime. As a result, soil NO emissions reduced O_3 by 1.1 ppb over the day. However, above 3m height the O_3 difference is positive (0.58 ppb) at all times and increases with height in the canopy. Especially, O_3 increments were in the range 1.4~1.6 ppb in the canopy (8~18m) and are greater above the canopy (18 to 30m) by 1.6 to 1.7 ppb. Throughout the growing season of 2018, below 30m soil NO emissions typically enhance O_3 production in the forest canopy atmosphere. Although soil emissions reduced O_3 at the surface (~3m), production at upper levels of the canopy outweighs this removal.

4.3.3 Impact of soil absorption on O_3

In the soil NO absorption scenario, the O_3 generally decreased compared to the no flux scenario (Table 4.3 and Fig. 4.6). All heights showed a decline in O_3, and there was no significant difference between heights ($p>0.1$). The heatwave period shows a dramatic decrease at all heights, with a reduction more than three times larger than in the other periods (Table 4.3), a significant difference ($p<0.001$). Although both positive and negative soil NO fluxes show an O_3 decrease at the ground surface, the mechanism is not the same. A positive soil flux led to increased titration of O_3, but with a negative soil flux, which removes NO from the atmosphere, there is depletion of precursors and O_3 production is reduced.

Table 4.3. Summary of the ozone difference (in ppb) due to soil NO absorption (mean ± 1 standard deviation).

Heights	Before Heatwave	Heatwave	Post Heatwave	Period average
H = 15.6m	-0.2±0.1	-0.9±0.3	-0.2±0.1	-0.5±0.5
H = 13.5m	-0.3±0.1	-0.9±0.4	-0.3±0.1	-0.5±0.4
H = 7.1m	-0.3±0.1	-1.0±0.4	-0.2±0.1	-0.5±0.4
H = 0.8m	-0.2±0.4	-0.9±0.6	0.0±0.2	-0.4±0.6
Average <30m	-0.2±0.2	-1.0±0.4	-0.2±0.2	-0.5±0.5

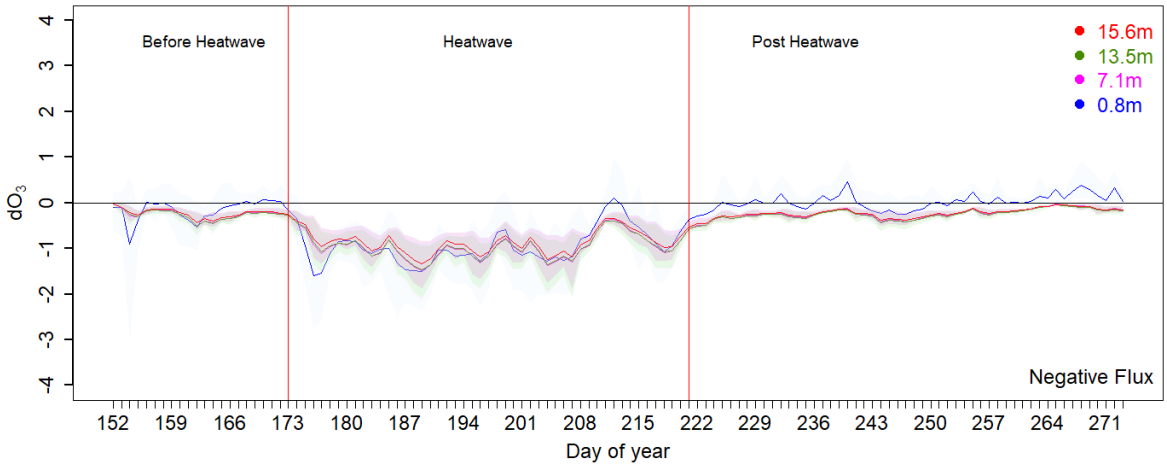

Fig. 4.6. Time series of simulated daily mean ozone difference (dO_3, ppb) at different heights due to soil NO absorption (f = -0.005 nmol m^2 s^{-1}). The shaded area represents the range of the daily maximum and minimum dO_3.

Similar to the scenario with the positive soil NO flux, daily minimum to maximum ranges were broader at all heights during the heatwave period. Also, the lowest height showed a larger range than the other heights. This scenario consistently removes NO from the atmosphere, limiting O_3 production and reducing titration, and predicts a smaller range than the positive flux scenario. However, while differing in sign, the magnitude of the changes in O_3 were similar not only overall (+0.6 vs. -0.5 ppb) but

also during the different periods (+0.3 vs. -0.2 ppb before heatwave, +1.2 vs. -1.0 ppb during the heatwave, and +0.2 vs. -0.2 ppb after the heatwave period). Considering that the applied soil NO sink is half the magnitude of the applied soil source (-0.005 vs. 0.011 nmol m^2 s^{-1}), it is clear that the impact of the soil NO flux on O_3 is not linear. These results suggest that soil NO absorption likely has a stronger impact on O_3 concentrations in the atmosphere than soil NO emissions at a surface level.

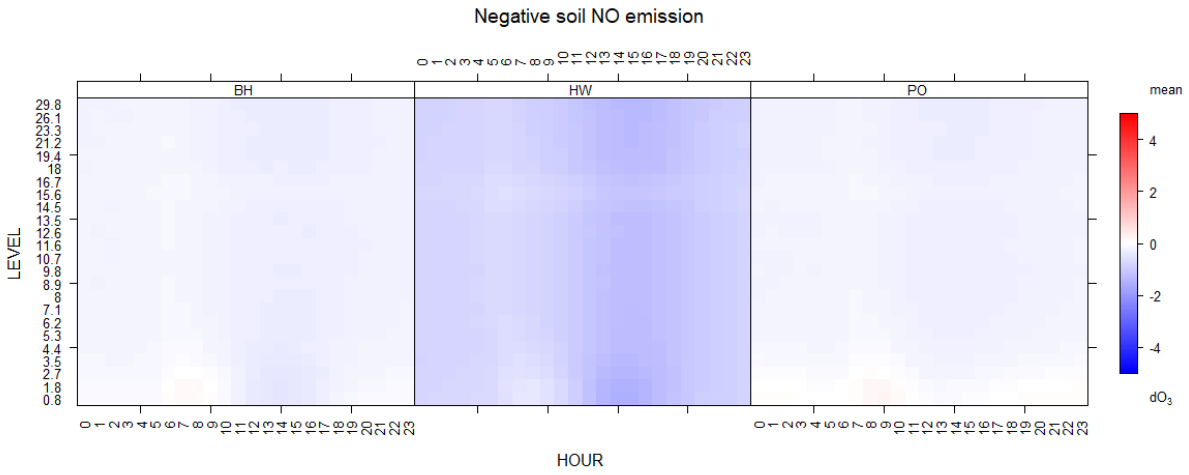

Fig. 4.7. Contour plot of O_3 difference (dO_3, ppb) due to soil NO uptake. Diurnal differences are shown for three different periods: before heatwave (BH), heatwave (HW), and post heatwave (PO).

The diurnal variation of the O_3 difference (dO_3 = soil uptake scenario – reference) with height under the soil NO absorption scenario is shown in Fig. 4.7. Almost all times and heights show a decline of O_3, but before and after the heatwave there is a small increase of O_3 near the surface in early morning. This small increase is likely to be due to the combined effect of soil NO uptake from the atmosphere and accumulation of O_3 at lower heights. The stable nocturnal boundary layer allows accumulation near the ground surface, but constant soil NO uptake limits titration that removes O_3 in the early morning.

However, there is clear decrease of O_3 at all times and heights during the heatwave period. The decrease in O_3 is largest in the afternoon coincides with the highest isoprene

in the atmosphere. The soil NO uptake scenario continuously removes NO and limits O_3 production. At the same time, isoprene reacts not only with OH but also with O_3, which consumes O_3. In consequence, more O_3 is consumed under higher concentrations of isoprene during the heatwave period than in the other periods. Thus, with limited O_3 production and consumption by BVOCs, soil NO absorption results in a decrease in O_3 at the ground surface even in the afternoon during the heatwave period.

4.3.4 Influence on photochemistry in the forest atmosphere

During the heatwave period, when soil fluxes are expected to have the largest impact on O_3, HO_x radicals (OH and HO_2), HONO, isoprene and methacrolein (MACR) + methyl vinyl ketone (MVK) were found to show a clear diel variation (Fig. 4.8). Both MACR and MVK (C_4H_6O) are the oxygenated products of isoprene oxidation, and we consider here the sum of MVK+MACR.

Both OH and HO_2 radicals increase with sunlight, rising from dawn at ~05:00 to a peak at 13:30, slightly later than the peak of the maximum sunlight intensity observed at noon (Ferracci et al., 2020). The major processes producing radicals are related through photolysis and photochemistry (Atkinson, 2000), and there is a time lag between the peak in solar radiation and maximum radical concentrations (Stone et al., 2012; Brune et al., 2016). Soil NO fluxes also affect the isoprene oxidation process and HO_x radical chemistry (Fig. 4.8). At the lowest height (0.8m) near the ground surface there is a bigger impact on both OH and HO_2 radicals than in the mid-canopy (Fig. 4.8a and 4.8c). At both heights, soil NO emissions increase and soil NO uptake decreases OH radicals compared to the reference (f=0).

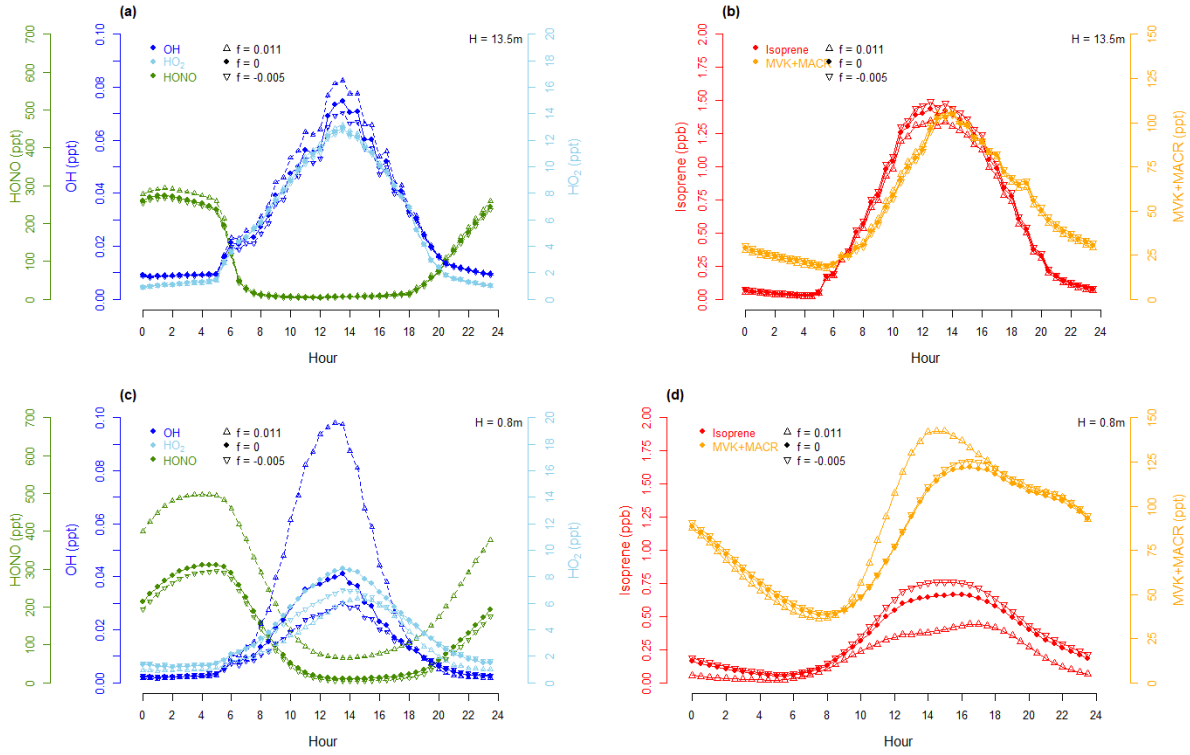

Fig. 4.8. Diurnal variations of HO_x radicals, including OH (blue) and HO_2 (skyblue), HONO (green), MVK+MACR (orange) and isoprene (red). Panel (a) and (c) display HO_x radicals and HONO at mid-canopy (13.5m) and ground level (0.8m), figure (b) and (d) show MVK+MACR and isoprene at the same heights, respectively. The lines with filled dots are the scenario with no soil flux, open triangle is for the positive soil flux, and open reverse triangle lines are the negative soil flux. The time resolution is every 30 minutes, The unit of isoprene is ppb, HO_x, HONO and MVK+MACR are in ppt levels.

OH radicals are principally generated by photolysis of O_3 followed by reaction with water vapour (Eq. 4.6 ~ 4.7). In addition, an early morning OH increase might be induced by the photolysis of nitrous acid (HONO), which is rapidly dissociated by weak sunlight in the early morning (Eq. 4.8).

$$O_3 + h\nu \rightarrow O^1D + O_2 \qquad \text{Eq. 4.6}$$

$$O^1D + H_2O \rightarrow 2OH \qquad \text{Eq. 4.7}$$

$$HONO + h\nu \rightarrow OH + NO \ (300nm < \lambda < 405nm) \qquad \text{Eq. 4.8}$$

The diel variations of HONO and HO_x radicals (Fig. 4.8a and 4.8c) strongly influence oxidation processes in this environment. OH increases rapidly in the early morning (05:00 ~ 06:00) following photolysis of HONO. A small decrease in OH was found during 06:00 ~ 07:30, but there is then a rapid increase again after 08:00. This suggests that early morning OH is initiated by photolysis of HONO, and photolysis of O_3 and the water vapour reaction take over generation of OH a little later in the morning. In addition, oxidation of NO to NO_2 supports HO_2 to OH conversion at the same time (Eq. 4.5), so the contribution of OH increases when NO is available, . Furthermore, the role of soil NO fluxes is clearly illustrated at the 0.8m height (Fig. 4.8c) after 06:00, where the difference between positive and negative scenarios starts to become larger. The positive soil NO flux continuously provides NO to the atmosphere and contributes to increasing OH from HO_2. On the other hand, the negative soil flux competes, consuming NO, resulting in lower OH.

HONO concentrations are higher with soil NO emission. HONO formation occurs through heterogeneous dark reaction of NO_2 and water vapour (Rohrer et al., 2005; Li et al., 2008), and also direct formation from NO and OH (Kleffmann and Gavriloaiei, 2005; Yang et al., 2014). As NO_x is essential to produce HONO, soil NO emissions supply NO_x to the atmosphere and contribute to HONO formation. High mixing ratios are found at nighttime, and these rapidly decrease with sunrise at 05:00. HONO at the lowest height (0.8m) starts to decrease 30min to 1 hour later than at higher levels, and the rate of decrease is smaller, because the canopy reduces sunlight exposure. The mixing ratios of HONO were almost depleted in daytime except at the surface for the positive soil NO flux scenario. NO emission from the soil supplies NO continuously to the atmosphere, allowing direct production of HONO, and this is greater than loss even during the daytime.

The mixing ratio of HO_2 radicals was not significantly different at the mid-canopy (13.5m) for any of the soil NO flux scenarios. However, both positive and negative soil NO fluxes contribute to a reduction in HO_2 near the surface. Emitted NO directly reacts with HO_2 to generate OH, and absorption of NO contributes to a low NO_x environment that limits oxidation of BVOCs (e.g. producing MVK and MACR) and HO_2 dominates the peroxy radical reactivity (Atkinson, 2000; Nguyen et al., 2014; Wennberg et al., 2018).

The diel patterns of isoprene (Fig. 4.8b and 4.8c) show that concentrations are higher during the daytime than the nighttime, and maximum concentrations are found in the afternoon. The dominant emission source of isoprene is plant leaves, and high solar radiation and increasing temperature are the major driving parameters for isoprene emission. The mid-canopy isoprene concentrations were estimated to be as much as twice those at the ground surface as they are close to the emission source. Moreover, OH and O_3 directly participate in oxidation of isoprene and generate MACR and MVK in the presence of NO during daylight hours (Pierotti et al., 1990; Wennberg et al., 2018). Isoprene increased after sunrise, and MVK+MACR started to increase after 08:00 in the morning, roughly 2 hours later than the isoprene increase. This time lag highlights the weak oxidation capacity in the early morning and indicates the time required to oxidise isoprene to MVK+MACR. The daytime isoprene concentrations at 0.8m remained at similar concentrations with a smaller variational range for several hours near the ground surface (Fig. 4.8d), and this is different from the mid-canopy (Fig. 4.8b) where isoprene diurnal variations showed a clear peak and high concentrations at mid-day. Isoprene emissions typically increase with solar radiation and temperature, and concentrations and fluxes are maximum in the afternoon (Park et al., 2011; Kim et al., 2015; Mo et al., 2018). Which indicates more isoprene loss and resulted the emission and loss rates are similar at the low height in the mid-day.

The mean MACR+MVK concentrations at ground level are approximately 58% higher than in the mid-canopy for the no-soil NO flux scenario. The maximum MACR+MVK concentrations at 13.5m height were found at 14:00 (Fig. 4.8b, all three scenarios), and those at 0.8m (Fig. 4.8d) peaked at 16:30 for the soil NO uptake and reference scenarios, but at 14:30 for the soil emission scenario. Although a higher isoprene concentration was estimated for the soil NO uptake scenario near the surface, MACR+MVK concentrations were similar to the reference. The soil NO uptake scenario absorbs near ground surface NO and leads to lower NO at 0.8m height than the other scenarios. Isoprene consumes more HO_x radicals under the low NO condition and HO_2 dominates the peroxy radical reactivity that limits MACR and MVK production (Nguyen et al., 2014; Wennberg et al., 2018). Therefore, MACR+MVK in the soil uptake and reference scenarios reached a maximum 2 hours or more later than in the soil NO emission scenario. As more isoprene is consumed by oxidation processes,

demand for OH increased and O_3 was also impacted by isoprene oxidation. These results demonstrate the important role of NO in isoprene oxidation, which contributes to isoprene and MACR+MVK diel variations and magnitudes.

Furthermore, as NO influences OH radicals and the isoprene oxidation process, the lifetime of isoprene is also affected by soil NO fluxes, especially close to the ground surface. At 13:30 when the OH concentrations are at a maximum during the day, the lifetime of isoprene at the 15.6m height decreases 9% with soil NO emissions and increases 6% with soil uptake. The impact is bigger close to the ground surface. The isoprene lifetime to OH at 0.8m height was estimated to be 3.1 hours in the reference scenario. The positive soil NO flux reduced the lifetime by more than 58%, (to 1.3 hours), and the soil uptake increased the isoprene lifetime by 38% (to 4.3 hours). These soil NO impacts on the isoprene lifetime provide strong evidence for the importance of soil NO fluxes on atmospheric oxidation capacity and photochemistry in the forest environment.

4.3.5 Influence of the forest canopy structure

As discussed, atmospheric photochemistry is influenced by meteorological conditions such as temperature and solar radiation. However, the vertical structure of the forest is also an important consideration. The vertical structure consists of three spaces with distinct physical features: trunk level space, canopy with leaves and free air above the canopy. In particular, the tree canopy plays an important role in both isoprene emission and physical deposition because the high density of leaves provides a large surface area.

The vertical profile of gaseous species at 13:30 (Fig. 4.9), the time that HO_x radicals are maximum, clearly shows the influence of the forest structure. Especially, the region within the canopy (8~18m) plays an important role for gas species.

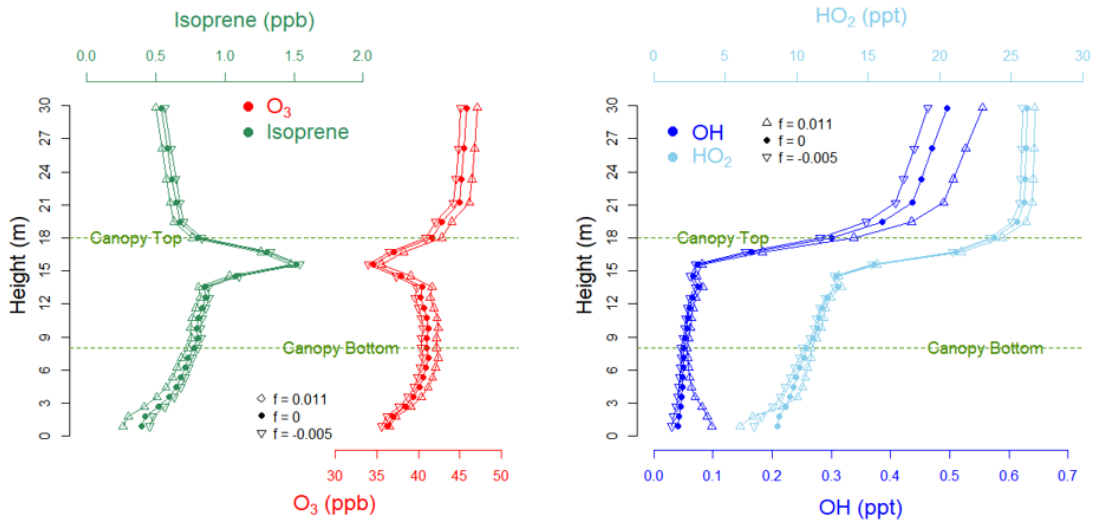

Fig. 4.9. Vertical profile at 13:30, when HO_x radicals are at a diurnal maximum. The left panel (a) displays O_3 (red) and isoprene (green) in ppb, the right panel (b) shows OH (blue) and HO_2 (skyblue) in ppt. The lines with filled circle indicate the reference (f=0), x marks and + marks indicate the negative and positive soil flux scenarios. The forest canopy is indicated with dotted lines (8–18m height).

Isoprene was found to gradual increase with height from the ground, with a large increase from 13.5m (0.81~0.88 ppb) to 15.6m (1.48~1.54 ppb), and a rapid decrease at the top of the canopy (0.76~0.83 ppb at 18m). The concentrations gradually decrease with height above the canopy. The vertical distribution indicates the height of the dominant isoprene emission source at 15.6m. The leaf density is usually high in the upper canopy (maximum leaf area index at 15.6m in Wytham Woods) but is less dense at the very top of the tree (e.g. Finco et al., 2018), while the bottom of the canopy is shaded by the leaves above so that there is less light exposure. Both light exposure and leaf temperature are important parameters that control isoprene emissions (Guenther et al., 1991; Guenther et al., 1993; Gunther et al., 2006). The leaf temperature is typically higher at the top of the canopy where they are directly exposed to solar radiation but is less low in the canopy where leaves are in shade (Rey-Sánchez et al., 2016). Accounting for leaf density, leaf temperature and light exposure, isoprene emissions are expected to be maximum in the upper canopy (15.6m) rather than at the top of the canopy. A positive soil NO emission flux decreases isoprene at all heights, and the soil NO uptake contributes to a small increase. As atmospheric NO contributes to isoprene oxidation,

bigger differences in isoprene concentrations are found at lower heights under the positive soil NO flux scenario.

Higher O_3 is found with elevated height in general (Fig. 4.9a), but distinctive below canopy (< 8m). A noticeable drop in O_3 was found in the upper canopy, centred on 15.6m, coinciding with the increase in isoprene. O_3 then increases again above the top of the canopy. The tree canopy consists of dense leaves and abundant isoprene emissions, and the vertical profile of O_3 is influenced not only by chemical consumption through isoprene oxidation, but also by dry deposition on the leaves. O_3 increased at all heights in the positive soil NO flux scenario and decreased in the negative soil NO flux case. These results indicate that daytime O_3 production in the forest is influenced by soil NO fluxes, and vertical distributions are affected by forest structures.

Both OH and HO_2 radicals were found to be high above the canopy but much lower in the upper canopy (Fig. 4.9b). Right above the canopy (19.5m) OH and HO_2 mixing ratios were 0.36~0.44 ppt and 25.0~26.0 ppt respectively, however, in the upper canopy OH was 0.07~0.08 ppt and HO_2 was 12.7~13.0 ppt. Although soil NO emissions supported higher HO_x mixing ratios in general, HO_2 below 2m height (e.g. 6.0 ppt at 0.8m) was lower than in other scenarios. At the same time, OH mixing ratios increased. At heights below 2m, HO_2 radicals react with NO emitted from the soil (Eq. 4.5) and convert NO to NO_2 generating OH. NO_x conversion with HO_x radicals also occurs at greater heights, so that soil NO emissions increase the total HO_x radical budget and soil NO uptake reduces it. The vertical profiles of HO_x radicals demonstrate the impact of the forest structure and emission sources on atmospheric chemistry. In summary, isoprene emission from the dense leaves in the canopy affects the consumption of HO_x radicals. The soil is a potential source and sink of NO, influencing HO_x cycling and limiting isoprene oxidation pathways.

Another important role of the tree canopy is its contribution to deposition (Fig. 4.10). The tree leaves provide a large surface area that allows dry deposition of O_3 from the atmosphere to the leaves. In accordance with the leaf area, the maximum O_3 deposition rates were estimated at 15.6m (3.7 ppb/min) during the heatwave period, which was almost five times higher than those at 13.5m (0.8 ppb/min). Furthermore, deposition rates were higher in the daylight hours than at night, as they are dependent on stomatal uptake (Fares et al., 2007; 2010). As stomatal conductance is influenced by

meteorological conditions (e.g. light exposure, temperature, and vapour pressure deficit), not only isoprene concentrations but also O_3 deposition rates were estimated to reach a maximum in the afternoon. In addition, under the positive soil NO emission scenario the dry deposition of O_3 was slightly higher (3.9 ppb/min) than in the reference and up to 7.1 ppb/min of O_3 were estimated to be deposited on the leaf surface. The O_3 dry deposition rate from the soil NO emission scenario was 4.8% higher than in the reference scenario at 15.6m height during the heatwave. On the other hand, soil NO uptake resulted in lower O_3, and the dry deposition rates were also smaller (3.6 ppb/min for average, up to 6.7 ppb/min). Although the soil NO flux does not directly affect stomatal conductance, it affects O_3 concentration in the air and influences the magnitude of O_3 deposition.

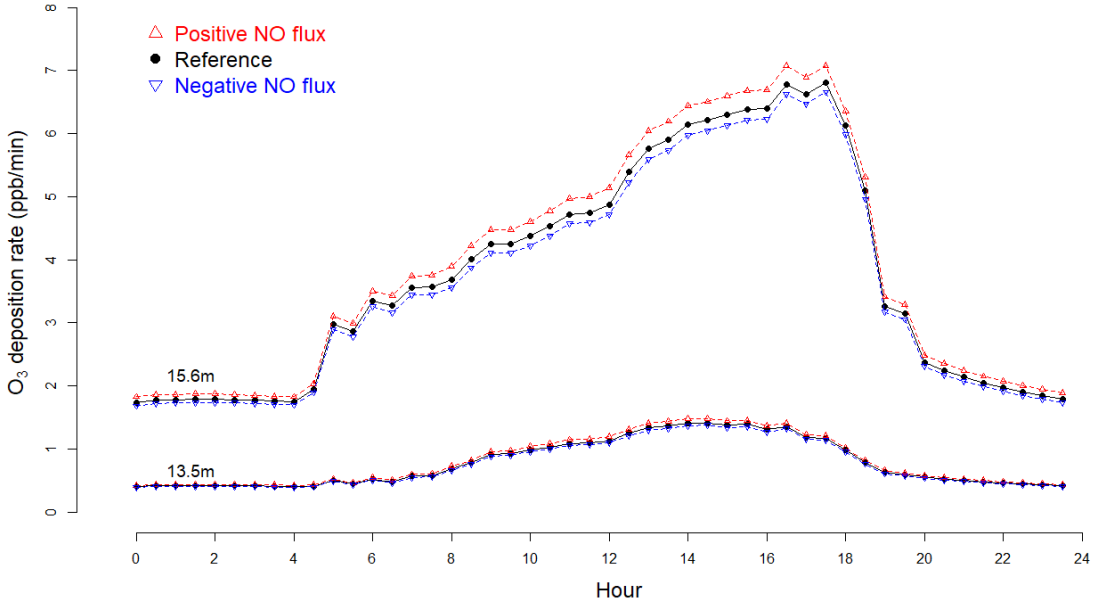

Fig. 4.10. Diel variations of O_3 deposition rates (ppb/min) during the heatwave period for different scenarios at the mid-canopy (13.5m) and top canopy (15.6m).

4.3.6 Future implications of the soil NO flux

As global climate change continues, soil NO emission is expected to increase in the future as surface temperatures get warmer (Schindlbacher et al., 2004; Medinets et al., 2016; Chapter 2). Therefore, the impact of soil emission is also expected to be bigger than in current environmental conditions. To investigate the implication of these projections, the soil NO flux was scaled by a factor of two (f=0.022) and four (f=0.044) to reflect the potential impacts of future climate change. Figure. 4.11 illustrates the model simulated mean O_3 concentrations of each period at four heights for the selected soil NO fluxes. O_3 concentrations linearly increase with increasing soil NO flux (R^2 >0.95, $p<0.05$), except at 0.8m height. NO is released from the surface which titrates O_3 and produces NO_2 in the atmosphere, and this NO_2 affects upper heights and generates O_3. Furthermore, NO to NO_2 conversion via peroxy radicals leads to O_3 production which increases O_3 concentrations at higher altitudes. These impacts are directly related to the magnitude of the soil NO flux. For instance, O_3 is 5% higher in the positive soil NO emission scenario (f=0.011) during the heatwave period at the top canopy. Increasing soil NO emissions (f=0.022 and 0.044) gives near-linear increases in O_3 concentrations of 9% and 17% compared to the reference, respectively. At trunk (7.1m) and canopy (13.5 and 15.6m) heights the O_3 increase is about three times greater in the heatwave period than in the periods before and after, which were similar (see regression equations in Fig. 4.11). At the ground surface height (0.8m) the relationships are negative and non-linear. Quadratic regressions provide a better fit for each period (R^2 >0.98) than linear regressions (e.g. heatwave $R^2 = 0.91$). Surface O_3 concentrations were decreased by soil fluxes under either soil NO emission or consumption.

These relationships demonstrate the importance of soil NO emissions on forest O_3 in the future. As a response to global warming and extreme climates including prolonged drought and heatwaves, the soil NO emission rates are likely to increase (Medinets et al., 2016; Chapter 2) and hence forest O_3 will also increase in forests at trunk heights and above. The increasing O_3 at the canopy heights could damage plant leaves and lead to a decline in plant activities such as photosynthesis and gross primary production.

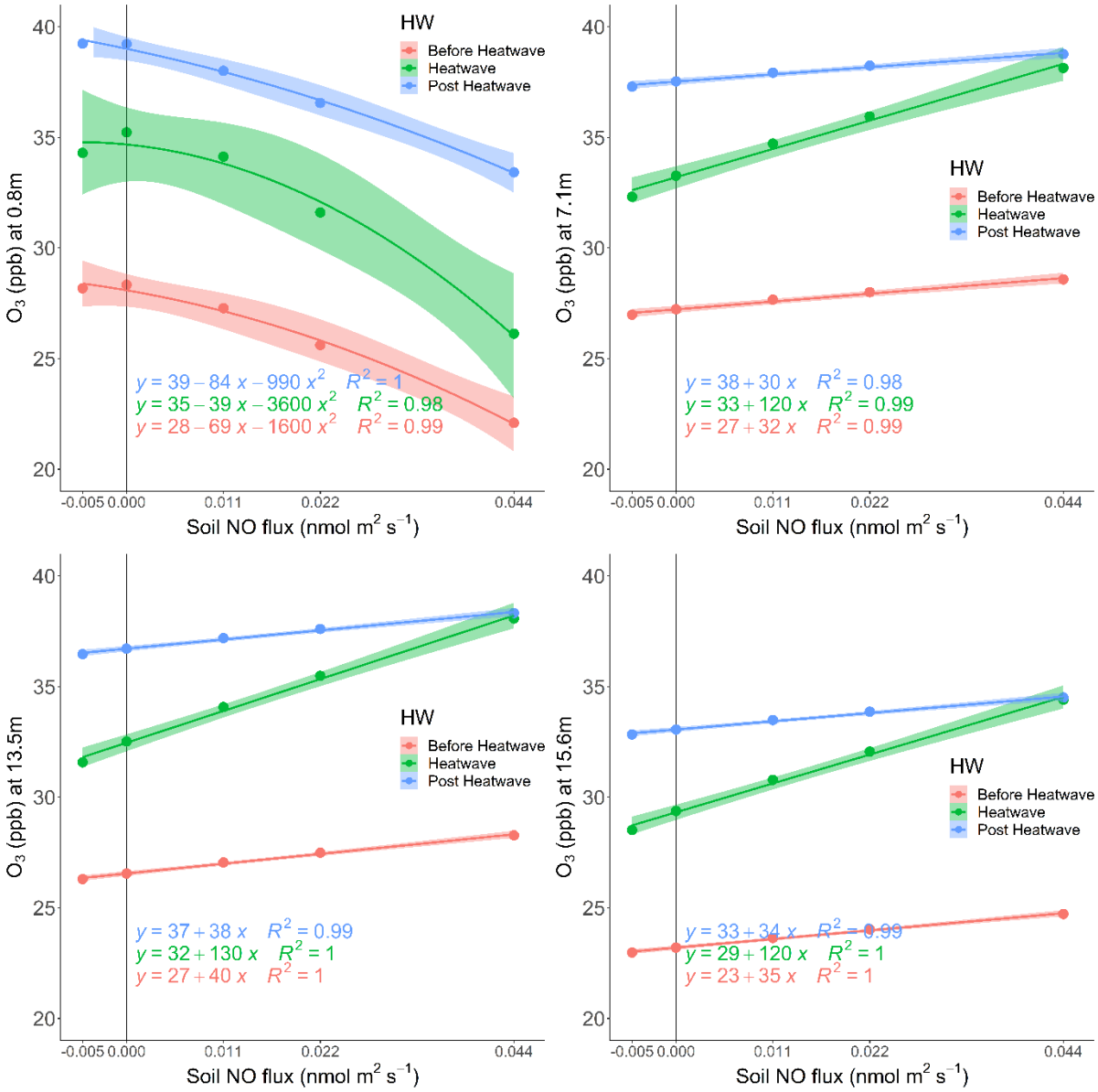

Fig. 4.11. Simulated changes in mean O_3 concentrations at each height in the forest under a broad range of soil NO emissions fluxes ($-0.005 \leq f \leq 0.044$) reflecting the effects of future climate change. Red points represent O_3 concentrations before the heatwave period, green and blue indicate the heatwave and post heatwave, respectively. The 95% confidence intervals are shown by the shaded areas on each regression line.

4.4 Conclusions

This study investigates the impact of soil NO fluxes on forest atmospheric chemistry during the growing season, including the effects of both soil emission and uptake. Although soil typically emits NO to the atmosphere, soil NO uptake can occur where soil nitrogen is limited. This study explores the impacts at Wytham Woods considering the vertical structure of the forest and a heatwave with prolonged drought period. With a soil NO emission flux (f=0.011 nmol m^{-2} s^{-1}, Chapter 2), O_3 concentrations at 0.8m height were reduced by 1.1~1.2 ppb due to titration by NO emitted from the soil, throughout the period. However, average O_3 concentrations below 30m height during the growing season were approximately 0.6 ppb higher than in a reference scenario with no soil emissions. The O_3 concentration increase was twice as large (1.2 ppb) during the heatwave period, reflecting the greater isoprene emission and more active photochemistry. The soil NO emissions also influenced HO_x radicals and the lifetime of the isoprene, for example, reducing the isoprene lifetime to removal by OH radicals by 58% at 0.8m height in the afternoon. In contrast, with a soil uptake flux (f=-0.005 nmol m^{-2} s^{-1}), absorbing NO from the atmosphere, O_3 concentrations during the growing season were about 0.5 ppb lower, and about 1.0 ppb lower during the heatwave period.

As global climate is changing, the atmosphere is getting warmer and more extreme conditions are expected. In response to these changes, soil NO emissions are expected to increase in the future. Forest atmospheres are characterised as NO_x-limited environments with abundant BVOCs and limited NO_x emission sources. Although soil NO fluxes and O_3 concentrations show a non-linear inverse relationship, the O_3 at heights above trunk levels linearly increases with soil NO emissions. Furthermore, the gradient during the heatwave period was found to be about 2.5 times higher than before the heatwave and up to 4 times higher than after the heatwave period.

This study demonstrates that the effect of soil NO emissions on the forest atmosphere are not negligible, and that the impacts are likely to be greater in the future. Furthermore, diurnal and vertical profiles of O_3 and HO_x radicals highlight the contribution of different emission sources; NO from the soil and isoprene from the tree canopy. In addition, the results could help in selecting measurement inlet heights for

forest campaigns and suggest that soil NO fluxes need to be measured to help with interpretation of atmospheric chemistry measurements below the canopy. Therefore, it would be valuable to conduct field observations not only measuring gas concentrations but also fluxes from a variety of sources such as soil and vegetation. Moreover, monitoring climatic and pedoclimatic conditions, and soil characteristics would be valuable to quantify and explain soil NO fluxes and to allow further interpretation of the impacts on the atmosphere and nitrogen cycle. Model simulations using this field data along with projections of future climate change would be highly valuable to improve understanding of the role and importance of soil NO fluxes on the forest atmosphere.

Supplementary materials for Chapter 4

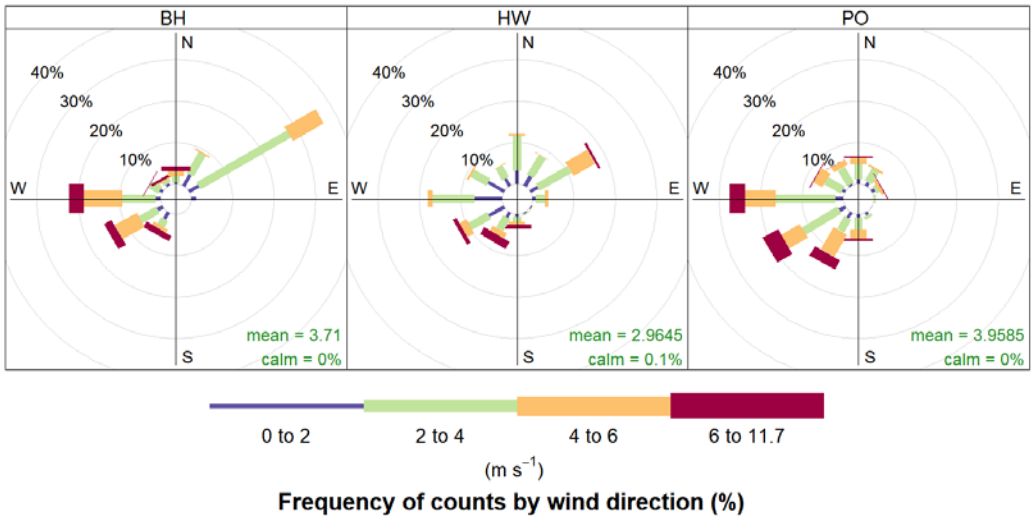

Fig. 4.S1. Windrose at the Oxford St. Ebbes during the growing season in 2018 (Jun-01 to Sep-30) split in the heatwave period. The wind data were collected from UK-Air (Defra) archive. The main wind directions were south-east for all periods, but also great frequency of north-east wind observed except post heatwave period as similar as observed in Wytham Woods (Ferracci et al., 2020). The heatwave period observed the lighter winds (mean = 3.0 m s^{-1}) than before (3.7 m s^{-1}) and post heatwave (4.0 m s^{-1}).

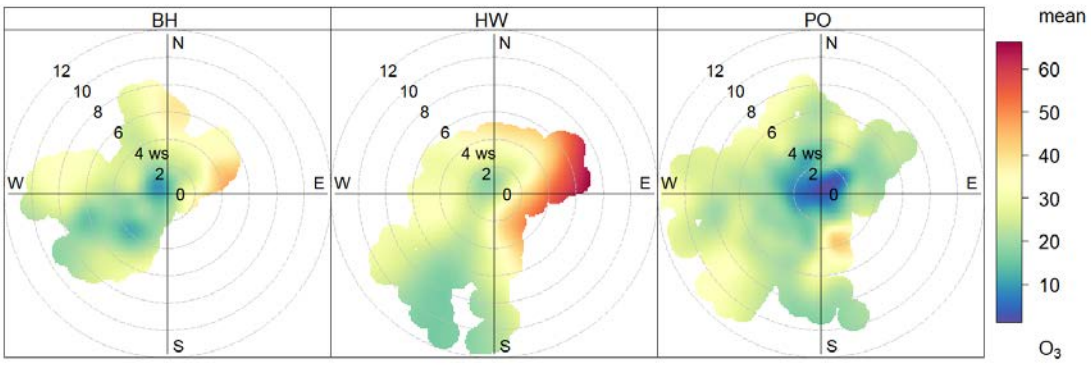

Fig. 4.S2. Polar plots showing O_3 concentration by wind speed and direction (polarPlot function in “openair” package in R) at the Oxford St. Ebbes monitoring site. Heatwave period O_3 concentrations were high under strong easterlies but low post heatwave O_3 when the winds were calm.

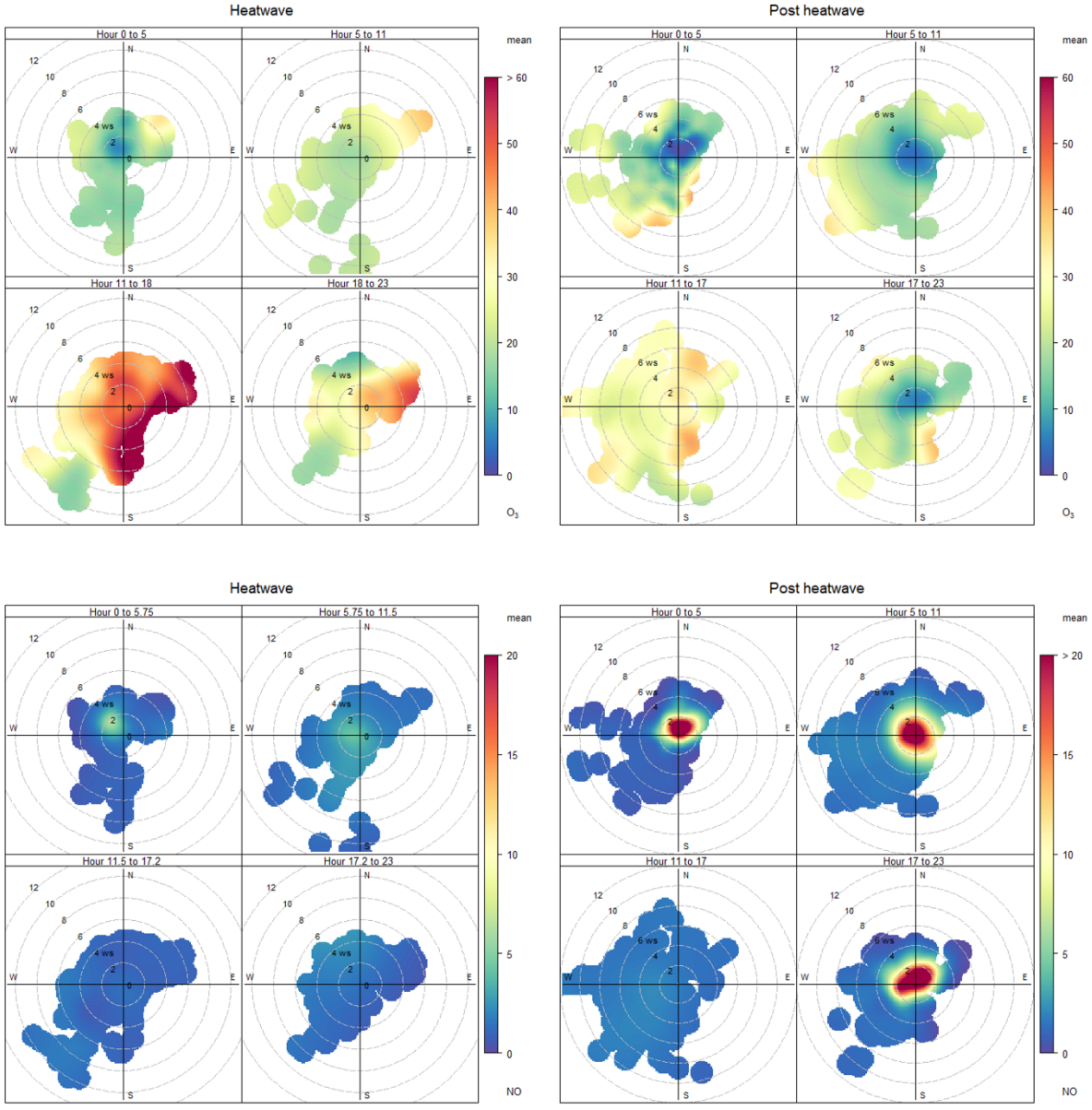

Fig. 4.S3. Polar plots showing O_3 and NO concentrations by wind speed and direction (polarPlot function in “openair” package in R) at the Oxford St. Ebbes monitoring site,

split in heatwave and post heatwave period and the hours of the day. High O_3 concentrations were observed accompanying east and south wind directions during 11~18h of the heatwave period. On the other hand, post heatwave O_3 was low when the winds were calm with high NO concentrations were observed. These bivariate polar plots could imply the potential sources influence at the location.

Chapter 5: Conclusions

This thesis has been motivated by the soil NO_x fluxes that provide an interaction between the atmosphere and biosphere. As an important atmospheric pollutant and precursor of air pollution that contributes to O_3 and aerosol formation, anthropogenic emissions of NO_x have been extensively investigated but the role of soils has been relatively neglected (Lu et al., 2021). In response to the rising issues of air pollution in urban areas, anthropogenic emissions have been controlled and reduced through government regulations and technological development. However, urban parks and greenspaces are getting larger as urban areas expand, and this suggests that biogenic emission sources including soil emissions should not be neglected. In addition, these biogenic emissions have increased and are likely to increase in the future responding to increasing air temperature (Fortems-Cheiney et al., 2021). Hence, biosphere-atmosphere interactions may become more important, and we need to understand their role and their impacts.

The objective of this research was to understand the role of soil NO emissions to the atmosphere. To achieve this, a pair of dynamic soil chambers were designed and field measurements were conducted to quantify soil NO emissions and investigate the driving factors. Previous studies determined the magnitude of the soil NO emissions along with soil characteristics and pedoclimate parameters such as soil water content and temperature (Schindlbacher et al., 2004; Schaufler et al., 2010), soil pH (Kesik et al., 2006) and vegetation (Pilegaard et al., 2006). However, as soil emissions are induced by microbial activities (Pilegaard, 2013), a specific focus in this thesis was placed on temporal variation to investigate the response of NO fluxes to changes in meteorological and pedoclimate parameters (Chapter 2). Subsequently, to investigate future soil NO fluxes and their response to climate change, soil samples were collected in ambient and atmospheric CO_2 elevated soils. The soils were incubated at four different temperatures to investigate the response of fluxes of both NO and NO_2 following predicted future climate change (Chapter 3). These soil NO emission rates were then used to explore the impacts on the atmosphere, especially photochemistry within the forest canopy, using a canopy gas exchange model (Ashworth et al., 2015).

Forests are relatively distant from large anthropogenic emission sources, and the contribution and impact of soil NO fluxes were expected to be much clearer than in urban areas (Chapter 4). Together, the results of these three studies provide insight into a little-investigated emission source. The body of work will therefore motivate greater interest in soil NO emissions, one of the most important biogenic sources of NO, and their interactions with the atmosphere. Understanding soil NO fluxes helps address the knowledge gap of emission sources and improves predictions of chemical composition changes in the atmosphere, e.g. O_3 and aerosol formation and loss.

This concluding chapter provides integrated insights from the findings and highlights the importance of soil NO fluxes, a key biosphere-atmosphere interaction pathway. Moreover, I address the most important directions to pursue in future work.

5.1 Key findings

In the field study in Chapter 2, atmospheric NO mixing ratios near the ground surface were significantly different from those measured at observatory inlet heights (e.g. Finco et al., 2018) through the field campaigns during the summer in an Australian Eucalyptus forest and in both summer and winter in a suburban greenspace in the UK. NO concentrations in an open-bottom sample chamber were always higher than in a closed bottom reference chamber, not only in the daytime but also in the nighttime. These in-situ continuous observations indicate that soil NO fluxes were always positive day and night, even in winter in suburban greenspace, which possibly reflects the characteristics of the soil respiration rates (Makita et al., 2018). Although NO was also emitted during the nighttime, the summer daytime NO fluxes were higher and found to have clear diel cycles with the diurnal variation of meteorological parameters. These observations indicate that the biological activities which govern soil NO fluxes are stimulated by the diurnal cycle of meteorological – pedoclimate factors. On the other hand, cold and wet meteorological conditions in winter potentially disturb biological activities, and could provide a seasonal minimum in soil NO flux under the low biological activity at the location. Furthermore, the majority of previous studies have focussed on soil NO emission rates from agricultural croplands (Skiba et al., 1992; Venterea et al., 2005, Schaufler et al., 2010), which are closely influenced by nitrogen application, although

some studies have investigated forest soil NO fluxes in the northern hemisphere (Schindlbacher et al., 2004; Butterbach-Bahl et al., 2009; Schaufler et al., 2010). This study provides additional soil NO emission inventories from a suburban greenspace in the residential area and from a forest in the southern hemisphere.

The results from the field observations suggest that soils are a clear source of NO to the atmosphere, and have a bigger impact near the ground surface. However, these soil NO fluxes can interact with isoprene emissions from the tree canopy and have a complex influence on forest O_3 and HO_x chemistry (Atkinson, 2000; Atkinson and Arey, 2003; Nguyen et al., 2014; Kim et al., 2015; Wennberg et al., 2018). The model simulations in Chapter 4 confirm that a soil NO emission flux of 0.011 nmol m^2 s^{-1} contributes to an O_3 reduction of 1.1 ppb at the ground surface, but an increase of 1.4 ppb at the top of the canopy, during a heatwave period. Soil NO emission not only affects NO_x – O_3 chemistry, but also influences VOC oxidation (Atkinson, 2000; Nguyen et al., 2014). At the ground surface, the soil NO emission scenario in Chapter 4 reduced isoprene lifetime by 58% in the afternoon, and vertical profiles and diurnal variations of HO_x radicals provide evidence of VOC oxidation and NO_x conversion.

Overall, soil NO fluxes tend to be positive and NO_2 fluxes are reported to be negative in European soils (Butterbach-Bahl et al., 1997; Schindlbacher et al., 2004; Schaufler et al., 2010). A series of laboratory experiments using forest soils (Chapter 3) found negative soil NO_2 fluxes as expected. However, soil NO fluxes were unexpectedly negative, which has previously only been observed where nitrogen availability in the soils is limited (unfertilised cropland in the UK, Skiba et al., 1992; boreal forest in Finland, Schindlbacher et al., 2004; Schaufler et al., 2010), and this contrasts with what has been observed in the field campaigns at other sites, and previous studies (Schindlbacher et al., 2004; Schaufler et al., 2010). During 10 consecutive days of monitoring NO_x fluxes from soils subjected to warming treatments, it was found that both NO and NO_2 fluxes were negative, which indicates soil uptake of NO_x from the atmosphere, and showed a clear temporal cycle (Chapter 3). Although the availability of nitrogen could govern the magnitude of the fluxes (Kesik et al., 2005; Pilegaard et al., 2006), Chapter 2 and 3 in this thesis found and confirmed that microbial activity in the soil was the key process affecting soil NO_x fluxes. My research also found that the NO fluxes from the elevated atmospheric CO_2 level soils showed less NO_x uptake than soils

under current ambient conditions. By applying temperature treatments that reflect the response to predicted future climate changes, I showed that the optimal soil temperature for NO_x fluxes will likely be altered by atmospheric CO_2 levels. This suggests that elevated atmospheric CO_2 levels might not just reduce soil NO fluxes (Hungate et al., 1997; Mosier et al., 2002), but also influence microbial responses to changing soil temperatures.

Even for conditions where the soil absorbs NO from the atmosphere, atmospheric composition near the ground surface could be affected by changes in NO fluxes (Finco et al., 2018), especially isoprene oxidation and O_3 production. My model simulations in Chapter 4 indicate that variations in O_3 and HO_x radicals at the ground surface due to soil NO fluxes were bigger than at heights above the ground surface, because of the proximity of the emission source and deposition surface. Furthermore, the overall contribution of soil NO fluxes to canopy O_3 concentrations was non-linear. I found that the response of O_3 to soil NO uptake was twice as high as the response to soil NO emissions. Soil NO absorption (-0.005 nmol m^2 s^{-1}) contributed 0.5 ppb of O_3 reduction below 30m height in the forest, similar to the O_3 increase (0.6 ppb) associated with NO emissions that are twice as large (0.011 nmol m^2 s^{-1}). Overall, O_3 concentrations were linear and increased with soil NO fluxes except at the ground surface (0.8m), where the correlation was negative and nonlinear due to O_3 removal by NO_x titration close to the emission source. In addition, the impacts of soil NO fluxes on O_3 concentrations at trunk height and above were distinctively higher (~ 4 times) during the heatwave period. The results from the model simulations denote the non-negligible influence of soil NO emissions on atmospheric composition, potentially critical under high-temperature conditions.

Throughout the field observations, lab experiments, and model simulations, the contributions of soil NO fluxes were bigger near the ground surface and under higher temperatures. Furthermore, these studies provide not only a quantitative determination and temporal variations of soil NO fluxes in different environments, but also an assessment of their impacts on forest O_3 and HO_x chemistry. Thus, this thesis provides a new perspective on rarely investigated soil NO fluxes and their impact on the forest atmosphere, and demonstrates that this previously overlooked source of NO emissions underpins important interactions along the biosphere-atmosphere continuum.

5.2 Limitations and future work

In this thesis, soil NO fluxes were measured in several different places for comparison and analysis with environmental parameters. However, soil NO fluxes differ substantially with location and observation time (Schindlbacher et al., 2004; Schaufler et al., 2010). Furthermore, the number of samples taken or instruments used, especially at in-situ field sites, might be insufficient to be fully representative, which somewhat hinders interpretation of the results. Although soil collars were rotated at the Australian site in Chapter 2 and a total of 24 soil samples (4 cores at 6 arrays) were collected from the Free-Air CO_2 Enrichment arrays in Chapter 3, they did not fully cover the biodiversity and environmental characteristics of the location. Furthermore, it is difficult to provide direct comparisons because the observation periods were different. Not only the time scale, but also the locations differ in climate, meteorological and soil conditions, and these affect biological activity and interactions. The lab experiments have the advantages to test hypotheses by controlling different parameters (e.g. soil temperature and moisture, nutrient supply, etc.) using collected soil samples (Schindlbacher et al., 2004; Kesik et al., 2005; Venterea et al., 2005; Schaufler et al., 2010). However, the system is artificial and the soils are separated from their interaction with plant roots and in-situ microbial activities. Therefore, future work should be conducted with nutrient application, not only nitrogen but also carbon and phosphorus, and ideally include long-term monitoring. This would motivate investigation not only of climate change (e.g. changes in pedoclimate parameters) but also nutrient transport or input through biological activities (e.g. root exudation and transport through soil water) and human activities (e.g. use of fertilisers).

Furthermore, model studies should also be encouraged. A 1-D model for the forest environment was used here to investigate the impact of soil NO fluxes on O_3 and HO_x radicals under different soil NO fluxes (Chapter 4). However, it is clear that soil fluxes could also have an influence on the atmosphere through O_3 and aerosol formation in many different locations and environments. For example, my work demonstrated that soil NO emissions in urban greenspaces are non-negligible (Chapter 3) and as urban parks and greenspaces are getting bigger (Haaland and Van Den Bosch, 2015), the

contributions of the soil NO fluxes will also increase. Thus, applying soil NO fluxes in chemistry and transport models covering a range of different spatial and temporal scales would help understanding the contribution of soil NO fluxes to the atmosphere at local and regional scales. By considering soil emissions as a non-negligible source of NO, these future studies could provide the missing all-day emission source of NO_x that affects atmospheric chemistry and provide another perspective to approach urban air quality issues.

Finally, NO plays an important role as a precursor of air pollution (on a relatively short time scale) and N_2O acts as a significant greenhouse gas contributing to global warming (a long-term impact), but both NO and N_2O are produced through the same processes of nitrification and denitrification (Butterbach-Bahl et al., 2013; Pilegaard, 2013). However, the partitioning ratio and conditions that govern the balance of NO and N_2O are still uncertain. Greenhouse gases including N_2O could increase global air temperature and hence potentially cause more frequent extremes, and more soil emissions are expected under these conditions as found in Chapter 4. Therefore, understanding of NO and N_2O from nitrification and denitrification in soils and their relative responses to environmental conditions could provide a wider perspective on the short-term and long-term interactions between the biosphere and atmosphere. Overall, my results and conclusions demonstrate that soil NO fluxes play potentially important roles in atmospheric composition and the nitrogen cycle, which have hitherto been largely ignored. Moreover, the demonstrated impacts of soil NO fluxes on forest O_3 and photochemistry, and my model projections, will motivate soil and nitrogen cycle studies to assess the impacts of climate change and the role of soil nitrogen-cycle processes on the atmosphere.

References

Adachi, M., Ishida, A., Bunyavejchewin, S., Okuda, T., Koizumi, H., 2009. Spatial and temporal variation in soil respiration in a seasonally dry tropical forest, Thailand. *J. Trop. Ecol.* 25, 531–539. https://doi.org/10.1017/S026646740999006X

AQEG, 2004. Air Quality Expert Group, Nitrogen dioxide in the United Kingdom. Air Quality Expert Group, Defra, London.

Ashworth, K., Chung, S.H., Griffin, R.J., Chen, J., Forkel, R., Bryan, A.M., Steiner, A.L., 2015. FORest Canopy Atmosphere Transfer (FORCAsT) 1.0: a 1-D model of biosphere–atmosphere chemical exchange. *Geosci. Model Dev.* 8(11), 3765-3784. https://doi.org/10.5194/gmd-8-3765-2015

Atkinson, R., 2000. Atmospheric chemistry of VOCs and NO_x. *Atmos. Environ.* 34, 2063–2101. https://doi.org/10.1016/S1352-2310(99)00460-4

Atkinson, R., Arey, J., 2003. Gas-phase tropospheric chemistry of biogenic volatile organic compounds: a review. *Atmos. Environ.* 37, 197–219. https://doi.org/10.1016/S1352-2310(03)00391-1

Australian Government Department of Climate Change E, the Environment and Water 2022. https://data.gov.au/dataset/ds-dga-043f58e0-a188-4458-b61c-04e5b540ae a4/distribution/dist-dga-9ec26edf-ea5b-4869-8c2c-38b41fb3a51d/details?q=, (accessed 21 Feb 2023).

Bamberger, I., Ruehr, N.K., Schmitt, M., Gast, A., Wohlfahrt, G., Arneth, A., 2017. Isoprene emission and photosynthesis during heatwaves and drought in black locust. *Biogeosciences 14*(15), 3649-3667. https://doi.org/10.5194/bg-14-3649-2017

Bao, H., Shrestha, K.L., Kondo, A., Kaga, A., Inoue, Y., 2010. Modeling the influence of biogenic volatile organic compound emissions on ozone concentration during summer season in the Kinki region of Japan. *Atmos. Environ.* 44(3), 421-431. https://doi.org/10.1016/j.atmosenv.2009.10.021

Barnard, R., Leadley, P.W., Hungate, B.A., 2005. Global change, nitrification, and denitrification: a review. *Global biogeochem. cycles 19*(1). https://doi.org/10.1029/2004GB002282

Bates, D., Mächler, M., Bolker, B., Walker, S., 2015. Fitting Linear Mixed-Effects Models Using lme4. *J. Stat. Softw.* 67(1), 1–48. https://doi.org/10.18637/jss.v067.i01

Bell, M.L., McDermott, A., Zeger, S.L., Samet, J.M., Dominici, F., 2004. Ozone and short-term mortality in 95 US urban communities, 1987-2000. *Jama* 292(19), pp.2372-2378. https://doi.rog/10.1001/jama.292.19.2372

Bertram, T.H., Heckel, A., Richter, A., Burrows, P.J., Cohen, R.C., 2005. Satellite measurements of daily variations in soil NO_x emissions. *Geophys. Res. Letts.* 32, L24812. https://doi.org/10.1029/2005GL024640

Blackmer, A.M., Robbins, S.G., Bremner, J.M., 1982. Diurnal variability in rate of emission of nitrous oxide from soils. *Soil Sci. Soc. Am. J.* 46 (5), 937–942. https://doi.org/10.2136/sssaj1982.03615995004600050011x

Blackmer, A.M., Cerrato, M.E., 1986. Soil properties affecting formation of nitric oxide by chemical reactions of nitrite. *Soil Sci. Soc. Am. J.* 50(5), 1215-1218. https://doi.org/10.2136/sssaj1986.03615995005000050025x

Bohler, S., Bagard, M., Oufir, M., Planchon, S., Hoffmann, L., Jolivet, Y., Hausman, J.F., Dizengremel, P., Renaut, J., 2007. A DIGE analysis of developing poplar leaves subjected to ozone reveals major changes in carbon metabolism. *Proteomics* 7(10), pp.1584-1599. https://doi.org/10.1002/pmic.200600822

Bolas, C.G., Ferracci, V., Robinson, A.D., Mead, M.I., Nadzir, M.S.M., Pyle, J.A., Jones, R.L., Harris, N.R., 2020. iDirac: a field-portable instrument for long-term autonomous measurements of isoprene and selected VOCs. *Atmos. Meas. Tech.* 13(2), 821-838. https://doi.org/10.5194/amt-13-821-2020

Boningari, T., Smirniotis, P.G., 2016. Impact of nitrogen oxides on the environment and human health: Mn-based materials for the NO_x abatement. *Current Opinion in Chemical Engineering* 13: 133-141, https://doi.org/10.1016/j.coche.2016.09.004

Borbon, A., Fontaine, H., Veillerot, M., Locoge, N., Galloo, J.C., Guillermo, R., 2001. An investigation into the traffic-related fraction of isoprene at an urban location. *Atmos. Environ.* 35(22), 3749-3760. https://doi.org/10.1016/S1352-2310(01)00170-4

Borowik, A., Wyszkowska, J., 2016. Impact of temperature on the biological properties of soil. *Int. Agrophys.* 30(1), 1-8.

Bremner, J., Blackmer, A.M., 1978. Nitrous oxide: emission from soils during nitrification of fertilizer nitrogen. *Science* 199, 295–296. https://doi.org/10.1126/science.199.4326.295

Brüggemann, N., Rosenkranz, P., Papen, H., Pilegaard, K., Butterbach-Bahl, K., 2005. Pure stands of temperate forest tree species modify soil respiration and N turnover. *Biogeosci. Discuss.* 2(2), pp.303-331.

Brune, W., Baier, B., Thomas, J., Ren, X., Cohen, R., Pusede, S., Browne, E., Goldstein, A., Gentner, D., Keutsch, F., Thornton, J., Harrold, S., Lopez-Hilfiker, F., Wennberg, P., 2016. Ozone production chemistry in the presence of urban plumes. *Faraday Discuss.* 189, 169–189. https://doi.org/10.1039/c5fd00204d

Buckingham, S., Anthony, S., Bellamy, P., Cardenas, L., Higgins, S., McGeough, K., Topp, C., 2014. Review and analysis of global agricultural N_2O emissions relevant to the UK. S*ci. Total Environ.* 487, 164–172. https://doi.org/10.1016/j.scitotenv.2014.02.122

Burris, R.H., Wilson, P.W., 1945. Biological nitrogen fixation. *Annu. Rev. Biochem.* 14(1), 685-708.

Butterbach-Bahl K., Gasche R., Breuer L., Papen, H., 1997. Fluxes of NO and N_2O from temperate forest soils: impact of forest type, N deposition and of liming on the NO and N_2O emissions. *Nutr. Cycl. Agroecosystems 48,* 79-90. https://doi.org/10.1023/A:1009785521107

Butterbach-Bahl, K., Kahl, M., Mykhayliv, L., Werner, C., Kiese, R., Li, C., 2009. A European-wide inventory of soil NO emissions using the biogeochemical models DNDC/Forest-DNDC. *Atmos. Environ.* 43, 1392–1402. https://doi.org/10.1016/j.atmosenv.2008.02.008

Butterbach-Bahl, K., Baggs, E.M., Dannenmann, M., Kiese, R., Zechmeister- Boltenstern, S., 2013. Nitrous oxide emissions from soils: how well do we understand the processes and their controls? *Philos. Trans. R. Soc. B Biol. Sci.* 368, 20130122 https://doi.org/10.1098/rstb.2013.0122

Campbell, P.K., Huemmrich, K.F., Middleton, E.M., Ward, L.A., Julitta, T., Daughtry, C. S., Burkart, A., Russ, A.L., Kustas, W.P., 2019. Diurnal and seasonal variations in chlorophyll fluorescence associated with photosynthesis at leaf and canopy scales. *Remote Sens.* (Basel) 11, 488. https://doi.org/10.3390/rs11050488

Carslaw, D.C., 2005. Evidence of an increasing NO_2/NO_x emissions ratio from road traffic emissions. *Atmos. Environ.* 39 (26), 4793–4802. https://doi.org/10.1016/j.atmosenv.2005.06.023

Carslaw, D.C., Ropkins, K., 2012. Openair - an R package for air quality data analysis. *Environ. Model. Softw.* Volume 27-28, 52-61. https://doi.org/10.1016/j.envsoft.2011.09.008

Chalk, P.M., Smith, C.J., 1983. Chemodenitrification. In: Freney, J.R., Simpson, J.R. (eds) Gaseous Loss of Nitrogen from Plant-Soil Systems. Developments in Plant and Soil Sciences, vol 9. Springer, Dordrecht. https://doi.org/10.1007/978-94-017-1662-8_3

Chameides, W.L., Lindsay, R.W., Richardson, J., Kiang, C.S., 1988. The role of biogenic hydrocarbons in urban photochemical smog: Atlanta as a case study. *Science* 241(4872), 1473-1475. DOI: 10.1126/science.34204

Chen, D., Li, Y., Wang, C., Liu, X., Wang, Y., Shen, J., Qin, J., Wu, J., 2019. Dynamics and underlying mechanisms of N_2O and NO emissions in response to a transient land-use conversion of Masson pine forest to tea field. *Sci. Total Environ.* 693, 133549 https://doi.org/10.1016/j.scitotenv.2019.07.355

Churchill S., Richmond B., MacCarthy J., Broomfield M., Brown P., Del Vento S., Galatioto F., Gorji S., Karagianni E., Misra A., Murrells T., Passant N., Pearson B., Richardson J., Stewart R., Thistlethwaite G., Travasso N., Tsagatakis I., Wakeling D., Walker C., Wiltshire J., Wong J., Yardley R. (Ricardo Energy & Environment). UK Informative Inventory Report (1990 to 2020), 2022.

Ciais, P., Sabine, C., Bala, G., Bopp, L., Brovkin, V., Canadell, J., Chhabra, A., DeFries, R., Galloway, J., Heimann, M., Jones, C., Quéré, C., Myneni, R.B., Piao, S., Thornton, P., 2013: Carbon and Other Biogeochemical Cycles. In: Climate Change 2013: The Physical Science Basis. Contribution of Working Group I to the Fifth Assessment Report of the Intergovernmental Panel on Climate Change [Stocker, T.F., Qin, D., Plattner, G.-K., Tignor, M., Allen, S.K., Boschung, J., Nauels, A., Xia, Y., Bex, V., Midgley, P.M. (eds.)]. Cambridge University Press, Cambridge, United Kingdom and New York, NY, USA.

COMEAP. Associations of long-term average concentrations of nitrogen dioxide with mortality. COMEAP Report, 2018.

Commonwealth of Australia 2022, Bureau of Meteorology. http://www.bom.gov.au/climate/data/, (accessed 17 May 2022).

Crawford, J.H., Ahn, J.Y., Al-Saadi, J., Chang, L., Emmons, L.K., Kim, J., Lee, G., Park, J.H., Park, R.J., Woo, J.H., Song, C.K., Hong, J.H., Hong, Y.D., Lefer, B.L., Lee, M., Lee, T., Kim, S., Min, K.E., Yum, S.S., Shin, H.J., Kim, Y.W., Choi, J.S., Park, J.S., Szykman, J.J., Long, R.W., Jordan, C.E., Simpson, I.J., Fried, A., Dibb, J.E., Cho, S., Kim, Y.P., 2021. The Korea–United States air quality (KORUS-AQ) field study. *Elem Sci Anth*. 9(1), p.00163. https://doi.org/10.1525/elementa.2020.00163

Davidson, E.A., Kingerlee, W., 1997. A global inventory of nitric oxide emissions from soils. *Nutr. Cycl. Agroecosystems* 48, pp.37-50. https://doi.org/10.1023/A:1009738715891

Davidson, E.A., Keller, M., Erickson, H.E., Verchot, L.V., Veldkamp, E., 2000. Testing a conceptual model of soil emissions of nitrous and nitric oxides: using two functions based on soil nitrogen availability and soil water content, the hole-in-the-pipe model characterizes a large fraction of the observed variation of nitric oxide and nitrous oxide emissions from soils. *Bioscience* 50(8), 667-680. https://doi.org/10.1641/0006-3568(2000)050[0667:TACMOS]2.0.CO;2

Delmas, R., Serça, D., Jambert, C., 1997. Global inventory of NO_x sources. *Nutr. Cycl. Agroecosystems* 48: 51-60. https://doi.org/10.1023/A:1009793806086

Denef, K., Bubenheim, H., Lenhart, K., Vermeulen, J., Van Cleemput, O., Boeckx, P., Müller, C., 2007. Community shifts and carbon translocation within metabolically-active rhizosphere microorganisms in grasslands under elevated CO_2. *Biogeosciences* 4, 769–779. https://doi.org/10.5194/bg-4-769-2007

Denman, K.L., Brasseur, G., Chidthaisong, A., Ciais, P., Cox, P.M., Dickinson, R.E., Hauglustaine, D., Heinze, C., Holland, E., Jacob, D., Lohmann, U., Ramachandran, S., da Silva Dias, P.L., Wofsy, S.C., Zhang, X., 2007. Couplings between changes in the climate system and biogeochemistry. In: Solomon, S., Qin, D., Manning, M., Chen, Z., Marquis, M., Averyt, K.B., Tignor, M., Miller, H.L. (Eds.), Climate Change 2007: The Physical Science Basis. Contribution of Working Group I to the Fourth Assessment Report of the Intergovernmental Panel On Climate Change. Cambridge University Press, Cambridge, United Kingdom and New York, NY, USA.

Department for Environment Food & Rural Affairs (DEFRA) data archive, United Kingdom, http://www.uk-air.defra.gov.uk/data/, (accessed 08 Jan 2024).

Deutsch, E.S., Bork, E.W., Willms, W.D., 2010. Separation of grassland litter and ecosite influences on seasonal soil moisture and plant growth dynamics. *Plant Ecol.* 209, 135-145. https://doi.org/10.1007/s11258-010-9729-6

Di Carlo, P., Brune, W.H., Martinez, M., Harder, H., Lesher, R., Ren, X., Thornberry, T., Carroll, M.A., Young, V., Shepson, P.B., Riemer, D., Apel, E., Campbell, C., 2004. Missing OH reactivity in a forest: Evidence for unknown reactive biogenic VOCs. *Science* 304(5671), 722-725. https://doi.org/10.1126/science.1094392

Doran, J., Berkowitz, C.M., Coulter, R.L., Shaw, W.J., Spicer, C.W., 2003. The 2001 Phoenix Sunrise experiment: vertical mixing and chemistry during the morning transition in Phoenix. *Atmos. Environ.* 37, 2365–2377. https://doi.org/10.1016/S1352-2310(03)00134-1

Drake, J.E., Gallet-Budynek, A., Hofmockel, K.S., Bernhardt, E.S., Billings, S.A., Jackson, R.B., Johnsen, K.S., Lichter, J., McCarthy, H.R., McCormack, M.L., Moore, D.J., Oren, R., Palmroth, S., Phillips, R.P., Pippen, J.S., Pritchard, S.G., Treseder K.K., Schlesinger W.H., DeLucia E.H., Finzi, A.C., 2011. Increases in the flux of carbon belowground stimulate nitrogen uptake and sustain the long-term enhancement of forest productivity under elevated CO_2. *Ecol. Lett.* 14(4), pp.349-357. https://doi.org/10.1111/j.1461-0248.2011.01593.x

Fares, S., Loreto, F., Kleist, E., Wildt, J., 2007. Stomatal uptake and stomatal deposition of ozone in isoprene and monoterpene emitting plants. *Plant Biology*, e69-e78. https://doi.org/10.1055/s-2007-965257

Fares, S., McKay, M., Holzinger, R., Goldstein, A.H., 2010. Ozone fluxes in a Pinus ponderosa ecosystem are dominated by non-stomatal processes: Evidence from long-term continuous measurements. *Agric. For. Meteorol. 150*(3), 420-431. https://doi.org/10.1016/j.agrformet.2010.01.007

Fares, S., Alivernini, A., Conte, A., Maggi, F., 2019. Ozone and particle fluxes in a Mediterranean forest predicted by the AIRTREE model. *Sci. Total Environ.* 682, 494-504. https://doi.org/10.1016/j.scitotenv.2019.05.109

Feig, G.T., Mamtimin, B., Meixner, F.X., 2008. Soil biogenic emissions of nitric oxide from a semi-arid savanna in South Africa. *Biogeosciences* 5(6), 1723-1738. https://doi.org/10.5194/bg-5-1723-2008

Ferracci, V., Bolas, C.G., Freshwater, R.A., Staniaszek, Z., King, T., Jaars, K., Otu-Larbi, F., Beale, J., Malhi, Y., Waine, T.W., Jones, R.L., Ashworth, K., Harris, N.R.P., 2020. Continuous isoprene measurements in a UK temperate forest for a whole growing season: Effects of drought stress during the 2018 heatwave. *Geophys. Res. Lett.* 47(15), p.e2020GL088885. https://doi.org/10.1029/2020GL088885

Finco, A., Coyle, M., Nemitz, E., Marzuoli, R., Chiesa, M., Loubet, B., Fares, S., Diaz-Pines, E., Gasche, R., Gerosa, G., 2018. Characterization of ozone deposition to a mixed oak–hornbeam forest–flux measurements at five levels above and inside the canopy and their interactions with nitric oxide. *Atmos. Chem. Phys.* 18(24), 17945-17961. https://doi.org/10.5194/acp-18-17945-2018

Finzi, A.C., Van Breemen, N., Canham, C.D., 1998. Canopy tree–soil interactions within temperate forests: species effects on soil carbon and nitrogen. *Ecol. Appl.* 8(2), 440-446. https://doi.org/10.1890/1051-0761(1998)008[0440:CTSIWT]2.0.CO;2

Firestone, M.K., Davidson, E.A., 1989. Microbiological basis of NO and N_2O production and consumption in soil. *Exchange of trace gases between terrestrial ecosystems and the atmosphere* 47, 7-21.

Forkel, R., Klemm, O., Graus, M., Rappenglück, B., Stockwell, W.R., Grabmer, W., Held, A., Hansel, A., Steinbrecher, R., 2006. Trace gas exchange and gas phase chemistry in a Norway spruce forest: A study with a coupled 1-dimensional canopy atmospheric chemistry emission model. *Atmos. Environ.* 40, 28-42. https://doi.org/10.1016/j.atmosenv.2005.11.070

Fortems-Cheiney, A., Broquet, G., Pison, I., Saunois, M., Potier, E., Berchet, A., Dufour, G., Siour, G., Denier van der Gon, H., Dellaert, S., Boersma, K., 2021. Analysis of the anthropogenic and biogenic NO_x emissions over 2008–2017: assessment of the trends in the 30 most populated urban areas in Europe. *Geophys. Res. Lett.* 48, e2020GL092206 https://doi.org/10.1029/2020GL092206

Fowler, D., Amann, M., Anderson, R., Ashmore, M., Cox, P., Depledge, M., Derwent, D., Grennfelt, P., Hewitt, N., Hov, O., Jenkin, M., Kelly, F., Liss, P., Pilling, M., Pyle, J., Slingo, J., Stevenson, D., 2008. Ground-level Ozone in the 21st Century: Future Trends, Impacts and Policy Implications. The Royal Society, ISBN: 978-0-85403-713-1, Issued: October 2008 RS1276.

Fowler, D., Coyle, M., Skiba, U., Sutton, M.A., Cape, J.N., Reis, S., Sheppard, L.J., Jenkins, A., Grizzetti, B., Galloway, J.N., Vitousek, P., Leach, A., Bouwman, A. F., Butterbach-Bahl,

K., Dentener, F., Stevenson, D., Amann, M., Voss, M., 2013. The global nitrogen cycle in the twenty-first century. *Philos. Trans. R. Soc. B Biol. Sci.* 368(1621), p.20130164. https://doi.org/10.1098/rstb.2013.0164

Fowler, D., Steadman, C.E., Stevenson, D., Coyle, M., Rees, R.M., Skiba, U.M., Sutton, M.A., Cape, J.N., Dore, A.J., Vieno, M., Simpson, D., Zaehle, S., Stocker, B.D., Rinaldi, M., Facchini, M.C., Flechard, C.R., Nemitz, E., Twigg, M., Erisman, J.W., Butterbach-Bahl, K., Galloway, J.N., 2015. Effects of global change during the 21st century on the nitrogen cycle. *Atmos. Chem. Phys.* 15(24), pp.13849-13893. https://doi.org/10.5194/acp-15-13849-2015

Fowler, D., Brimblecombe, P., Burrows, J., Heal, M.R., Grennfelt, P., Stevenson, D.S., Jowett, A., Nemitz, E., Coyle, M., Liu, X., Chang, Y., Fuller, G.W., Sutton, M.A., Klimont, Z., Unsworth, M.H., Vieno, M., 2020. A chronology of global air quality. *Philos. Trans. R. Soc. A* 378, 20190314. https://doi.org/10.1098/rsta.2019.0314

Fumagalli, I., Gruening, C., Marzuoli, R., Cieslik, S., Gerosa, G., 2016. Long-term measurements of NO_x and O_3 soil fluxes in a temperate deciduous forest. *Agric. For. Meteorol.* 228, 205–216. https://doi.org/10.1016/j.agrformet.2016.07.011

Galbally, I.E., 1989. Factors controlling NO_x emissions from soils. *Exchange of trace gases between terrestrial ecosystems and the atmosphere* pp.23-37.

Gao, W., Wesely, M.L., Doskey, P.V., 1993. Numerical modeling of the turbulent diffusion and chemistry of NO_x, O_3, isoprene, and other reactive trace gases in and above a forest canopy. *J. Geophys. Res. Atmos.* 98(D10), 18339-18353. https://doi.org/10.1029/93JD01862

Gao, W., Tie, X., Xu, J., Huang, R., Mao, X., Zhou, G., Chang, L., 2017. Long-term trend of O_3 in a mega City (Shanghai), China: Characteristics, causes, and interactions with precursors. *Sci. Total Environ.* 603, 425-433. https://doi.org/10.1016/j.scitotenv.2017.06.099

Garrido, F., Hénault, C., Gaillard, H., Pérez, S., Germon, J.C., 2002. N_2O and NO emissions by agricultural soils with low hydraulic potentials. *Soil Biol. Biochem.* 34(5), 559-575. https://doi.org/10.1016/S0038-0717(01)00172-9

Geng, F., Tie, X., Guenther, A., Li, G., Cao, J., Harley, P., 2011. Effect of isoprene emissions from major forests on ozone formation in the city of Shanghai, China. *Atmos. Chem. Phys.* 11(20), 10449-10459. https://doi.org/10.5194/acp-11-10449-2011

Geyer, A., Stutz, J., 2004. Vertical profiles of NO_3, N_2O_5, O_3, and NO_x in the nocturnal boundary layer: 2. Model studies on the altitude dependence of composition and chemistry. *J. Geophys. Res. Atmos.* (D12), 109. https://doi.org/10.1029/2003JD004211

Goldberg, D.L., Anenberg, S.C., Lu, Z., Streets, D.G., Lamsal, L.N., McDuffie, E.E., Smith, S.J., 2021. Urban NO_x emissions around the world declined faster than anticipated between 2005 and 2019. *Environ. Res. Lett.* 16, 115004 https://doi.org/10.1088/1748-9326/ac2c34

Goldstein, A.H., Galbally, I.E., 2007. Known and unexplored organic constituents in the earth's atmosphere. *Environ. Sci. Technol.* 41(5), 1514-1521.

Griffin, R.J., Dabdub, D., Seinfeld, J.H., 2002. Secondary organic aerosol 1. Atmospheric chemical mechanism for production of molecular constituents. *J. Geophys. Res. Atmos.* 107(D17), 4332. https://doi.org/10.1029/2001JD000541

Griffin, R.J., Dabdub, D. and Seinfeld, J.H., 2005. Development and initial evaluation of a dynamic species-resolved model for gas phase chemistry and size-resolved gas/particle partitioning associated with secondary organic aerosol formation. *J. Geophys. Res. Atmos.* 110,D05304. https://doi.org/10.1029/2004JD005219

Guenther, A.B., Monson, R.K., Fall, R., 1991. Isoprene and monoterpene emission rate variability: observations with eucalyptus and emission rate algorithm development. *J. Geophys. Res. Atmos.* 96(D6), 10799-10808. https://doi.org/10.1029/91JD00960

Guenther, A.B., Zimmerman, P.R., Harley, P.C., Monson, R.K., Fall, R., 1993. Isoprene and monoterpene emission rate variability: model evaluations and sensitivity analyses. *J. Geophys. Res. Atmos.* 98(D7), pp.12609-12617. https://doi.org/10.1029/93JD00527

Guenther, A., Hewitt, C.N., Erickson, D., Fall, R., Geron, C., Graedel, T., Harley, P., Klinger, L., Lerdau, M., McKay, W.A., Pierce, T., Scholes, B., Steinbrecher, R., Tallamraju, R., Taylor, J., Zimmerman, P., 1995. A global model of natural volatile organic compound emissions. *J. Geophys. Res. Atmos.* 100(D5), pp.8873-8892. https://doi.org/10.1029/94JD02950

Guenther, A., Karl, T., Harley, P., Wiedinmyer, C., Palmer, P.I., Geron, C., 2006. Estimates of global terrestrial isoprene emissions using MEGAN (Model of Emissions of Gases and Aerosols from Nature). *Atmos. Chem. Phys.* 6(11), 3181-3210. https://doi.org/10.5194/acp-6-3181-2006

Guenther, A.B., Jiang, X., Heald, C.L., Sakulyanontvittaya, T., Duhl, T.A., Emmons, L.K.,Wang, X., 2012. The Model of Emissions of Gases and Aerosols from Nature version 2.1 (MEGAN2. 1): an extended and updated framework for modeling biogenic emissions. *Geosci. Model Dev.* 5(6), pp.1471-1492. https://doi.org/10.5194/gmd-5-1471-2012

Haaland, C., Van Den Bosch, C.K., 2015. Challenges and strategies for urban green-space planning in cities undergoing densification: A review. *Urban For. Urban Green.* 14(4), 760-771. https://doi.org/10.1016/j.ufug.2015.07.009

Hart, K.M., Curioni, G., Blaen, P., Harper, N.J., Miles, P., Lewin, K.F., Nagy, J., Bannister, E.J., Cai, X.M., Thomas, R.M., Krause, S., Tausz, M., MacKenzie, A.R., 2020. Characteristics of free air carbon dioxide enrichment of a northern temperate mature forest. *Glob. Chang. Biol.* 26(2), pp.1023-1037. https://doi.org/10.1111/gcb.14786

Hayatsu, M., Tago, K., Saito, M., 2008. Various players in the nitrogen cycle: diversity and functions of the microorganisms involved in nitrification and denitrification. *Soil Sci. Plant Nutr.* 54(1), 33-45. https://doi.org/10.1111/j.1747-0765.2007.00195.x

Heil, J., Vereecken, H., Brüggemann, N., 2016. A review of chemical reactions of nitrification intermediates and their role in nitrogen cycling and nitrogen trace gas formation in soil. *Eur. J. Soil Sci.* 67 (1), 23–39. https://doi.org/10.1111/ejss.12306

Her, J.J., Huang, J.S., 1995. Influences of carbon source and C/N ratio on nitrate/nitrite denitrification and carbon breakthrough. *Bioresour. Technol.* 54(1), 45-51. https://doi.org/10.1016/0960-8524(95)00113-1

Hidy, G.M., Blanchard, C.L., Baumann, K., Edgerton, E., Tanenbaum, S., Shaw, S., Knipping, E., Tombach, I., Jansen, J., Walters, J., 2014. Chemical climatology of the southeastern United States, 1999–2013. *Atmos. Chem. Phys.* 14(21), 11893-11914. https://doi.org/10.5194/acp-14-11893-2014

Huang, Y., Zou, J., Zheng, X., Wang, Y., Xu, X., 2004. Nitrous oxide emissions as influenced by amendment of plant residues with different C: N ratios. *Soil Biol. Biochem.* 36, 973–981. https://doi.org/10.1016/j.soilbio.2004.02.009

Hudman, R.C., Moore, N.E., Mebust, A.K., Martin, R.V., Russell, A.R., Valin, L.C., Cohen, R.C., 2012. Steps towards a mechanistic model of global soil nitric oxide emissions: implementation and space based-constraints. *Atmos. Chem. Phys.* 12(16), pp.7779-7795. https://doi.org/10.5194/acp-12-7779-2012

Hungate, B.A., Lund, C.P., Pearson, H.L., Chapin, F.S., 1997. Elevated CO_2 and nutrient addition after soil N cycling and N trace gas fluxes with early season wet-up in a California annual grassland. *Biogeochemistry* 37, 89-109. https://doi.org/10.1023/A:1005747123463

Im, U., Incecik, S., Guler, M., Tek, A., Topcu, S., Unal, Y.S., Yenigun, O., Kindap, T., Odman, M.T., Tayanc, M., 2013. Analysis of surface ozone and nitrogen oxides at urban, semi-rural and rural sites in Istanbul, Turkey. *Sci. Total Environ.* 443, 920–931. https://doi.org/10.1016/j.scitotenv.2012.11.048

IPCC, 2007. Climate Change, the Scientific Basis. Contribution of Working Group I to the Fourth Assessment Report of Intergovernmental Panel on Climate Change (IPCC). Cambridge University Press, Cambridge

Jacob, D.J., 1999. Introduction to atmospheric chemistry. Princeton university press.

Jakoby, G., Rog, I., Megidish, S., Klein, T., 2020. Enhanced root exudation of mature broadleaf and conifer trees in a Mediterranean forest during the dry season. *Tree Physiol.* 40, 1595–1605. https://doi.org/10.1093/treephys/tpaa092

Jauregui, I., Rothwell, S.A., Taylor, S.H., Parry, M.A., Carmo-Silva, E., Dodd, I.C., 2018. Whole plant chamber to examine sensitivity of cereal gas exchange to changes in evaporative demand. *Plant Methods* 14 (1), 1–13. https://doi.org/10.1186/s13007-018-0357-9

Kansal, A., 2009. Sources and reactivity of NMHCs and VOCs in the atmosphere: A review. *J. Hazard. Mater.* 166(1), 17-26. https://doi.org/10.1016/j.jhazmat.2008.11.048

Kesik, M., Ambus, P., Baritz, R., Brüggemann, N., Butterbach-Bahl, K., Damm, M., Duyzer, J., Horváth, L., Kiese, R., Kitzler, B., Leip, A., Li, C., Pihlatie, M., Pilegaard, K., Seufert, G., Simpson, D., Skiba, U., Smiatek, G., Vesala, T., Zechmeister-Boltenstern, S., 2005. Inventories of N_2O and NO emissions from European forest soils. *Biogeosciences 2*(4), 353-375. https://doi.org/10.5194/bg-2-353-2005

Kesik, M., Blagodatsky, S., Papen, H., Butterbach-Bahl, K., 2006. Effect of pH, temperature and substrate on N_2O, NO and CO_2 production by Alcaligenes faecalis p. *J. Appl. Microbiol.* 101 (3), 655–667. https://doi.org/10.1111/j.1365- 2672.2006.02927.x

Kim, S., Kim, S.Y., Lee, M., Shim, H., Wolfe, G.M., Guenther, A.B., He, A., Hong, Y., Han, J., 2015. Impact of isoprene and HONO chemistry on ozone and OVOC formation in a

semirural South Korean forest. *Atmos. Chem. Phys.* 15(8), 4357-4371. https://doi.org/10.5194/acp-15-4357-2015

Kleffmann, J., Gavriloaiei, T., Hofzumahaus, A., Holland, F., Koppmann, R., Rupp, L., Schlosser, E., Siese, M., Wahner, A., 2005. Daytime formation of nitrous acid: A major source of OH radicals in a forest. *Geophys. Res. Lett.* 32(5). https://doi.org/10.1029/2005GL022524

Klemedtsson, L., Von Arnold, K., Weslien, P., Gundersen, P., 2005. Soil CN ratio as a scalar parameter to predict nitrous oxide emissions. *Glob. Chang. Biol.* 11, 1142–1147. https://doi.org/10.1111/j.1365-2486.2005.00973.x

Kuznetsova, A., Brockhoff, P.B., Christensen, R.H.B., 2017. lmerTest package: tests in linear mixed effects models. *J. Stat. Softw.* 82(13). https://doi.org/10.18637/jss.v082.i13

Lantz, A.T., Allman, J., Weraduwage, S.M., Sharkey, T.D., 2019. Isoprene: New insights into the control of emission and mediation of stress tolerance by gene expression. *Plant Cell Environ.* 42(10), 2808-2826. https://doi.org/10.1111/pce.13629

Leitner, S., Homyak, P.M., Blankinship, J.C., Eberwein, J., Jenerette, G.D., Zechmeister-Boltenstern, S., Schimel, J.P., 2017. Linking NO and N_2O emission pulses with the mobilization of mineral and organic N upon rewetting dry soils. *Soil Biol. Biochem.* 115, 461-466. https://doi.org/10.1016/j.soilbio.2017.09.005

Li, S., Matthews, J., Sinha, A., 2008. Atmospheric hydroxyl radical production from electronically excited NO_2 and H_2O. *Science* 319(5870), 1657-1660. https://doi.org/10.1126/science.1151443

Lu, X., Ye, X., Zhou, M., Zhao, Y., Weng, H., Kong, H., Li, K., Gao, M., Zheng, B., Lin, J., Zhou, F., Zhang, Q., Wu, D., Zhang, L., Zhang, Y., 2021. The underappreciated role of agricultural soil nitrogen oxide emissions in ozone pollution regulation in North China. *Nature Communications*, *12*(1), p.5021. https://doi.org/10.1038/s41467-021-25147-9

Ludwig, J., Meixner, F.X., Vogel, B., Förstner, J., 2001. Soil-air exchange of nitric oxide: An overview of processes, environmental factors, and modeling studies. *Biogeochemistry 52*, 225-257. https://doi.org/10.1023/A:1006424330555

Luria, M., Weisinger, R., Peleg, M., 1990. CO and NO_x levels at the center of city roads in Jerusalem. *Atmos. Environ. Part B. Urban Atmos.* 24, 93–99. https://doi.org/10.1016/0957-1272(90)90014-L

Machefert, S.E., Dise, N.B., Goulding, K.W.T., Whitehead, P.G., 2002. Nitrous oxide emission from a range of land uses across Europe. *Hydrol. Earth Syst. Sci.* 6(3), 325-338. https://doi.org/10.5194/hess-6-325-2002

Mackenzie, R., Curioni, G., Hart, K., Harper, N., (2020) BIFoR FACE environmental monitoring data.

Makita, N., Kosugi, Y., Sakabe, A., Kanazawa, A., Ohkubo, S., Tani, M., 2018. Seasonal and diurnal patterns of soil respiration in an evergreen coniferous forest: evidence from six years of observation with automatic chambers. *PLoS ONE* 13, e0192622. https://doi.org/10.1371/journal.pone.0192622

Matejovic, I., 1997. Determination of carbon and nitrogen in samples of various soils by the dry combustion. *Commun. Soil Sci. Plant Anal.* 28, 1499–1511. https://doi.org/10.1080/00103629709369892

McDowell, N., Bowling, D., Bond, B., Irvine, J., Law, B., Anthoni, P., Ehleringer, J., 2004. Response of the carbon isotopic content of ecosystem, leaf, and soil respiration to meteorological and physiological driving factors in a Pinus ponderosa ecosystem. *Global Biogeochem. Cycles* 18. https://doi.org/10.1029/2003GB002049

McDuffie, E.E., Smith, S.J., O'Rourke, P., Tibrewal, K., Venkataraman, C., Marais, E.A., Zheng, B., Crippa, M., Brauer, M., Martin, R.V., 2020. A global anthropogenic emission inventory of atmospheric pollutants from sector-and fuel-specific sources (1970–2017): an application of the Community Emissions Data System (CEDS). *Earth System Science Data*, 12(4):3413-42. https://doi.org/10.5194/essd-12-3413-2020

Medinets, S., Skiba, U., Rennenberg, H., Butterbach-Bahl, K., 2015. A review of soil NO transformation: associated processes and possible physiological significance on organisms. *Soil Biol. Biochem.* 80, 92–117. https://doi.org/10.1016/j.soilbio.2014.09.025

Medinets, S., Gasche, R., Skiba, U., Schindlbacher, A., Kiese, R., Butterbach-Bahl, K., 2016. Cold season soil NO fluxes from a temperate forest: drivers and contribution to annual budgets. *Environ. Res. Lett.* 11, 114012 https://doi.org/10.1088/1748-9326/11/11/114012

Medinets, S., Gasche, R., Kiese, R., Rennenberg, H., Butterbach-Bahl, K., 2019. Seasonal dynamics and profiles of soil NO concentrations in a temperate forest. *Plant Soil* 445, 335–348. https://doi.org/10.1007/s11104-019-04305-5

Medinets, S., White, S., Cowan, N., Drewer, J., Dick, J., Jones, M., Andrews, C., Harvey, D., Skiba, U., 2021. Impact of climate change on soil nitric oxide and nitrous oxide emissions

from typical land uses in Scotland. *Environ. Res. Lett.* 16, 055035 https://doi.org/10.1088/1748-9326/abf06e

Mei, B., Zheng, X., Xie, B., Dong, H., Yao, Z., Liu, C., Zhou, Z., Wang, R., Deng, J., Zhu, J., 2011. Characteristics of multiple-year nitrous oxide emissions from conventional vegetable fields in southeastern China. *J. Geophys. Res. Atmos.* 116(D12). https://doi.org/10.1029/2010JD015059

Middleton, J.T., Kendrick, J.B., Schwalm, H.W., 1950. Injury to herbaceous plants by smog or air pollution. *Plant Disease Reporter* **34**, 245–252.

Mo, Z., Shao, M., Wang, W., Liu, Y., Wang, M., Lu, S., 2018. Evaluation of biogenic isoprene emissions and their contribution to ozone formation by ground-based measurements in Beijing, China. *Sci. Total Environ.* 627, 1485-1494. https://doi.org/10.1016/j.scitotenv.2018.01.336

Mosier, A.R., Morgan, J.A., King, J.Y., Lecain, D., Milchunas, D.G., 2002. Soil-atmosphere exchange of CH_4, CO_2, NO_x, and N_2O in the Colorado shortgrass steppe under elevated CO_2. *Plant and Soil* 240, 201-211. https://doi.org/10.1023/A:1015783801324

Mosier, A.R., Pendall, E., Morgan, J.A., 2003. Effect of water addition and nitrogen fertilization on the fluxes of CH_4, CO_2, NO_x, and N_2O following five years of elevated CO_2 in the Colorado Shortgrass Steppe. *Atmos. Chem. Phys.* 3(5), pp.1703-1708. https://doi.org/10.5194/acp-3-1703-2003, 2003

Monteith J., Unsworth M. Principles of Environmental Physics; Arnold E., Ed: Butterworth-Heinemann: London, UK, 1990.

Mouat, A.P., Paton-Walsh, C., Simmons, J.B., Ramirez-Gamboa, J., Griffith, D.W., Kaiser, J., 2022. Measurement report: observation of long-lived volatile organic compounds from the 2019–2020 Australian wildfires during the COALA campaign. *Atmos. Chem. Phys.* 22, 11033–11047. https://doi.org/10.5194/acp-22-11033-2022

Muhr, J., Goldberg, S.D., Borken, W., Gebauer, G., 2008. Repeated drying–rewetting cycles and their effects on the emission of CO_2, N_2O, NO, and CH_4 in a forest soil. *J. Plant Nutr. Soil Sci.* 171(5), 719-728. https://doi.org/10.1002/jpln.200700302

National Atmospheric Emission Inventory. https://naei.beis.gov.uk/emissionsapp/, (accessed 21 Feb 2023).

Nguyen, T.B., Crounse, J.D., Schwantes, R.H., Teng, A.P., Bates, K.H., Zhang, X., St. Clair, J.M., Brune, W.H., Tyndall, G.S., Keutsch, F.N., Seinfeld, J.H., Wennberg, P.O., 2014.

Overview of the Focused Isoprene eXperiment at the California Institute of Technology (FIXCIT): mechanistic chamber studies on the oxidation of biogenic compounds. *Atmos. Chem. Phys.* 14(24), pp.13531-13549. https://doi.org/10.5194/acp-14-13531-2014

Norman, J.M., 1979. Modeling the complete crop canopy, in: Modification of the Aerial Environment of Plants, edited by Barfield, B.J and Gerber, J.F., ASAE Monogr. *Am. Soc. Agric. Eng.* 249-277.

Norman, J.M., Campbell, G.S., 1983. Application of a plant environment model to problems in irrigation, in: Advances in irrigation, Vol. II., 155–188, edited by: Hillel, D. I., Academic Press, New York.

Ocheltree, T., Nippert, J., Prasad, P., 2014. Stomatal responses to changes in vapor pressure deficit reflect tissue-specific differences in hydraulic conductance. *Plant Cell Environ.* 37, 132–139. https://doi.org/10.1111/pce.12137

Oswald, R., Behrendt, T., Ermel, M., Wu, D., Su, H., Cheng, Y., Breuninger, C., Moravek, A., Mougin, E., Delon, C., Loubet, B., Pommerening-Röser, A., Sörgel, M., Pöschl, U., Hoffmann, T., Andreae, M.O., Meixner, F.X., Trebs, I., 2013. HONO emissions from soil bacteria as a major source of atmospheric reactive nitrogen. *Science* 341(6151), pp.1233-1235. https://doi.org/10.1126/science.1242266

Otu-Larbi, F., Bolas, C.G., Ferracci, V., Staniaszek, Z., Jones, R.L., Malhi, Y., Harris, N.R., Wild, O., Ashworth, K., 2020. Modelling the effect of the 2018 summer heatwave and drought on isoprene emissions in a UK woodland. *Glob. Chang. Biol.* 26(4), pp.2320-2335. https://doi.org/10.1111/gcb.14963

Otu-Larbi, F., Conte, A., Fares, S., Wild, O., Ashworth, K., 2021. FORCAsT-gs: Importance of stomatal conductance parameterization to estimated ozone deposition velocity. *J. Adv. Model. Earth Syst.* 13(9), p.e2021MS002581. https://doi.org/10.1029/2021MS002581

Park, C., Schade, G.W., Boedeker, I., 2011. Characteristics of the flux of isoprene and its oxidation products in an urban area. *J. Geophys. Res. Atmos.* 116(D21). https://doi.org/10.1029/2011JD015856

Pierotti, D., Wofsy, S.C., Jacob, D., Rasmussen, R.A., 1990. Isoprene and its oxidation products: Methacrolein and methyl vinyl ketone. *J. Geophys. Res. Atmos.* 95(D2), pp.1871-1881. https://doi.org/10.1029/JD095iD02p01871

Pilegaard, K., Hummelshøj, P., Jensen, N.O., 1999. Nitric oxide emission from a Norway spruce forest floor. *J. Geophys. Res. Atmos.* 104(D3), 3433-3445. https://doi.org/10.1029/1998JD100050

Pilegaard, K., Skiba, U., Ambus, P., Beier, C., Brüggemann, N., Butterbach-Bahl, K., Dick, J., Dorsey, J., Duyzer, J., Gallagher, M., Gasche, R., Horvath, L., Kitzler, B., Leip, A., Pihlatie, M.K., Rosenkranz, P., Seufert, G., Vesala, T., Westrate, H., Zechmeister-Boltenstern, S., 2006. Factors controlling regional differences in forest soil emission of nitrogen oxides (NO and N_2O). *Biogeosciences* 3(4), pp.651-661. https://doi.org/10.5194/bg-3-651-2006

Pilegaard, K., 2013. Processes regulating nitric oxide emissions from soils. *Philos. Trans. R. Soc. B Biol. Sci.* 368, 20130126 https://doi.org/10.1098/rstb.2013.0126

Pinheiro, J.C., Bates, D.M., 2000. Linear Mixed-Effects Models: Basic Concepts and Examples. In: Mixed-Effects Models in S and S-PLUS. Statistics and Computing. Springer, New York, NY. 3-56. https://doi.org/10.1007/0-387-22747-4_1

Poth, M., Focht, D.D., 1985. 15^N kinetic analysis of N_2O production by Nitrosomonas europaea: an examination of nitrifier denitrification. *Appl. Environ. Microbiol.* 49(5), 1134-1141. https://doi.org/10.1128/aem.49.5.1134-1141.1985

R Core Team, 2021. R: A Language and Environment For Statistical Computing. R Foundation for Statistical Computing, Vienna, Austria. URL. http://www.R-project. org/. (Version 4.0.5)

R Core Team, 2023. R: A Language and Environment For Statistical Computing. R Foundation for Statistical Computing, Vienna, Austria. URL. http://www.R-project. org/. (Version 4.3.1)

Ramirez-Gamboa, J., Paton-Walsh, C., Galbally, I., Simmons, J., Guerette, E.-A., Griffith, A.D., Chambers, S.D., Williams, A.G, 2020. Seasonal variation of biogenic and anthropogenic VOCs in a semi-urban area near Sydney, Australia. *Atmosphere* (Basel) 12, 47. https://doi.org/10.3390/atmos12010047

Ran, L., Zhao, C.S., Xu, W.Y., Lu, X.Q., Han, M., Lin, W.L., Yan, P., Xu, X.B., Deng, Z.Z., Ma, N., Liu, P.F., Yu, J., Liang, W.D., Chen, L.L., 2011. VOC reactivity and its effect on ozone production during the HaChi summer campaign. *Atmos. Chem. Phys.* 11(10), 4657-4667. https://doi.org/10.5194/acp-11-4657-2011

Rey-Sánchez, A.C., Slot, M., Posada, J.M., Kitajima, K., 2016. Spatial and seasonal variation in leaf temperature within the canopy of a tropical forest. *Clim. Res.* 71(1), pp.75-89. https://doi.org/10.3354/cr01427

Robertson, G.P., 1989. Nitrification and denitrification in humid tropical ecosystems: potential controls on nitrogen retention. *Mineral nutrients in tropical forest and savanna ecosystems.* 9:55-69.

Robertson, G.P., Groffman, P.M., 2007. Nitrogen transformations. In: Paul, E.A. (Ed.), Soil Microbiology, Ecology, and Biochemistry, third ed. Springer, New York, 341-364.

Rohrer, F., Bohn, B., Brauers, T., Brüning, D., Johnen, F.J., Wahner, A., Kleffmann, J., 2005. Characterisation of the photolytic HONO-source in the atmosphere simulation chamber SAPHIR. *Atmos. Chem. Phys.* 5(8), 2189-2201. https://doi.org/10.5194/acp-5-2189-2005

Rubio, V.E., Detto, M., 2017. Spatiotemporal variability of soil respiration in a seasonal tropical forest. *Ecol. Evol.* 7, 7104–7116. https://doi.org/10.1002/ece3.3267

Sanchez, D., Seco, R., Gu, D., Guenther, A., Mak, J., Lee, Y., Kim, D., Ahn, J., Blake, D., Herndon, S., Jeong, D., Sullivan, J.T., Mcgee, T., Park, R., Kim, S., 2021. Contributions to OH reactivity from unexplored volatile organic compounds measured by PTR-ToF-MS–a case study in a suburban forest of the Seoul metropolitan area during the Korea–United States Air Quality Study (KORUS-AQ) 2016. *Atmos. Chem. Phys.* 21(8), 6331-6345. https://doi.org/10.5194/acp-21-6331-2021

Sari, D., İncecik, S., Ozkurt, N., 2016. Surface ozone levels in the forest and vegetation areas of the Biga Peninsula, Turkey. *Sci. Total Environ. 571*, pp.1284-1297. http://dx.doi.org/10.1016/j.scitotenv.2016.07.168

Sartelet, K.N., Couvidat, F., Seigneur, C., Roustan, Y., 2012. Impact of biogenic emissions on air quality over Europe and North America. *Atmos. Environ.* 53, 131-141. https://doi.org/10.1016/j.atmosenv.2011.10.046

Sayer, E.J., 2006. Using experimental manipulation to assess the roles of leaf litter in the functioning of forest ecosystems. *Biol. Rev.* 81(1), 1-31. https://doi.org/10.1017/S1464793105006846

Sayer, E.J., Baxendale, C., Birkett, A.J., Br´echet, L.M., Castro, B., Kerdraon-Byrne, D., Lopez-Sangil, L., Rodtassana, C., 2021. Altered litter inputs modify carbon and nitrogen storage in soil organic matter in a lowland tropical forest. *Biogeochemistry* 156, 115–130. https://doi.org/10.1007/s10533-020-00747-7

Schaufler, G., Kitzler, B., Schindlbacher, A., Skiba, U., Sutton, M., Zechmeister- Boltenstern, S., 2010. Greenhouse gas emissions from European soils under different land use: effects of soil moisture and temperature. *Eur. J. Soil Sci.* 61, 683–696. https://doi.org/10.1111/j.1365-2389.2010.01277.x

Schindlbacher, A., Zechmeister-Boltenstern, S., Butterbach-Bahl, K., 2004. Effects of soil moisture and temperature on NO, NO_2, and N_2O emissions from European forest soils. *J. Geophys. Res. Atmos.* 109. https://doi.org/10.1029/2004JD004590

Schreiber, F., Wunderlin, P., Udert, K.M., Wells, G.F., 2012. Nitric oxide and nitrous oxide turnover in natural and engineered microbial communities: biological pathways, chemical reactions, and novel technologies. *Front. Microbiol.* 3, 372. https://doi.org/10.3389/fmicb.2012.00372

Seok, B., Helmig, D., Ganzeveld, L., Williams, M., Vogel, C., 2013. Dynamics of nitrogen oxides and ozone above and within a mixed hardwood forest in northern Michigan. *Atmos. Chem. Phys.* 13, 7301–7320. https://doi.org/10.5194/acp-13-7301-2013

Sgouridis, F., Reay, M., Cotchim, S., Ma, J., Radu, A., Ullah, S., 2023. Stimulation of soil gross nitrogen transformations and nitrous oxide emission under Free air CO_2 enrichment in a mature temperate oak forest at BIFoR-FACE. *Soil Biol. Biochem.* 109072. https://doi.org/10.1016/j.soilbio.2023.109072

Shen, Y., Xiao, Z., Wang, Y., Xiao, W., Yao, L., Zhou, C., 2023. Impacts of agricultural soil NO_x emissions on O_3 over Mainland China. *J. Geophys. Res. Atmos.* 128(4), e2022JD037986. https://doi.org/10.1029/2022JD037986

Shoun, H., Fushinobu, S., Jiang, L., Kim, S.W., Wakagi, T., 2012. Fungal denitrification and nitric oxide reductase cytochrome P450nor. *Philos. Trans. R. Soc. B Biol. Sci*. 367(1593), 1186-1194. https://doi.org/10.1098/rstb.2011.0335

Sierra, J., 2002. Nitrogen mineralization and nitrification in a tropical soil: effects of fluctuating temperature conditions. *Soil Biol. Biochem.* 34(9), 1219-1226. https://doi.org/10.1016/S0038-0717(02)00058-5

Sillman, S., 1999. The relation between ozone, NO_x and hydrocarbons in urban and polluted rural environments. *Atmos. Environ.* 33, 1821–1845. https://doi.org/10.1016/S1352-2310(98)00345-8

Simmons J.B., Paton-Walsh C., Mouat A.P., Kaiser J., Humphries R.S., Keywood M., Sutresna A., Griffith D.W.T., Naylor T., Ramirez-Gamboa J., 2021. The Gas and aerosol phase

composition of smoke plumes from the 2019-2020 Black Summer bushfires and potential implications for human health. https://doi.org/10.21203/rs.3.rs-1062663/v1

Sindelarova, K., Granier, C., Bouarar, I., Guenther, A., Tilmes, S., Stavrakou, T., Müller, J.F., Kuhn, U., Stefani, P., Knorr, W., 2014. Global data set of biogenic VOC emissions calculated by the MEGAN model over the last 30 years. *Atmos. Chem. Phys.* 14(17), 9317-9341. https://doi.org/10.5194/acp-14-9317-2014

Skiba, U., Hargreaves, K.J., Fowler, D., Smith, K.A., 1992. Fluxes of nitric and nitrous oxides from agricultural soils in a cool temperate climate. *Atmos. Environ. Part A Gen. Top.* 26 (14), 2477–2488. https://doi.org/10.1016/0960-1686(92)90100-Y

Skiba, U., Fowler, D., Smith, K.A., 1997. Nitric oxide emissions from agricultural soils in temperate and tropical climates: sources, controls and mitigation options. *Nutr. Cycl. Agroecosystems* 48, pp.139-153. https://doi.org/10.1023/A:1009734514983

Skiba, U., Medinets, S., Cardenas, L., Carnell, E., Hutchings, N., Amon, B., 2021. Assessing the contribution of soil NO_x emissions to European atmospheric pollution. *Environ. Res. Lett.* 16, 025009 https://doi.org/10.1088/1748-9326/abd2f2

Slemr, F., Seiler, W., 1984. Field measurements of NO and NO_2 emissions from fertilized and unfertilized soils. *J. Atmos. Chem.* 2, 1-24. https://doi.org/10.1007/BF00127260

Spott, O., Russow, R., Stange, C.F., 2011. Formation of hybrid N2O and hybrid N2 due to codenitrification: First review of a barely considered process of microbially mediated N-nitrosation. *Soil Biol. Biochem.* 43(10), 1995-2011. https://doi.org/10.1016/j.soilbio.2011.06.014

Stark, J.M., 1996. Modeling the temperature response of nitrification. *Biogeochemistry.* 35, 433-445. https://doi.org/10.1007/BF02183035

Stehfest, E., Bouwman, L., 2006. N_2O and NO emission from agricultural fields and soils under natural vegetation: summarizing available measurement data and modeling of global annual emissions. *Nutr. Cycl. Agroecosystems* 74, 207-228. https://doi.org/10.1007/s10705-006-9000-7

Steinbrecher, R., Hauff, K., Hakola, H., Rössler, J., 1999. A revised parameterisation for emission modelling of isoprenoids for boreal plants. *Biogenic VOC emissions and photochemistry in the boreal regions of Europe–Biphorep, edited by Laurila, T. and Lindfors, V*, (70), 29-43.

Stewart, H.E., Hewitt, C.N., Bunce, R.G.H., Steinbrecher, R., Smiatek, G., Schoenemeyer, T., 2003. A highly spatially and temporally resolved inventory for biogenic isoprene and monoterpene emissions: Model description and application to Great Britain. *J. Geophys. Res. Atmos.* 108(D20). https://doi.org/10.1029/2002JD002694

Stone, D., Whalley L.K., Heard, D.E., 2012. Tropospheric OH and HO_2 radicals: field measurements and model comparisons. *Chem. Soc. Rev.* 41, 6348-6404. https://doi.org/10.1039/c2s35140d

Su, H., Cheng, Y., Oswald, R., Behrendt, T., Trebs, I., Meixner, F.X., Andreae, M.O., Cheng, P., Zhang, Y., Pöschl, U., 2011. Soil nitrite as a source of atmospheric HONO and OH radicals. *Science* 333(6049), 1616-1618. https://doi.org/10.1126/science.1207687

Taylor, K.E., 2001. Summarizing multiple aspects of model performance in a single diagram. *J. Geophys. Res. Atmos.* 106(D7), 7183-7192. https://doi.org/10.1029/2000JD900719

Thomas, M.V., Malhi, Y., Fenn, K.M., Fisher, J.B., Morecroft, M.D., Lloyd, C.R., Taylor, M.E., McNeil, D.D., 2011. Carbon dioxide fluxes over an ancient broadleaved deciduous woodland in southern England. *Biogeosciences* 8(6), 1595-1613. https://doi.org/10.5194/bg-8-1595-2011

Thorn, K.A., Mikita, M.A., 2000. Nitrite fixation by humic substances nitrogen-15 nuclear magnetic resonance evidence for potential intermediates in chemodenitrification. *Soil Sci. Soc. Am. J.* 64(2), 568-582. https://doi.org/10.2136/sssaj2000.642568x

Toma, Y., Hatano, R., 2007. Effect of crop residue C: N ratio on N_2O emissions from Gray Lowland soil in Mikasa, Hokkaido, Japan. *Soil Sci. Plant Nutr.* 53, 198–205. https://doi.org/10.1111/j.1747-0765.2007.00125.x

Torsten-Hoffmann, SunCalc© 2022, http://suncalc.org/. (accessed 10 August 2022).

UK Met Office. 2019. Heatwave. Retrieved from https://www.metoffice.gov.uk/weather/learn-about/weather/types-of-weather/temperature/heatwave

Van Cleemput, O., Patrick Jr, W.H., McIlhenny, R.C., 1976. Nitrite decomposition in flooded soil under different pH and redox potential conditions. *Soil Sci. Soc. Am. J.* 40(1), 55-60. https://doi.org/10.2136/sssaj1976.03615995004000010018x

Van Cleemput, O., Baert, L., 1984. Nitrite: a key compound in N loss processes under acid conditions?. *Plant Soil*, 76, 233-241. https://doi.org/10.1007/BF02205583

Velasco, E., Roth, M., Tan, S., Quak, M., Nabarro, S., Norford, L., 2013. The role of vegetation in the CO_2 flux from a tropical urban neighbourhood. *Atmos. Chem. Phys.* 13, 10185–10202. https://doi.org/10.5194/acp-13-10185-2013

Venterea, R.T., Rolston, D.E., Cardon, Z.G., 2005. Effects of soil moisture, physical, and chemical characteristics on abiotic nitric oxide production. *Nutr. Cycl. Agroecosystems* 72, 27–40. https://doi.org/10.1007/s10705-004-7351-5

Visser, A.J., Ganzeveld, L.N., Finco, A., Krol, M.C., Marzuoli, R., Boersma, K.F., 2022. The combined impact of canopy stability and soil NO_x exchange on ozone removal in a temperate deciduous forest. *J. Geophys. Res. Biogeosci.* 127(10), p.e2022JG006997. https://doi.org/10.1029/2022JG006997

Vuong, Q.V., Chalmers, A.C., Jyoti Bhuyan, D., Bowyer, M.C., Scarlett, C.J, 2015. Botanical, phytochemical, and anticancer properties of the Eucalyptus species. *Chem. Biodivers.* 12 (6), 907–924. https://doi.org/10.1002/cbdv.201400327

Wagner, P., Kuttler, W., 2014. Biogenic and anthropogenic isoprene in the near-surface urban atmosphere—A case study in Essen, Germany. *Sci. Total environ.* 475, 104-115. https://doi.org/10.1016/j.scitotenv.2013.12.026

Wan, Y., Ju, X., Ingwersen, J., Schwarz, U., Stange, C.F., Zhang, F., Streck, T., 2009. Gross nitrogen transformations and related nitrous oxide emissions in an intensively used calcareous soil. *Sci. Soc. Am. J.* 73(1), pp.102-112. https://doi.org/10.2136/sssaj2007.0419

Wang, B., Lee, X., Theng, B.K., Cheng, J., Yang, F., 2015. Diurnal and spatial variations of soil NO_x fluxes in the northern steppe of China. *J. Environ. Sci.* 32, 54-61. https://doi.org/10.1016/j.jes.2014.11.011

Wei, D., Alwe, H.D., Millet, D.B., Bottorff, B., Lew, M., Stevens, P.S., Shutter, J.D., Cox, J.L., Keutsch, F.N., Shi, Q. and Kavassalis, S.C., Murphy, J.G., Vasquez, K.T., Allen, H.M., Praske, E., Crounse, J.D., Wennberg, P.O., Shepson, P.B., Bui, A.A.T., Wallace, H.W., Griffin, R.J., May, N.W., Connor, M., Slade, J.H., Pratt, K.A., Wood, E.C., Rolling, M., Deming, B.L., Anderson, D.C., Steiner A.L., 2021. FORest Canopy Atmosphere Transfer (FORCAsT) 2.0: model updates and evaluation with observations at a mixed forest site. *Geosci. Model Dev.* 14(10), 6309-6329. https://doi.org/10.5194/gmd-14-6309-2021

Weng, H., Lin, J., Martin, R., Millet, D.B., Jaeglé, L., Ridley, D., Keller, C., Li, C., Du, M., Meng, J., 2020. Global high-resolution emissions of soil NO_x, sea salt aerosols, and

biogenic volatile organic compounds. *Sci. Data* 7(1), 148. https://doi.org/10.1038/s41597-020-0488-5

Wennberg, P.O., Bates, K.H., Crounse, J.D., Dodson, L.G., McVay, R.C., Mertens, L.A., Nguyen, T.B., Praske, E., Schwantes, R.H., Smarte, M.D., St Clair, J.M., Teng, A.P., Zhang, X., Seinfeld, J.H., 2018. Gas-phase reactions of isoprene and its major oxidation products. *Chem. Rev.* 118(7), 3337-3390. https://doi.org/10.1021/acs.chemrev.7b00439

WHO, 2006. Air Quality Guidelines: Global Update 2005: Particulate Matter, Ozone, Nitrogen Dioxide, and Sulfur Dioxide. World Health Organization.

Wrage, N., Velthof, G.L., Van Beusichem, M.L., Oenema, O., 2001. Role of nitrifier denitrification in the production of nitrous oxide. *Soil Biol. Biochem.* 33(12-13), pp.1723-1732. https://doi.org/10.1016/S0038-0717(01)00096-7

Yamulki, S., Harrison, R.M., Goulding, K.W.T., Webster, C.P., 1997. N_2O, NO and NO_2 fluxes from a grassland: effect of soil pH. *Soil Biol. Biochem.* 29(8), 1199-1208. https://doi.org/10.1016/S0038-0717(97)00032-1

Yang, Q., Su, H., Li, X., Cheng, Y., Lu, K., Cheng, P., Gu, J., Guo, S., Hu, M., Zeng, L., Zhu, T., Zhang, Y., 2014. Daytime HONO formation in the suburban area of the megacity Beijing, China. *Sci. China Chem.* 57, 1032-1042. https://doi.org/10.1007/s11426-013-5044-0

Yu, Z., Elliott, E.M., 2021. Nitrogen isotopic fractionations during nitric oxide production in an agricultural soil. *Biogeosciences* 18, 805–829. https://doi.org/10.5194/bg-18-805-2021

Zhang, X., Ward, B.B., Sigman, D.M., 2020. Global nitrogen cycle: critical enzymes, organisms, and processes for nitrogen budgets and dynamics. *Chem. Rev.* 120(12), 5308-5351. https://doi.org/10.1021/acs.chemrev.9b00613

Zhang, Y., Hu, X.M., Leung, L.R., Gustafson Jr, W.I., 2008. Impacts of regional climate change on biogenic emissions and air quality. *J. Geophys. Res. Atmos.* 113(D18). https://doi.org/10.1029/2008JD009965

Ziegler, C., Kulawska, A., Kourmouli, A., Hamilton, L., Shi, Z., MacKenzie, A.R., Dyson, R.J., Johnston, I.G., 2023. Quantification and uncertainty of root growth stimulation by elevated CO_2 in a mature temperate deciduous forest. *Sci. Total Environ.* 854, 158661. https://doi.org/10.1016/j.scitotenv.2022.158661

Zumft, W.G., Cárdenas, J., 1979. The inorganic biochemistry of nitrogen bioenergetic processes. *Naturwissenschaften* 66(2), 81-88. https://doi.org/10.1007/BF00373498

Zumft, W.G., 1997. Cell biology and molecular basis of denitrification. *Microbiol. Mol. Biol. Rev.* 61(4), 533-616. https://doi.org/10.1128/mmbr.61.4.533-616.1997